An Abstract of the thesis of

Lingzhou Li Canfield for the degree of Doctor of Philosophy in Physics presented on June 10, 1992.

Title: Local Field Effects on Dielectric Properties of Solids

Abstract approved: Redacted for Privacy

Professor Allen Wasserman

Local field effects on the dielectric properties of solids have been studied for three-dimensional and two-dimensional crystals by using two kinds of dipole models: an atomic dipole model in which dipoles coincide with atom sites and a bond dipole model in which dipoles are placed along bond directions. Local fields at the dipole sites and at the interstitial sites are calculated in a self-consistent manner. Both the three and two dimensional model give results in the form of the classical Lorentz-Lorenz relation. The formulas for calculating the dipole sums have been obtained by applying the Born-Ewald method in three and two dimensions. Lorentz factors for several three and two dimensional crystal structures have been calculated.

Elasto-optic (Pockels) constants have been studied for the rare gas solid Xenon. Pockels constants have also been calculated for some selected tetrahedral crystals using both dipole models.

Local Field Effects on Dielectric Properties of Solids

by

Lingzhou Li Canfield

A THESIS

submitted to

Oregon State University

in partial fulfillment of

the requirements for the

degree of

Doctor of Philosophy

Completed June 10, 1992

Commencement June 1993

Approved:

Redacted for Privacy

Professor of Physics in charge of major

Redacted for Privacy

Chairman of the Department of Physics

Redacted for Privacy

Dean of Graduate School

Date thesis is presented June 10, 1992

Typed by Lingzhou L. Canfield for Lingzhou L. Canfield

Acknowledgements

I would like to express my deep gratitude to my advisor, Professor Allen Wasserman, for his guidance during the course of this work. I would like to express my sincere appreciation to Dr. William Hetherington and Dr. Henri Jansen, for their interested in the work, their valuable suggestions about the thesis and their encouragement. I would like to express my sincere appreciation to our department head, Dr. Kenneth Krane, for his encouragement throughout the course of my study.

I would also like to express my special thanks to my husband, Philip Canfield, for his constant support, encouragement and assistance. He helped with all the plotting in this work and also helped to correct my English. Many times I wasn't sure I could continue this work, however, he was always there to cheer me up and encourage me to go on. Without his support, I could never have finished it.

I also want to thank my parents — especially my mother, Dr. Qingmei Liu, who spent almost two years helping in taking care of my baby, Jason, so that I could concentrate on my research. The majority of this work was done during that period of time.

Thanks are also given to all my family in laws, and all my friends. Their support and encouragement made the finishing of this work much easier.

TABLE OF CONTENTS

LIST OF FIGURES

LIST OF TABLES

LOCAL FIELD EFFECTS ON DIELECTRIC PROPERTIES OF SOLIDS

CHAPTER I

INTRODUCTION

1.1 Microscopic and Macroscopic Fields

A weak external electric field applied to a crystal will displace electronic charges and produce an internal polarization. The dielectric response $\epsilon(\vec{r},\vec{r}';t-t')$ is defined by relating the microscopic displacement vector $\vec{D}(\vec{r},t)$ to the microscopic local electric field $\vec{E}(\vec{r}',t')$ at the position $\vec{r}'$ and time t' †:

$$\vec{D}(\vec{r},t) = \iint \epsilon(\vec{r},\vec{r}';t-t')\vec{E}(\vec{r}',t')d\vec{r}'dt'. \qquad (1.1)$$

In contrast the macroscopic relation from Maxwell equations is

$$< \vec{D} > = \epsilon(\omega) < \vec{E} >, \qquad (1.2)$$

where ϵ is the measured dielectric constant, with $< \vec{D} >$ and $< \vec{E} >$ the macroscopic average fields. It is the relationship between microscopic and macroscopic quantities, and the bearing it has on

---

† CGS units are used throughout this work.

measured and calculated optical properties, that forms the main body of this work.

For a better understanding of the problem, we rewrite Eq.(1.1) in a different way. In a perfect crystal, translational symmetry requires that

$$\epsilon(\vec{r}+\vec{R},\vec{r}'+\vec{R};t-t') = \epsilon(\vec{r},\vec{r}';t-t'), \tag{1.3}$$

where $\vec{R}$ denotes a lattice vector. Taking the Fourier transform of Eq.(1.1) then gives the relation:

$$\vec{D}(\vec{q}+\vec{G};\ \omega) = \sum_{\vec{G}'} \epsilon(\vec{q}+\vec{G},\vec{q}+\vec{G}';\ \omega)\vec{E}(\vec{q}+\vec{G}';\ \omega), \tag{1.4}$$

where $\vec{q}$ is a wave vector confined to the first Brillouin zone and $\vec{G}$ and $\vec{G}'$ are reciprocal lattice vectors for any crystal symmetry. Thus the allowed values of $\vec{q}+\vec{G}$ cover the infinite range of wave vectors and the simple $\vec{G}$ and $\vec{G}'$ dependence of $\epsilon(\vec{q}+\vec{G},\vec{q}+\vec{G}';\ \omega)$ reflects the crystal symmetry. If the external field is a long-wavelength optical field then $\vec{q}$ corresponds to the external wave vector in the medium (i.e. $\vec{q}=\vec{q}'/n$, $\vec{q}'$ is the external wave vector, n is the refractive index of the medium), and ω is its frequency.

Notice that in Eq.(1.1), which is in coordinate-time space, or in Eq.(1.4), which is in wave vector-frequency space, the electric fields are the microscopic fields which contain small-scale (unit cell) fluctuations — historically called local fields. Local fields arise from the external field and the induced polarization

distributed throughout the crystal. Due to the inhomogeneity in the charge distribution these unit cell scale variations occur even if the applied external field is uniform.

Metals (in which the electrons are often modeled as a highly delocalized free electron gas) have negligible microscopic field fluctuations. So the derived microscopic fields will also be uniform. The quantum mechanically obtained microscopic screening dielectric function will therefore correspond to the macroscopic average value. However, for covalent and ionic crystals, where there are local accumulations of polarizable electrons, the screening response will reflect local field variations within the unit cell. In a crystal, it is the local field that actually determines how the charge is polarized, which in turn determines the macroscopic dielectric response by an average of the microscopic quantities over a unit cell. Taking the $\vec{G} = 0$ and $\vec{G}' = 0$ term in Eq.(1.4), gives the macroscopic relation

$$\mathbf{D}(\vec{q};\ \omega) = \epsilon(\vec{q};\ \omega)\mathbf{E}(\vec{q};\ \omega). \tag{1.5}$$

In the optical limit $\vec{q}=0$ Eq. (1.5) becom s the macrosBMp725Maxwell relation Eq.(1.2). The detailed relationship between the microscopic and macroscopic electric fields will be discussed later in this chapter and in Chapter II.

1.2 Dielectric Constant and the Lorentz - Lorenz Relation

The complex dielectric constant

$$\epsilon(\omega) = \epsilon_1(\omega) + i\,\epsilon_2(\omega) \tag{1.6}$$

contains a complete description of the linear optical properties of matter. For example the optical absorption coefficient $\eta(\omega)$ is related to the imaginary part of the dielectric function $\epsilon_2(\omega)$ by $\eta(\omega) = \frac{\omega}{c}\,\epsilon_2(\omega)$, and the complex index of refraction $n(\omega)$ is defined by

$$n(\omega) = \sqrt{\epsilon(\omega)}, \tag{1.7}$$

which in turn determines the reflectivity at normal incidence $R = |\frac{1 - n}{1 + n}|^2$. Moreover, light scattering and harmonic generation cross-sections can be modeled by considering variations of the complex dielectric constant with the crystal under strain.

Comparison between measured dielectric constants and those calculated from microscopic models must be done with care. The measured dielectric constant is a bulk property defined through Maxwell equations in terms of macroscopic average fields. On the other hand, dielectric constants calculated from quantum mechanical models are usually found as linear and non-linear screening responses of a polarizable system to an external electric field.

The relation between macroscopic and microscopic fields was first studied, over 100 years ago, by Mossotti (1847) and Clausius

(1879). They independently anticipated a relationship between the macroscopic dielectric constant and the microscopic atomic polarizability which was later theoretically obtained by Lorentz (1880) from the following arguments.

Consider a cubic crystal consisting of identical polarizable dipoles with polarizability $\alpha(\omega)$ at each site. Let there be an external electric field $\vec{E}_{ext}$ (due to external charges). The microscopic dipoles are polarized by the microscopic field $\vec{E}_L$ at their sites which, as a result of the fields from all the other dipoles, are clearly not the same as the external field. The microscopic dipoles acquire moments according to

$$\vec{p}(\omega) = \alpha(\omega)\ \vec{E}_L, \tag{1.8}$$

and the average polarization vector within the crystal is the sum of these dipole moments

$$\vec{P} = N\ \alpha(\omega)\ \vec{E}_L, \tag{1.9}$$

where N is the number of dipoles (n) per unit volume (a^3), a being the lattice constant and therefore $N = n/a^3$. However, the polarization vector defines the macroscopic electric susceptibility χ

$$\vec{P} = \chi\ \vec{E}, \tag{1.10}$$

where $\vec{E}$ is the macroscopic averaged electric field within matter.

The macroscopic dielectric constant ϵ is defined from χ by

$$\epsilon = 1 + 4\pi\chi. \tag{1.11}$$

The local field $\vec{E}_L$ can be estimated by using the Lorentz spherical cavity argument in a cubic crystal to find[1]

$$\vec{E}_L = \vec{E} + \frac{4\pi}{3}\vec{P}. \tag{1.12}$$

Substituting Eq.(1.9) into Eq.(1.12), we have

$$\vec{E}_L = \frac{\vec{E}}{1 - \frac{4\pi}{3}N\alpha(\omega)}, \tag{1.13}$$

so the local field has the same direction as the macroscopic average field. Comparison with Eq(1.9) and (1.10) yields

$$\epsilon = 1 + \frac{4\pi\ N\alpha(\omega)E_L}{E}, \tag{1.14}$$

from which it is found that

$$\epsilon = 1 + \frac{4\pi\ N\alpha(\omega)}{1 - \frac{4\pi}{3}N\alpha(\omega)}. \tag{1.15}$$

This demonstrates the difference between a microscopic description (via $\alpha(\omega)$ in this model) and the macroscopic (measured) dielectric

function. Eq.(1.15) is the so-called Lorentz - Lorenz (L-L) formula and the factor $4\pi/3$ is called the Lorentz factor (L-factor) for cubic crystals.

1.3 Quantum Local Field Theory and the L-L Relation

Apart from the obvious limitation that the L-L relation is only valid for cubic symmetry, it may seem like the L-L formula is a hopelessly naive approach to what is a complex quantum mechanical many body problem. In general, the L-factor is crystal structure dependent, which is beyond the Lorentz theory[2]. However, within this simple L-L formula

$$\chi = \frac{\chi_o}{1 - L\chi_o} = \chi_o \{1 + L\chi_o + (L\chi_o)^2 + (L\chi_o)^3 + ...\}, \qquad (1.16)$$

lies the suggestion of a summation of Feynman diagrams, hinting perhaps at some form of Random Phase Approximation (RPA).

From the general method for obtaining the Maxwell measured dielectric constant from the fully local field corrected microscopic dielectric response, originally developed by Adler (1962)[3], Wiser (1963)[4] and Sinha et al. (1973)[5,6,7], the macroscopic dielectric constant $\epsilon(\omega)$ with local field effect included is given by[3,4]

$$\epsilon(\omega) = \lim_{\vec{q}\to 0} \frac{1}{\epsilon^{-1}(\vec{q}+\vec{G},\vec{q}+\vec{G}';\ \omega)} \Bigg|_{\substack{\vec{G}=0 \\ \vec{G}'=0}} . \qquad (1.17)$$

Here ϵ^{-1} is the inverse dielectric matrix and $\vec{q}\to 0$ is the

long-wavelength (optical) limit. If one considers the limit of tightly bound electrons, neglects the overlap of electronic wave functions belonging to different sites and uses the dipole approximation, one finds results analogous to the classical Lorentz - Lorenz relation.

This has been most clearly discussed by Onodera[8] and we state here his result. If the unit cell contains one atom, the dielectric constant is

$$\epsilon(\omega) = \lim_{\vec{q}\to 0}\{ 1 + \frac{4\pi\, a(\omega)}{1 - \frac{4\pi e^2}{3}[\sum_{G} |f(\vec{q}+\vec{G})|^2 - \sum_{G\neq 0} |f(\vec{G})|^2]}\}, \quad (1.18)$$

where $a(\omega) = e^2|f(0;\omega)|^2$ is the free-atom polarizability and $f(\vec{q}+\vec{G})$ is the polarizability between a pair of localized Wannier states $\varphi_\mu(\vec{r})$ and $\varphi_\xi(\vec{r})$

$$f(\vec{q}+\vec{G}) = \int d^3r\ \varphi^*_\xi(\vec{r}) e^{-i(\vec{q}+\vec{G})\cdot\vec{r}} \varphi_\mu(\vec{r}). \quad (1.19)$$

Onodera[8] is careful to point out that while the third term in the denominator corresponds to the RPA result the second term, which is the subtracted self polarization of charge in a unit cell, is essential to give the L-L result. The removal of self polarization corresponds to going beyond RPA and including the exchange contribution in the Feynman diagrams.

In principle, if the Wannier functions of the solid are known, the self-consistent local field calculation of the dielectric matrix

can be done by using the many body quantum theory which we have described above. However, determination of the Wannier functions of a solid is very complicated and in most cases is too difficult to be practical, although linear combination of atomic orbitals (LCAO) calculations are often useful. Moreover, for the more general case of a non-cubic crystal or a crystal with several atoms per unit cell, the dielectric matrix is not so easily obtained. But having seen even a restrictive quantum justification for the L-L form, it may be that a direct " classical" evaluation of the dielectric function in the spirit of L-L can be an useful approach.

A number of investigations have been reported into the local field effect in semiconductors and insulators[9,10]. Hanke and Sham[11,12,13,14] expressed the dielectric response in Wannier states, by writing the single-electron Bloch wave in terms of a set of well localized wave functions describing the inhomogeneity of the charge distribution. The localization of the Wannier functions describes precisely the physical origin of the charge inhomogeneity. Notice that in Eq.(1.19), the first non-vanishing term in the multipole expansion (i.e. $e^{-i\vec{k}\cdot\vec{r}} \simeq 1 - i\vec{k}\cdot\vec{r}$) corresponds to the appearance of a dipole. If we assume that the well localized Wannier states are the physical origin of the dipole, then we can still use the point dipole model to evaluate the local fields and the dielectric constant in the solids.

1.4 This Work

The L-L relation is justifiable for solids with electrons tightly bound to the atom, but is questionable for covalent crystals[10] in which the electron wave functions are sufficiently spread out to form bonds bridging atomic sites. Yet this is a case we wish to consider here. As an alternative if we assume that the well localized bonds are the actual dipoles (i.e the bond dipole model) then we can consider a relationship between the bond polarizability and the dielectric constant.

In this work we use the point dipole model to calculate the self consistent local field at each dipole's site and the dielectric constants of solids. We also examine the variation of local field strength at the interstitial sites in a unit cell, which may be very useful for studying defects in solids and understanding local field related light absorption or light scattering enhancements.

In this work the following assumptions are made. We assume that the frequency of the external field is in the optical range but far from resonances which allows us to be concerned only with the contributions from the electrons in the solid and to ignore the frequency dependence of the dielectric function.

In the point dipole limit, the local field at an arbitrary position in the unit cell is the external field plus the field due to all the interacting polarized electrons, i.e all the dipoles, in the solid. In Cartesian coordinates, the i^{th} component of the local field at an arbitrary position in the unit cell can be written as

$$E_L^i(\vec{q},\vec{r}) = E_{ext}^i(\vec{q}',\vec{r}) + \Sigma'_{\ell,m} \frac{3(\vec{x}_{\ell m}\cdot\vec{p}_m)x^i_{\ell m} - x^2_{\ell m}\, p^i_m}{x^5_{\ell m}} \exp(i\vec{q}\cdot\vec{x}_{\ell m}), \quad (1.20)$$

where $\vec{x}_{\ell m} = \vec{r} - \vec{r}_\ell - \vec{r}_m$, $\vec{r}$ is an arbitrary position in the unit cell, $\vec{r}_\ell$ is the lattice vector, $\vec{r}_m$ is the position of the m^{th} dipole basis in the unit cell (see Fig. 1.1), $\vec{p}_m$ is the dipole moment at the m^{th} basis, $\vec{q}$ is the propagation wave vector in the solid, $\vec{q}'$ is the external wave vector where $\vec{q} = n\vec{q}'$ with n the index of refraction of the material, and ω is the frequency of the external field. If this point is a dipole site, then this dipole must be excluded from the dipole field sum. The prime in the sum indicates that the dipole at the site of interest is excluded from the sum. Since we are only considering the long wave length limit of the external field, the phase difference of the local fields at different unit cells can be ignored.

Mahan[15] has pointed out that Eq.(1.20) is not a static electric field since the retardation effect from the dipoles is already rigorously included in the instantaneous dipole sums. A brief review of Mahan's work on this subject is presented in Appendix P.

With the help of the Ewald method[16] to calculate the dipole summations, we can solve for the self-consistent local field at any arbitrary position in a unit cell, including at each dipole's position. We can also evaluate the macroscopic average field in the

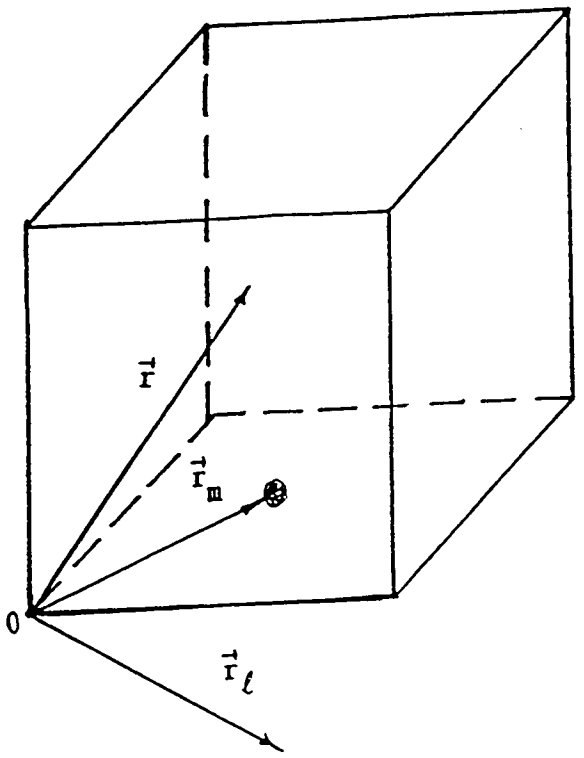

Figure 1.1 Schematic illustration of $\vec{r}$, $\vec{r}_1$ and $\vec{r}_m$.

solid which is the zero-order Fourier transform of the local fields. This allows us to examine the local field effects on the dielectric properties of the solids. A review of the Ewald method and a derivation of the macroscopic average field in the medium will be given in Chapter II.

In Chapter III, the method will be applied to the atomic dipole (polarized atoms) and bond dipole (hybrid orbitals in the classical dipole limit) models. We also examine the Lorentz -factor for different crystal structures and discuss the results from the self-consistent local field calculations for the two kinds of dipole models.

The self-consistent local field calculations are used to examine the effect on Brillouin scattering in solids in Chapter IV. The elasto-optic (Pockels) constants which are related to the Brillouin scattering cross section[17,18], represent the coupling of a photon and an acoustic phonon. They are determined by the change in the dielectric tensor due to an elastic strain. In Chapter IV, we have calculated the elasto-optical constants of compounds with the diamond and zinc blende structure by using the two kinds of dipole models.

In Chapter V, the self-consistent local field calculations have been extended to surfaces. In this case, some spatial averages which are zero in the original L-L argument are non-zero. For the two kinds of dipole models two dimensional local field equations and calculations are presented. Local fields at an arbitrary point on the surface are evaluated and the L-factor for different two dimensional surface structures are also calculated.

Finally, a summary of this work and the conclusions are presented in Chapter VI. Future work that may extend the analysis and application of this work are also discussed.

CHAPTER II

BORN-EWALD METHOD AND ITS APPLICATION

2.1 Introduction

From Chapter I, the i^{th} component of the dipole electric field at an arbitrary position $\vec{r}$ in a unit cell of a crystal is

$$E_p^i(\vec{r}) = \Sigma'_{\ell,m} \frac{3\,(\vec{x}_{\ell m}\cdot\vec{p}_m)x^i_{\ell m} - x^2_{\ell m}p^i_m}{x^5_{\ell m}} \exp(i\vec{q}\cdot\vec{x}_{\ell m}), \qquad (2.1)$$

where $\vec{x}_{\ell m} = \vec{r} - \vec{r}_\ell - \vec{r}_m$, $\vec{r}_\ell$ is the lattice vector and $\vec{r}_m$ is the position of the m^{th} dipole basis in a primitive cell (see Fig. 1.1). $\vec{p}_m$ is the dipole moment at the m^{th} site and $\vec{q}$ is the wave vector in the crystal. The prime on the sum means the self contribution of the dipole is excluded. We define two functions S_5^{ij} and S_3, which are related to the dipole field by

$$S_5^{ij}(\vec{q},\vec{r},m) = \Sigma'_\ell \frac{x^i_{\ell m}\, x^j_{\ell m}}{x^5_{\ell m}} \exp(i\vec{q}\cdot\vec{x}_{\ell m}),\ i \ \&\ j = 1..3, \qquad (2.2)$$

and

$$S_3(\vec{q},\vec{r},m) = \Sigma'_\ell \frac{1}{x^3_{\ell m}} \exp(i\vec{q}\cdot\vec{x}_{\ell m}). \qquad (2.3)$$

We can also define a function S_{ij},

$$S_{ij}(\vec{q},\vec{r},m) = 3S_5^{ij}(\vec{q},\vec{r},m) - \delta_{ij}S_3(\vec{q},\vec{r},m), \quad i \& j = 1..3. \quad (2.4)$$

Then, the dipole field of Eq.(2.1) can be rewritten as:

$$E_p^i(\vec{q},\vec{r}) = \Sigma_{m,j}\, S_{ij}(\vec{q},\vec{r},m)p_m^j, \quad i \& j = 1..3. \quad (2.5)$$

The dipole sum in Eq.(2.4) is absolutely convergent when $\vec{q} \neq 0$ but is conditionally convergent for an infinite lattice when $\vec{q} = 0$. Because the sum has no unique limit when $\vec{q} = 0$, its limiting value depends entirely on the direction by which the point $\vec{q} = 0$ is approached or, equivalently, the results depends on the order in which the terms are summed. However, for a finite lattice, a direct evaluation of Eq.(2.4) for $\vec{q}$=0 case is zero. All these points have been discussed in detail by Cohen and Keffer[19].

For either case the real space lattice sum converges too slowly to be computationally practical.

The Born-Ewald method[16,20,21] is the canonical method for evaluating this type of lattice summation because it accomplishes three important things: (1) it separates the conditionally convergent term, (2) it accelerates the convergence, and (3) it obtains the correct $\vec{q}$ dependence for small $\vec{q}$ which can not be obtained by a finite real space sum. The first point will be mentioned later in the discussion and the second point is discussed in next section. The Ewald method[16] was further developed by Misra[20] and Born and Bradburn[21]. In addition it has been widely applied by many other authors who have contributed to its evaluations and

applications[22,23,24,25]. However, throughout all these consequent extensions to the Born-Ewald method, the essential features were still retained and are used here.

2.2 Born-Ewald Method For Dipole Summations

Consider a Bravais lattice with m basis dipoles in each primitive cell. Each basis dipole is located on a sublattice. In particular, the diamond crystal has two basis atoms in one primitive cell with each basis atoms part of a face-center-cubic (fcc) sublattice. So the diamond structure can be thought of as two interpenetrating fcc sublattices.

We have introduced the two dipole sums $S_5^{ij}(\vec{q},\vec{r},m')$ and $S_3(\vec{q},\vec{r},m')$ in section 2.1. They are the sums at position $\vec{r}$ in the unit cell due to the dipoles on sublattice m′. If the position we are interested is the M^{th} dipole site, i.e. take $\vec{r}$ at the M^{th} dipole site (Capital M stands for one of the lattice points in the m^{th} sublattice), then the sums $S_5^{ij}(\vec{q},M,m')$ and $S_3(\vec{q},M,m')$ are the sums at the M^{th} dipole site due to the m'^{th} (m′ = 1..m) sublattice in the solid. If m′ = m, then the sum is over an imperfect lattice for which the M^{th} point must be excluded. If m′ ≠ m, then the sum is over a perfect lattice but at a point which is on a different sublattice. A perfect lattice here means that the lattice is perfectly periodic.

To simplify the derivation of $S_5^{ij}(\vec{q},M,m')$ and $S_3(\vec{q},M,m')$ in the Born-Ewald expression, we define:

$$S_n(\vec{q},\vec{r},m) = \Sigma'_{\ell} \frac{1}{x^n_{\ell m}} \exp(i\vec{q}.\vec{x}_{\ell m}), \quad (n > 0), \tag{2.6a}$$

and note that

$$S^{ij}_n(\vec{q},\vec{r},m) = - \frac{\partial}{\partial q_i} \frac{\partial}{\partial q_j} S_n(\vec{q},\vec{r},m). \tag{2.6b}$$

We will use this result to simplify the derivation later.

The Born-Ewald method is based on using Euler's integral for the Γ-function,

$$\Gamma(n/2)\ x^{-n}_{\ell m} = \int_0^{\infty} t^{(n/2\ -\ 1)} \exp(-x^2_{\ell m}\ t)\ dt, \ (n=1,2,3..). \tag{2.7}$$

The relationships between the perfect lattice sum and the sum excluding the point $\vec{x}_{\ell m} = 0$ is:

$$\Sigma'_{\ell}\exp(-x^2_{\ell m}t + i\vec{q}\cdot\vec{x}_{\ell m}) = \Sigma_{\ell} \exp(-x^2_{\ell m}t + i\vec{q}\cdot\vec{x}_{\ell m}) - 1, \tag{2.8}$$

and the similar expression

$$\Sigma'_{\ell}x^i_{\ell m}\cdot x^j_{\ell m}\exp(-x^2_{\ell m}t + i\vec{q}\cdot\vec{x}_{\ell m}) = \Sigma_{\ell}x^i_{\ell m}\cdot x^j_{\ell m}\exp(-x^2_{\ell m}t + i\vec{q}\cdot\vec{x}_{\ell m}). \tag{2.9}$$

The Fourier transform of the perfect lattice sum is given by:

$$\Sigma_{\ell} \exp(-x^2_{\ell m}t + i\vec{q}\cdot\vec{x}_{\ell m}) = \Sigma_G\ C_G \exp(i\vec{G}\cdot\vec{r}), \tag{2.10}$$

where $\vec{G}$ is a reciprocal lattice vector. By substituting (2.7), and (2.8) into (2.6a), the Fourier transform is,

$$C_G = \frac{1}{V_c} \int_{\text{cell}} \exp(-i\vec{G}\cdot\vec{r}) \{\Sigma_\ell \exp(-x_{\ell m}^2 t + i\vec{q}\cdot\vec{x}_{\ell m})\} d^3\vec{r}, \qquad (2.11)$$

where, $V_c = a^3/4$ is the volume of the primitive cell and a being the lattice constant for diamond and zinc blende structures. We may interchange the order of integration and summation and change the integration variable from $\vec{r}$ to $\vec{x}_{\ell m} = \vec{r} - \vec{r}_\ell - \vec{r}_m$. The resulting integral (see Appendix A) is,

$$C_G = \frac{1}{V_c} \left(\frac{\pi}{t}\right)^{3/2} \exp\left[-i\vec{G}\cdot\vec{r}_m - \frac{(\vec{G} - \vec{q})^2}{4t}\right], \qquad (2.12)$$

which can be inserted into Eq.(2.10) to give

$$\Sigma_\ell \exp(-x_{\ell m}^2 t + i\vec{q}\cdot\vec{x}_{\ell m}) = \Sigma_G \frac{1}{V_c}\left(\frac{\pi}{t}\right)^{3/2} \cdot\exp\left[-i\vec{G}\cdot\vec{r}_m - \frac{(\vec{G} - \vec{q})^2}{4t}\right] \exp(i\vec{G}\cdot\vec{r}). \qquad (2.13)$$

If we define

$$\sigma = \Sigma_\ell \exp(-x_{\ell m}^2 t + i\vec{q}\cdot\vec{x}_{\ell m}), \qquad (2.14)$$

then we have

$$- \frac{\partial}{\partial q_i} \frac{\partial}{\partial q_j} \sigma = \Sigma_\ell \, x^i_{\ell m} \cdot x^j_{\ell m} \exp(-x^2_{\ell m} \, t + i\vec{q}\cdot\vec{x}_{\ell m})$$
$$= \Sigma_G \, D^{ij}_G \exp(i\vec{G}\cdot\vec{r}), \qquad (2.15)$$

where D^{ij}_G is (see Appendix A),

$$D^{ij}_G = \frac{1}{V_c} \left(\frac{\pi}{t}\right)^{3/2} \left[\frac{1}{2\,t} \, \delta_{ij} - \frac{(G_i - q_i)\cdot(G_j - q_j)}{4\,t^2}\right]$$
$$\cdot \exp\left[-i\vec{G}\cdot\vec{r}_m - \frac{(\vec{G} - \vec{q})^2}{4\,t}\right]. \qquad (2.16)$$

This leads to

$$\Sigma_\ell \, x^i_{\ell m} \cdot x^j_{\ell m} \exp(-x^2_{\ell m} t + i\vec{q}\cdot\vec{x}_{\ell m}) = \Sigma_G \frac{1}{V_c} \left(\frac{\pi}{t}\right)^{3/2} \left[\frac{1}{2\,t} \, \delta_{ij} - \right.$$
$$\left. \frac{(G_i - q_i)\cdot(G_j - q_j)}{4\,t^2}\right] \cdot \exp\left[-i\vec{G}\cdot\vec{r}_m - \frac{(\vec{G} - \vec{q})^2}{4\,t}\right] \cdot \exp(i\vec{G}\cdot\vec{r}). \qquad (2.17)$$

Eq.(2.13) and Eq.(2.17) are called the theta function transformations. They will be used later to obtain the final results.

We now use Euler's integral to rewrite S_n as:

$$S_n(\vec{q},\vec{r},m) = \frac{1}{\Gamma(n/2)} \int_0^\infty \{t^{(n/2 - 1)} [\Sigma'_\ell \exp(-x^2_{\ell m} t + i\vec{q}\cdot\vec{x}_{\ell m})]\} dt. \qquad (2.18)$$

We can break the above integral into the sum of two integrals; the first extending from 0 to some parameter μ and the second from μ to

∞. In the first integral we use (2.8), the theta function transformation (2.13) and the integral

$$\int_0^{\mu} t^{(n/2 - 1)}\, dt = \frac{2\mu^{n/2}}{n}. \tag{2.19}$$

S_n can be written as:

$$S_n(\vec{q},\vec{r},m) = \frac{1}{\Gamma(n/2)} \{ [\frac{\pi^{3/2}}{V_c}\Sigma_G \exp(-i\vec{G}\cdot\vec{r}_m)\cdot\exp(i\vec{G}\cdot\vec{r}) \int_0^{\mu} t^{(n-5)/2} \cdot\exp(-\frac{(\vec{G}-\vec{q})^2}{4t})dt - \frac{2\mu^{n/2}}{n}] + \int_{\mu}^{\infty} t^{(n/2 - 1)} [\Sigma'_{\ell} \exp(-x_{\ell m}^2 t + i\vec{q}\cdot\vec{x}_{\ell m})]\, dt\}. \tag{2.20}$$

Finally we replace t by s^{-1} in the first integral to give

$$S_n(\vec{q},\vec{r},m) = \frac{1}{\Gamma(n/2)}\{ [\frac{\pi^{3/2}}{V_c}\Sigma_G \exp(-i\vec{G}\cdot\vec{r}_m)\cdot\exp(i\vec{G}\cdot\vec{r})\int_{1/\mu}^{\infty} s^{(1-n)/2} \cdot\exp(\frac{-(\vec{G}-\vec{q})^2}{4s})\, ds - \frac{2\mu^{n/2}}{n}] + \int_{\mu}^{\infty} t^{(n/2 - 1)} [\Sigma'_{\ell} \exp(-x_{\ell m}^2 t + i\vec{q}\cdot\vec{x}_{\ell m})]\, dt\}. \tag{2.21}$$

$S_n(\vec{q},\vec{r},m)$ is the n^{th} order lattice sum at position $\vec{r}$ due to the m^{th} sublattice. Taking n = 1, we can get the lattice potentials sum which is used in the Madelung sum, while n = 3 and 5 give the dipole sum. In general, taking a different order of n will give a different

order of multipole sum.

Now introduce the incomplete gamma function which is defined as

$$\Gamma(m,x) = \int_x^\infty t^{m-1} \exp(-t)\, dt \tag{2.22}$$

and satisfies the recurrence formula

$$\Gamma(m+1,\ x) = m\Gamma(m,x)+x^m\exp(-x). \tag{2.23}$$

We also have

$$\begin{aligned} \Gamma(1,x) &= \exp(-x), \\ \Gamma(0,x) &= E_1(x), \\ \Gamma(1/2,x) &= \sqrt{\pi}\ \{(1-F(\sqrt{x})\}, \end{aligned} \tag{2.24}$$

where $E_1(x)$ is the exponential integral

$$E_1(x) = \int_x^\infty \frac{\exp(-t)}{t}\, dt \tag{2.25}$$

and $F(x)$ is the error function integral

$$F(x) = 2\sqrt{\pi} \int_o^x \exp(-t^2)\, dt. \tag{2.26}$$

To calculate the dipole sum at the M^{th} dipole site we define this point to be the origin and take $\vec{r} = 0$ in the dipole sum. The final results of S_3 and S_5^{ij} at the M^{th} dipole site due to the m' sublattice can be written as:

$$S_3(\vec{q},M,m') = \frac{2\pi}{V_c} \Sigma_G \exp(-i\vec{G}\cdot\vec{r}_{m'})\cdot E_1(x_G) - \delta_{m,m'} \frac{4\eta^3}{3\sqrt{\pi}}$$
$$+ \Sigma'_\ell \frac{1}{x^3_{\ell m'}} \exp(i\vec{q}\cdot\vec{x}_{\ell m'}) \left[1 - F(x_r) + \frac{2x_r}{\sqrt{\pi}} \exp(-x_r^2)\right]. \quad (2.27)$$

Using Eq.(2.6b) we have

$$S_5^{ij}(\vec{q},M,m') = \frac{2\pi}{3V_c} \Sigma_G \exp(-i\vec{G}\cdot\vec{r}_{m'})\cdot \left[E_1(x_G)\ \delta_{ij} \right.$$
$$\left. - \frac{2G'_i\ G'_j}{G'^2} \exp(-x_G)\right] + \Sigma'_\ell \frac{x^i_{\ell m'} x^j_{\ell m'}}{x^5_{\ell m'}} \exp(i\vec{q}\cdot\vec{x}_{\ell m'})\cdot[1 - F(x_r)$$
$$+ \frac{2x_r}{\sqrt{\pi}} \exp(-x_r^2) + \frac{4x_r^3}{3\sqrt{\pi}} \exp(-x_r^2)], \quad (2.28)$$

where $\vec{G}$ is the reciprocal lattice vector, $\vec{G}' = \vec{G} - \vec{q}$, $x_G = G'^2 / 4\eta^2$, $x_r = \eta\, x_1$, and the parameter $\eta = \sqrt{\mu}$ is called the Ewald parameter.

To calculate the dipole sum at an arbitrary position $\vec{r} \neq \vec{r}_\ell$ and $\vec{r}_m$ which is a sum over a perfect sublattice due to the m^{th} sublattice, the term $\delta_{m,m'} \frac{4\eta^3}{3\sqrt{\pi}}$ in Eq.(2.27) vanishes, because it comes from the exclusion of the dipole's self contribution. That is,

$$S_3(\vec{q},\vec{r},m) = \frac{2\pi}{V_c} \Sigma_G \exp(-i\vec{G}\cdot\vec{r}_{m'}) \exp(i\vec{G}\cdot\vec{r})\cdot E_1(x_G)$$

$$+ \Sigma'_\ell \frac{1}{x^3_{\ell m'}} \exp(i\vec{q}\cdot\vec{x}_{\ell m'}) \left[1 - F(x_r) + \frac{2x_r}{\sqrt{\pi}} \exp(-x_r^2)\right], \qquad (2.27')$$

and

$$S_5^{ij}(\vec{q},\vec{r},m) = \frac{2\pi}{3V_c} \Sigma_G \exp(-i\vec{G}\cdot\vec{r}_{m'}) \exp(i\vec{G}\cdot\vec{r})\cdot \left[E_1(x_G)\, \delta_{ij} \right.$$

$$\left. - \frac{2G'_i\, G'_j}{G'^2} \exp(-x_G)\right] + \Sigma'_\ell \frac{x^i_{\ell m'} x^j_{\ell m'}}{x^5_{\ell m'}} \exp(i\vec{q}\cdot\vec{x}_{\ell m'})\cdot[1 - F(x_r)$$

$$+ \frac{2x_r}{\sqrt{\pi}} \exp(-x_r^2) + \frac{4x_r^3}{3\sqrt{\pi}} \exp(-x_r^2)]. \qquad (2.28')$$

The value of η is arbitrary and can be carefully chosen to make the summations over real space and reciprocal space converge at the same rate. By choosing the optimum value of the Ewald parameter η, the summations will converge rapidly. Furthermore, we can prove that the dipole summations are independent of η by showing,

$$\frac{\partial S_3(\vec{q},\vec{r},m)}{\partial \eta} = 0 \quad \left(\text{or } \frac{\partial S_3(\vec{q},\mathbf{M},m')}{\partial \eta} = 0\right), \qquad (2.29)$$

$$\frac{\partial S_5^{ij}(\vec{q},\vec{r},m)}{\partial \eta} = 0 \quad \left(\text{or } \frac{\partial S_5^{ij}(\vec{q},\mathbf{M},m')}{\partial \eta} = 0\right). \qquad (2.30)$$

This is established in Appendix B. The dipole sums we have just evaluated using the Born-Ewald method can be used in any kind of crystal structure and is not restricted to a cubic crystal. However, for simplification we consider the cubic crystal to check our analysis. Tables 2.1 and 2.2 give the dipole sums for a simple cubic

Table 2.1 The independence of the Ewald parameter of the dipole sums. Different Ewald parameter η are in put with N = 3 where N is the number of terms taken in the sums. The calculation is based on a simple cubic (SC) structure, so there is only one dipole in a unit cell. The dipole sums are calculated at the dipole's site. The wave vector $\vec{q}$ in the solid is along the $\hat{z}$ direction and has the value $q \cdot a = 4.1931 \times 10^{-3}$, where a is the lattice constant.

η	S_3	S_5^{11}	S_5^{12}	S_5^{22}	S_5^{13}	S_5^{23}	S_5^{33}
1.25	77.9271	27.3720	0.0000	27.3720	0.0000	0.0000	23.1832
1.50	77.9271	27.3720	0.0000	27.3720	0.0000	0.0000	23.1832
1.75	77.9271	27.3720	0.0000	27.3720	0.0000	0.0000	23.1832
2.00	77.9271	27.3720	0.0000	27.3720	0.0000	0.0000	23.1832

Table 2.2 The convergence of the dipole sums. With Ewald parameter η = 1.75 and all other conditions the same as in Table 2.1. N is the number of terms taken in the sums in both real space and wave vector space.

N	S_3	S_5^{11}	S_5^{12}	S_5^{22}	S_5^{13}	S_5^{23}	S_5^{33}
1	77.9270	27.3719	0.0000	27.3719	0.0000	0.0000	23.1831
2	77.9271	27.3720	0.0000	27.3720	0.0000	0.0000	23.1832
3	77.9271	27.3720	0.0000	27.3720	0.0000	0.0000	23.1832
6	77.9271	27.3720	0.0000	27.3720	0.0000	0.0000	23.1832
9	77.9271	27.3720	0.0000	27.3720	0.0000	0.0000	23.1832

crystal with different values of η and number of terms N taken for the sums in both real space and wave vector space. We can see immediately that the dipole sums are independent of Ewald parameter η and that they converge very quickly.

2.3 The Macroscopic Average Field

As mentioned in Chapter 1, the local field $\vec{E}_L(\vec{r})$ is equal to the external field plus the contribution of the fields from all the dipoles in the solid except the self contribution if $\vec{r}$ is at a dipole site, i.e.

$$E_L^i(\vec{q},\vec{r}) = E_{ext}^i(\vec{q},\vec{r}) + E_p^i(\vec{q},\vec{r}), \tag{2.31}$$

where $E_p^i(\vec{q},\vec{r})$ is the dipole field defined in Eq.(2.1). The macroscopic average field is an average of the local fields over the unit cell. The i^{th} component of the macroscopic average field $< E^i >$ in the solid is the zero order Fourier component of the local field:

$$< E^i(\vec{q}) > = \frac{1}{V_c} \int_{cell} E_L^i(\vec{q},\vec{r})\, dr^3. \tag{2.32}$$

It is this macroscopic average field which satisfies the Maxwell equations in the medium. Using Eq.(2.31), the i^{th} component of the macroscopic average field can be rewritten as the the external field plus the averaged dipole field over the primitive cell, i.e.

$$< E^i(\vec{q}) > = E^i_{ext} + \frac{1}{V_c} \int_{cell} E^i_p(\vec{q}.\vec{r})\, dr^3, \qquad (2.33)$$

Now let us calculate the second term of Eq.(2.33). We want the Fourier transform of $E^i_p(\vec{q},\vec{r})$ and then take the $\vec{G} = 0$ term which will give us the macroscopic average of the dipole field. Notice that when $\vec{r}$ is not taken at the dipole site (i.e. $\vec{r} \neq \vec{r}_\ell$ or $\vec{r}_m$), the dipole sum is over a perfect lattice. Even in the case where $\vec{r}$ is at the M^{th} dipole site, the sum over $m' \neq m$ sublattice is still over a perfect lattice. Only the case of $S_{ij}(\vec{q},M,m)$ which is the sum at the M^{th} dipole site over its own sublattice must exclude the self contribution. Therefore only this sum is over an imperfect lattice. From Eq.(2.5), we know that the Fourier transform of the dipole field E_p is equivalent to the Fourier transform of S_{ij}. For the sums over a perfect lattice and using Euler's integral again, we can rewrite S_n which was defined in Eq.(2.6a) as

$$S_n(\vec{q},\vec{r}\neq\vec{r}_m,m) = \frac{1}{\Gamma(n/2)} \int_0^\infty \{t^{(n/2\,-\,1)} \Sigma_l \exp(-x_l^2\, t + i\vec{q}\cdot\vec{x}_l)\}dt. \qquad (2.34)$$

Using the theta function transformation in section 2.2, we obtain the Fourier transform of S_3 and S_5^{ij}:

$$S_3(\vec{q},\vec{r},m) = \lim_{\epsilon\to 0} \frac{1}{\Gamma(3/2)} \int_\epsilon^\infty t^{1/2}\{ \Sigma_G \frac{1}{V_c} \left(\frac{\pi}{t}\right)^{3/2} \exp[i\vec{G}\cdot\vec{r}_m - \frac{(\vec{G} - \vec{q})^2}{4\,t}]\cdot\exp(i\vec{G}\cdot\vec{r})\}\, dt. \qquad (2.35)$$

$$S_5^{ij}(\vec{q},\vec{r},m) = \lim_{\epsilon\to 0} \frac{1}{\Gamma(5/2)}\int_{\epsilon}^{\infty} \frac{\pi^{3/2}}{V_c}\{\Sigma_G[\frac{1}{2\,t}\delta_{ij} - \frac{(G_i - q_i)\cdot(G_j - q_j)}{4\,t^2}]$$

$$\cdot\exp[i\vec{G}\cdot\vec{r}_m - \frac{(\vec{G} - \vec{q})^2}{4\,t}]\cdot\exp(i\vec{G}\cdot\vec{r})\}\,dt. \qquad (2.36)$$

Thus, for the $\vec{G} = 0$ term (which does not depend on $\vec{r}$ so its dependence is suppressed) in Eq.(2.35) and (2.36):

$$< S_3(\vec{q},m) >|_{G=0} = \lim_{\epsilon\to 0}\frac{1}{\Gamma(3/2)} \frac{(\pi)^{3/2}}{Vc}\int_{\epsilon}^{\infty} t^{-1}\exp(-\frac{q^2}{4\,t})\,dt, \qquad (2.37)$$

$$< S_5^{ij}(\vec{q},m) >|_{G=0} = \lim_{\epsilon\to 0}\frac{1}{\Gamma(5/2)} \frac{(\pi)^{3/2}}{Vc}\int_{\epsilon}^{\infty} (\frac{t^{-1}}{2}\,\delta_{ij} - \frac{q_i q_j}{4\,t^2})$$

$$\cdot\exp(-\frac{q^2}{4\,t})\,dt. \qquad (2.38)$$

For the sums over an imperfect lattice only $S_3(\vec{q},\mathbf{M},m)$ requires special attention, since from Eq.(2.9) the sum $S_5^{ij}(\vec{q},\mathbf{M},m)$ is the same as $S_5^{ij}(\vec{q},\mathbf{M},m')$, which is over a perfect lattice. Also from Eq.(2.8), the imperfect lattice sum $S_3(\vec{q},\mathbf{M},m)$ is related to a perfect lattice which means we can take the Fourier transform. By a change of variable, the zero order Fourier component of the $S_3(\vec{q},\mathbf{M},m)$ can finally be written as

$$< S_3(\vec{q},\mathbf{M},m) >|_{G=0} = \lim_{\epsilon\to 0}\{\frac{1}{\Gamma(3/2)} \frac{(\pi)^{3/2}}{Vc}\int_{\epsilon}^{\infty} t^{-1}\exp(-\frac{q^2}{4\,t})\,dt$$

$$- \frac{2\,\epsilon^{3/2}}{3}\}. \qquad (2.39)$$

In the limit $\epsilon \to 0$, it has the same form as Eq.(2.37).

If we set

$$I(\epsilon) = \int_{\epsilon}^{\infty} t^{-1} \exp(- \frac{q^2}{4\,t}) \, dt, \tag{2.40}$$

then we can write

$$< S_3(\vec{q},m) >|_{G=0} = \lim_{\epsilon \to 0} \frac{2\pi}{V_c} I(\epsilon), \tag{2.41}$$

and

$$< S_5^{ij}(\vec{q},m) >|_{G=0} = \lim_{\epsilon \to 0} \frac{4\pi}{3V_c} \left(\frac{I(\epsilon)}{2} \delta_{ij} - \frac{q_i\, q_j}{q^2} \right). \tag{2.42}$$

The second term in (2.42) is from the integral over the second term in (2.38). Using Eq.(2.4), the zero order Fourier component of S_{ij} is

$$\begin{aligned} S_{ij}(\vec{q},m)|_{G=0} &= \Sigma_j \; 3 < S_5^{ij}(\vec{q},m) >|_{G=0} - \delta_{ij} < S_3(\vec{q},m) >|_{G=0} \\ &= - \frac{4\pi}{V_c} \frac{q_i\, q_j}{q^2}, \end{aligned} \tag{2.43}$$

which is the quantity we are really interested in. The $I(\omega)$ canceled between $< S_5^{ij}(\vec{q},m) >|_{G=0}$ and $< S_3(\vec{q},m) >|_{G=0}$. Therefore $< E_p^i >$ can be written as:

$$< E_p^i > = \frac{1}{V_c} \int_{cell} E_p^i(r) \, dr^3$$

$$= \Sigma_{m,j} S_{ij}(\vec{q},m)|_{G=0} \cdot p_m^j$$

$$= -\frac{4\pi}{V_c} \Sigma_{m,j} \frac{q_i\, q_j\, p_m^j}{q^2}, \qquad (2.44')$$

or

$$< \vec{E}_p > = -\frac{4\pi}{V_c} \frac{\vec{q}}{|\vec{q}|} \Sigma_m \{ \frac{\vec{q}}{|\vec{q}|} \cdot \vec{p}_m \}, \qquad (2.44)$$

where, $\vec{p}_m$ is the dipole moment at the site of the m^{th} basis. Notice that $< \vec{E}_p >$ is along the direction of the wave vector, but does not depend on the magnitude of the wave vector. The macroscopic average field can then be written as:

$$< \vec{E}(\vec{q}) > = \vec{E}_{ext} - \frac{4\pi}{V_c} \frac{\vec{q}}{|\vec{q}|} \Sigma_m \{ \frac{\vec{q}}{|\vec{q}|} \cdot \vec{p}_m) \}, \qquad (2.45)$$

which is valid for any kind of crystal structure.

2.4 Discussions

In the beginning of this Chapter, we mentioned the conditional convergence of the dipole sums. The Born-Ewald method enables one to separate out this troublesome term, which is in Eq.(2.43) and gives the second term of Eq.(2.45). Physically, when the optical limit $q \to 0$ is taken, the value of the second term in Eq.(2.45) strongly depends on the direction in which $\vec{q}$ goes to zero. This in fact reflects the surface shape effect. So when $\vec{q}=0$, the second term in Eq.(2.45) is actually the depolarization field due to the surface polarization charges. For example with a slab shaped sample, the depolarization

field is well known to be $-4\pi P$. The second term in Eq.(2.45) gives this result when $\vec{q}$ is in the same direction as the polarization vector (i.e. the macroscopic average field), which is the longitudinal case, and taking the limit $\vec{q} \to 0$. Thus, for $\vec{q} = 0$ the situation must be considered with care since the dipole field $\vec{E}_p(\vec{q}=0)$ can take on any value depending on which direction the $\vec{q}$ goes to zero. We can partition this term to

$$\vec{E}_p(q=0) = -N\vec{P}+L\vec{P}, \tag{2.46}$$

where, N is the shape dependent depolarization factor[2,7,26] and corresponds to the G=0 term in the dipole sums. The depolarization factor N is extensively tabulated in the literature[27]. L is the so-called Lorentz factor which is only dependent on the crystal structure and corresponds to all G≠0 terms in the dipole sums. So at the $\vec{q}$=0 limit, the local field can be written as:

$$\begin{aligned} \vec{E}_L(\vec{q}=0) &= \vec{E}_{ext} - N\vec{P} + L\vec{P}, \\ &= \langle \vec{E}(\vec{q}=0) \rangle + L\vec{P}. \end{aligned} \tag{2.47}$$

The macroscopic average field in this limit can be written as

$$\langle \vec{E}(\vec{q}=0) \rangle = \vec{E}_{ext} - N\vec{P}. \tag{2.48}$$

However, the conditional convergence of the dipole sums does not occur for $\vec{q} \neq 0$. For small $\vec{q} > 0$, the dipole sum defined in Eq.(2.4)

is absolutely convergent, i.e. it has only one finite limit and does not depend on the order in which the sum is taken. Therefore the dipole field $\vec{E}_p(\vec{q}\neq 0)$ is not shape dependent, and the local field $\vec{E}_L(\vec{q})$ does not include the depolarization factor. This is the case we are going to calculate and discuss in Chapter III.

Let's consider a crystal with one atom per primitive cell, i.e. m = 1. We rewrite the dipole sum S_{ij} (which was defined by Eq.(2.4) and is a sum for all G) at the dipole site (by taking $\vec{r}=0$) to be two terms, one is the G=0 term (which is in Eq.(2.43)), and another term which is for all $G\neq 0$. The second term only depends on the crystal structure and is regular at $\vec{q}=0$. We will see later that this term is actually related to the L-factor, i.e. (for simplicity the variables m and $\vec{r}$ are left out in the following equations since they are for the special case of m=1 and $\vec{r}=0$)

$$\begin{aligned} S_{ij}(\vec{q}) &= S_{ij}(\vec{q})|_{G=0} + S_{ij}(\vec{q})|_{G\neq 0} \\ &= -\frac{4\pi}{V_c}\left(\frac{q_i q_j}{q^2}\right) + L_{ij}/V_c, \end{aligned} \tag{2.49}$$

where L_{ij} is independent of $\vec{q}$ for $|\vec{q}| \ll |\vec{G}|$. For a cubic crystal, we know that $L_{ij} = (4\pi/3)\delta_{ij}$. Eq.(2.49) then becomes

$$S_{ij}(\vec{q}) = \frac{4\pi}{3V_c}\left[\delta_{ij} - 3\left(\frac{q_i q_j}{q^2}\right)\right], \tag{2.50}$$

which is exactly the same as Cohen and Keffer[19] obtained by a different approach. From this equation, we see that the dipole sum

matrix S_{ij} is insensitive to the magnitude of q. However, the G=0 term depends on the direction of the $\vec{q}$ and the sums $S_5^{ij}(\vec{q},M,m')$ and $S_3(\vec{q},M,m')$ (Eq.(2.27) and Eq.(2.28)) depend on the magnitude and the direction of $\vec{q}$. Table 2.3 lists the dipole sums S_3, S_5^{ij} and S_{ij} for different values of q for the simple cubic crystal as a check. The results clearly demonstrate that Eq.(2.50) is satisfied. In fact, the insensitivity of S_{ij} to the magnitude of q is valid for any crystal structure, even non-cubic crystals. Table 2.4 shows the insensitivity of S_{ij} to the magnitude of q for the simple tetragonal (ST) structure (Fig. 2.1) with the lattice ratio c/a = 0.8. Therefore in the following calculations the local fields and the dielectric constants are insensitive to the magnitude of q.

We also want to point out here that S_{ij} can be evaluated at any arbitrary position in a unit cell. This capability can help us to calculate the local field at any arbitrary point in a unit cell (we will discuss this further in Chapter III). However, only S_{ij} at the dipole's site is related to the L-factor, which is a tensor in general (see Tables 2.3 and 2.4). The L-factor is originally defined by $L_{ij} = V_c \cdot S_{ij}(\vec{q}=0)|_{G\neq 0}$. However, since $S_{ij}(\vec{q})|_{G\neq 0}$ is regular at $\vec{q}=0$ and S_{ij} is insensitive to q for small $\vec{q}$, so $S_{ij}(\vec{q}=0)|_{G\neq 0} = S_{ij}(\vec{q}\neq 0)|_{G\neq 0}$. This is also shown in Table 2.4. From Eq.(2.43), if $\vec{q}$ is along the $\hat{k}$ direction only, then $S_{ij}(\vec{q}\neq 0)|_{G=0} = 0$ for i and $j \neq k$, even for non-cubic crystals. So $S_{ij}(\vec{q}\neq 0)|_{\text{all } G} = S_{ij}(\vec{q}\neq 0)|_{G\neq 0}$ for i and $j \neq k$. Therefore we can calculate the L-factor from $S_{ij}(\vec{q}\neq 0)|_{\text{all } G}$ for i and $j \neq k$. For a crystal with only one atom per primitive cell, we have

Table 2.3 The insensitivity of the magnitude of the wave vector for the dipole sum of a simple cubic structure. For wave vector $\vec{q}$ along the z direction, where q·a is dimensionless and a is the lattice constant. All the dipole sums are calculated at the dipole's site. $S_5^{i\neq j} = 0.0$ and $S_{i\neq j} = 0.0$ are not listed in the table.

q·a = 4.1931×	S_3	S_5^{11}	S_5^{22}	S_5^{33}	S_{11}	S_{22}	S_{33}
10^{-2}	48.9931	17.7273	17.7273	13.5386	4.1888	4.1888	-8.3773
10^{-3}	77.9271	27.3720	27.3720	23.1832	4.1888	4.1888	-8.3775
10^{-4}	106.8622	37.0170	37.0170	32.8282	4.1888	4.1888	-8.3776
10^{-6}	164.7324	56.3071	56.3071	52.1183	4.1888	4.1888	-8.3776

$L = S_{11}/a^3 = S_{22}/a^3 = \frac{4\pi}{3} \cong 4.1888$ (taking a^3 as unity).

Table 2.4 The insensitivity of the magnitude of the wave vector for the dipole sum of a simple tetragonal structure. The lattice ratio c/a = 0.8, and $\vec{q}$ is along the x direction. All dipole sums are calculated at the dipole's site. From Eq.(2.43), $S_{22}(\vec{q})|_{G=0} = S_{33}(\vec{q})|_{G=0} = 0$, so $S_{ii}(\vec{q})|_{\text{all } G} = S_{ii}(\vec{q})|_{G\neq 0} \equiv S_{ii}(\vec{q})$ for $i\neq 1$. $S_{i\neq j} = 0.0$ are not listed in the table.

q·a = 4.1931×	$S_{11}(\vec{q})\|_{\text{all } G}$	$S_{22}(\vec{q})$	$S_{33}(\vec{q})$
10^{-2}	-12.4404	3.2675	9.1729
10^{-5}	-12.4404	3.2675	9.1729
q=0,G≠0		3.2675	9.1729

$S_{11}(q=0)|_{G\neq 0} = S_{11}(\vec{q})|_{\text{all } G} - S_{11}(\vec{q})|_{G=0} = -12.4404+4\pi/0.8 = 3.2675$. So $L_{xx}=L_{yy}=2.6140$, $L_{zz}=7.3383$ and $L_{xx}+L_{yy}+L_{zz}=4\pi$. $S_{11}+S_{22}+S_{33}=0$ is also satisfied for both $\vec{q}=0$ and $\vec{q}\neq 0$ case.

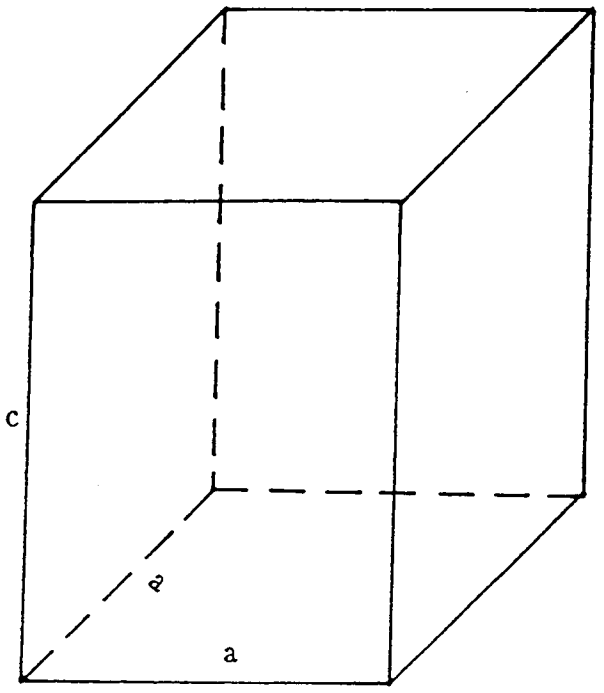

Figure 2.1 Simple tetragonal crystal structure.

$$L_{ij} \equiv V_c \cdot S_{ij}(\vec{q}=0)|_{G\neq 0} = V_c \cdot S_{ij}(\vec{q}\neq 0)|_{G\neq 0} \text{ with } |\vec{q}| << |\vec{G}| \qquad (2.51)$$
$$= V_c \cdot S_{ij}(\vec{q}\neq 0)|_{\text{all } G} \text{ (with i and j } \neq k).$$

However, if there are m basis atoms per primitive cell, since the local field at each atom's site are the same in the atomic dipole model (S_{ij}s are the coefficients of the coupled self-consistent local field equations, we will discuss this point in Chapter III), so we can simply add them together to have

$$nL_{ij} = V_c \cdot \Sigma_{m'} S_{ij}(\vec{q},m,m')|_{\text{all } G} \text{ (with i and j } \neq k), \qquad (2.52)$$

where n is the number of atoms per unit cell. For the bond dipole model, the L -factor is not so easy to obtain since the local fields at each bond dipole's site may be different, we can not simply add the S_{ij} together for different m. The difference between the atomic model and the bond dipole model will be further discussed in Chapter III.

Since the self contribution has been excluded in the dipole field, $\vec{E}_p$ satisfies $\nabla \cdot \vec{E}_p = 0$ anywhere in the crystal (or equivalently the potential ψ due to all other dipoles satisfies $\nabla^2 \psi = 0$). This result gives (in the principle axis)

$$(S_{11}+S_{22}+S_{33})\ \nabla \cdot \vec{P} = 0. \qquad (2.53)$$

For the $\vec{q}\neq 0$ case, $\nabla \cdot \vec{P} = \vec{q} \cdot \vec{P}$ which in general $\neq 0$, so we must have

$$S_{11}+S_{22}+S_{33}=0. \tag{2.54}$$

This result can also be observed in Tables 2.3 and 2.4. For the $\vec{q}=0$ case,

$$\nabla\cdot\vec{P} = \begin{cases} 0, & \text{off dipole's site} \\ 4\pi\rho_d, & \text{at the dipole's site,} \end{cases} \tag{2.55}$$

where ρ_d is the induced polarization charge density. So even for the $\vec{q}=0$ case, Eq.(2.54) holds at the dipole's site. Then, using the definition of L-factor in Eq.(2.51), Eq.(2.43), and Eq.(2.54), we have

$$L_{11}+L_{22}+L_{33}= 4\pi. \tag{2.56}$$

This result is identical to the results obtained by Mueller[28] and later by Colpa[7] and Purvis and Taylor[2](differing in definition by a factor 4π), but in this work it is from an entirely different approach. We obtained Eq.(2.56) without any additional assumptions. Also the method we used here for calculating the L-factor seems much simpler than the method of Purvis and Taylor[2] who take the $\vec{q}=0$ case in the dipole sum, choose special sample shapes and carefully order the summations to avoid the conditional convergence.

CHAPTER III

METHOD OF SELF-CONSISTENT LOCAL FIELD CALCULATIONS

3.1 Two Models of Local Dipoles

From Chapter I and II we know that the local field in a solid is the external field plus the dipole sum, which depends on the dipole moments residing on the sites in the crystal. The dipole moment is proportional to the self-consistent local field determined from the local dipole model used. Here, we use two kinds of dipole models: (1) the Atomic Dipole Model (ADM) in which the polarizable charge distribution is placed at the atomic sites, and (2) the Bond Dipole Model (BDM) in which the polarizable charge distribution is placed at middle of the bonds between the atoms and is only polarizable along the bonds.

For cubic materials, the atomic dipole moment is defined as the atomic polarizability times the local field at atom's position:

$$\vec{p}_{ADM}(m) = \alpha \cdot \vec{E}_L(m). \tag{3.1}$$

For the diamond and zinc blende structure, shown in Figure 3.1, we have two atomic dipoles in each primitive cell, which are located at (0,0,0) and $(\frac{1}{4},\frac{1}{4},\frac{1}{4})$ in the unit cell, with the lattice constant a taken to be unity. As we have discussed in Chapter I, the atomic dipole model has been widely used in the local field

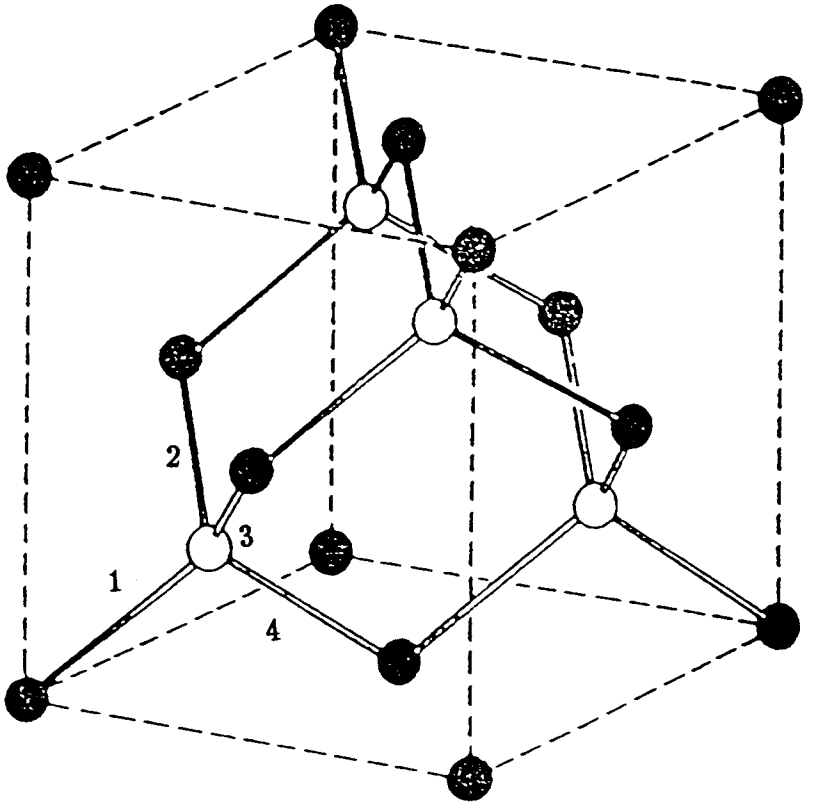

Figure 3.1 Crystal structure of zinc blende, showing the tetrahedral bond arrangement. If the two kinds of atoms are the same, it is the diamond structure. The numbers on the bonds indicate the four bond dipoles.

corrections in the past. It was assumed that the medium has been uniformly polarized and the L-L theory of the susceptibility,

$$\chi_{L\text{-}L} = \frac{N\,a}{1 - \frac{4\pi}{3} N\,a} \qquad (3.2)$$

is based on this model.

The bond dipole model arises from the overlap of quantum sp^3 hybridized orbital theory[29,30,31,32] along the bond directions. Figure 3.2 shows the bond orbitals in the linear combination of atomic orbitals (LCAO) quantum theory. The normalized wave function of the sp^3 hybrids and the directions in which the charge density is greatest are:

$$|h_1> = \frac{1}{2}\,[\,|s> + |p_x> + |p_y> + |p_z>] \text{ with } [111] \text{ orientation},$$
$$|h_2> = \frac{1}{2}\,[\,|s> + |p_x> - |p_y> - |p_z>] \text{ with } [1\bar{1}\bar{1}] \text{ orientation},$$
$$|h_3> = \frac{1}{2}\,[\,|s> - |p_x> + |p_y> - |p_z>] \text{ with } [\bar{1}1\bar{1}] \text{ orientation},$$
$$|h_4> = \frac{1}{2}\,[\,|s> - |p_x> - |p_y> + |p_z>] \text{ with } [\bar{1}\bar{1}1] \text{ orientation}.$$

The sp^3 hybridized orbitals give the four tetrahedral directions, which will be the direction of the bonds. The magnitude of the bond dipole moment is proportional to the projected local field at the middle of the bond along the bond directions. The i^{th} component of the bond dipole moment is defined as:

$$p^i_{BDM}(m) = a\,\Sigma_k\,\{E^k_L \cdot d^k(m)\}\,d^i(m), \quad (i, k=1..3), \qquad (3.3)$$

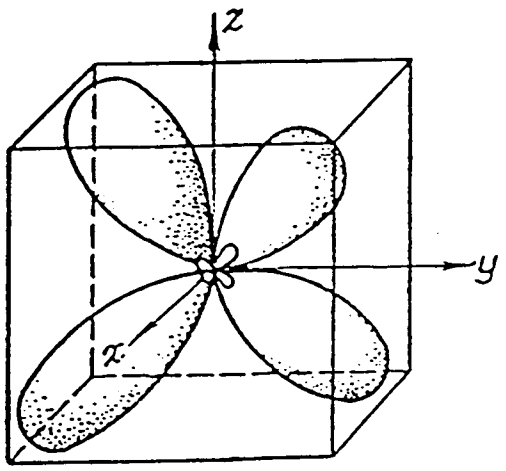

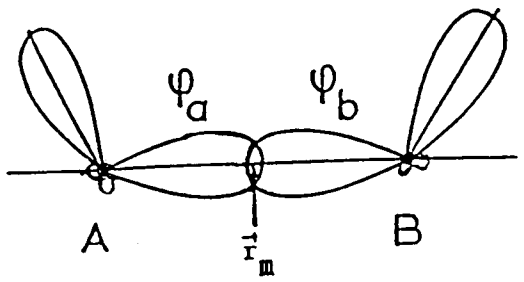

Figure 3.2 The sp^3 hybridized bond orbitals in LCAO theory.

where the bond polarizability a is assumed isotropic and independent of field, $d^i(m)$ is the unit direction of the m^{th} bond, and m=1..4.

There are four bond directions in the tetrahedral structure given by:

$$\begin{aligned}
\vec{d}(1) &= \frac{1}{\sqrt{3}}\,(1,1,1) \\
\vec{d}(2) &= \frac{1}{\sqrt{3}}\,(1,\bar{1},\bar{1}) \\
\vec{d}(3) &= \frac{1}{\sqrt{3}}\,(\bar{1},1,\bar{1}) \\
\vec{d}(4) &= \frac{1}{\sqrt{3}}\,(\bar{1},\bar{1},1).
\end{aligned} \tag{3.4}$$

For the diamond and zinc blende structure, we have four bond dipoles per primitive cell, along the four directions. They are located at: (0.125, 0.125, 0.125), (0.125, 0.375, 0.375), (0.375, 0.125, 0.375), (0.375, 0.375, 0.125), which are indicated in Fig.(3.1).

3.2 Self-Consistent Local Field Calculations:

In this section, we will calculate two kinds of self-consistent local fields: (1) at the dipole sites and (2) at an arbitrary position in the unit cell which is off a dipole's site.

The self-consistent local fields at the dipole sites are determined by a set of coupled linear equations[33,34,35,36,37]. Even for a simple cubic crystal with only one atom per unit cell, the three components of the local field are still coupled. The minimum dimension of the matrix is equal to three times the number of dipoles per primitive cell.

The local field at the m^{th} dipole's site is equal to the

external field plus the contribution of the fields from all the other dipoles at this point, except the self contribution. We will use the equations developed in Chapter II to calculate the dipole sums at the dipole's site. Each dipole moment is proportional to the local field at that point. The assumption of a field independent polarizability simplifies the calculation to coupled linear equations. However, an assumption of a non-linear field dependent polarizability, although introducing coupled non-linear equations, lies within the scope of the present formalism and constitutes an interesting problem in itself.

We write the i^{th} component of the local field at site M (which is on one of the m^{th} dipole sublattice) as:

$$E_L^i(\vec{q},M) = E_{ext}^i + \Sigma_{m',j} S_{ij}(\vec{q},M,m') \cdot p_{m'}^j, \qquad (3.5)$$

where $m'=1..m$ and M runs from 1 to m. The sums $S_{ij}(\vec{q},M,m')$ are the m'^{th} sublattice at the M dipole's site in a primitive cell. Notice that only when $m = m'$ are the sums $S_{ij}(\vec{q},M,m)$ over an imperfect sublattice (the self contribution has been excluded). The parameter $\vec{q}$ in the local field on the left hand side of Eq.(3.5) indicates that the limit q = 0 has NOT been taken, so the dipole sums are absolutely convergent and do not include surface effects (or equivalently the depolarization factor). From this equation we can see that using different dipole models will result in different equations. In each model we need to calculate $S_{ij}(\vec{q},M,m')$ for $m'=1..m$ and for M at all the sites (M = 1..m) to get the right coefficients for the local

field equations.

For the atomic dipole model, we shall use the ADM dipole moment, substitute Eq.(3.1) into Eq.(3.5), then the i^{th} component of the local field equation at the m^{th} site is:

$$E_L^i(\vec{q},M) = E_{ext}^i + \alpha \Sigma_{m',j} S_{ij}(\vec{q},M,m') \cdot E_L^j(\vec{q},m'), \quad M=1..m. \qquad (3.6)$$

We shall write out the local field equations at all the different dipole sites in the primitive cell, i.e. M = 1..m for a total of m dipoles in a primitive cell. This gives us the coupled linear equations for the local fields. For the diamond and zinc blende structure there are two atoms per primitive cell so we have M = 1, 2. From Eq.(3.6), we notice that the three components of the local fields are coupled to each other as well. Therefore, we have six linear coupled equations to solve for the atomic dipole model for a cubic tetrahedral structure.

For the bond dipole model, we shall use the BDM dipole moment, substitute Eq.(3.3) into Eq.(3.5). Consequently the i^{th} component of the local field equation at the m^{th} site is:

$$E_L^i(\vec{q},M) = E_{ext}^i + \alpha \Sigma_{m',k} E_L^k(\vec{q},m') d^k(m') \cdot \Sigma_j S_{ij}(\vec{q},M,m') \cdot d^j(m'), \quad (3.7)$$

where M = 1..m and $d^i(m)$ is the i^{th} component of the unit vector of the bond direction at the m^{th} site. For the diamond and zinc blende structure there are four bond dipoles per primitive cell, which are along the four bond directions. Since the i^{th} component of the local

field at the m^{th} dipole is not only coupled to all the other dipole fields in the primitive cell, but also coupled to its own other components, we have twelve linear coupled equations to solve for the bond dipole model for a cubic tetrahedral structure.

The matrix form of the linear coupled equations in both models can be written as:

$$E_L = (I - A)^{-1} E_{ext}, \tag{3.8}$$

where E_L is the vector of the local fields, $(I - A)$ is the coefficient matrix for the local fields, and E_{ext} is the constant external field vector. The elements of the coefficient matrix A_{ij} depends on which model is used and results of $S_{ij}(\vec{q},M,m')$ as well as the dipole polarizability per unit volume (α/a^3). The self-consistent local fields can be obtained by solving these linear equations. We know that S_{ij} depends on crystal structure. For a given crystal structure, the dipole sums are fixed and the matrix A scales with the polarizability α/a^3. Figure 3.3 is a schematic representation of the self-consistent local field as a function of the polarizability per unit cell α/a^3 with a given crystal structure. Notice the divergence in the local field which we may call the local field catastrophe, corresponds to a phase transition happening at that point. For large α/a^3, the local field associated with a charge in the lattice is so strong that it displaces the charge from its usual position until it reaches a new equilibrium. The new state of

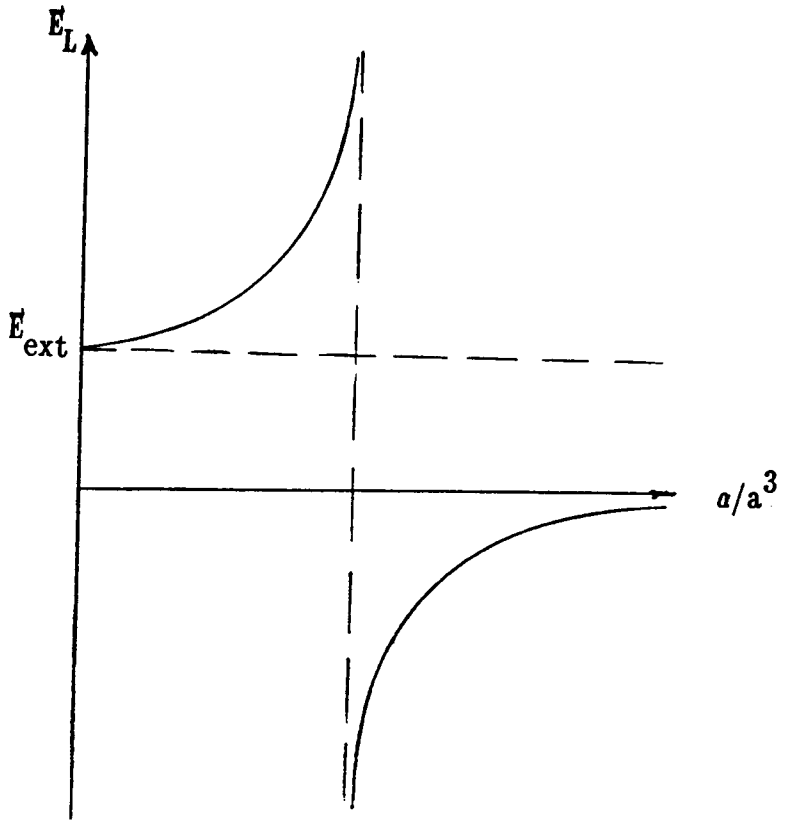

Figure 3.3 Schematic diagram of the self-consistent local field as function of the polarizability.

the solid permits a finite polarization even in zero applied field which is called the ferroelectric state.

For the atomic dipole model, the local field at the M dipole site has the form (in principle axis and $\vec{q}$ is along the k)

$$E_L^j(\vec{q}\neq 0,M) = \frac{E_{ext}^j}{(1 - a\Sigma_{m'}S_{jj}(\vec{q},M,m'))}, \tag{3.9a}$$

$$E_L^j(\vec{q}=0,M) = \frac{E_{ext}^j}{(1 - L_{jj}Na)}, \tag{3.9b}$$

where N=n/abc, n is the number of atoms per unit cell, and a, b, and c are the lattice constants. From Chapter II we have shown that when $\vec{q}$ is along the k direction, for a crystal which has M basis atoms per primitive cell, $\Sigma_{m'}S_{jj}(\vec{q},M,m') = nL_{jj}/V_c$ for $j\neq k$, but $\Sigma_{m'}S_{kk}(\vec{q},M,m') = (nL_{kk}-4\pi)/V_c$. So the local field depends on the direction of $\vec{q}$ since S_{ij} depends on the direction of $\vec{q}$. So we find that the relation between the $\vec{q}=0$ local field and the $\vec{q}\neq 0$ local field is (For simplicity the variable M is ignored since for the ADM the local field at different atomic sites is the same),

$$E_L^i(\vec{q}\neq 0)=E_L^i(\vec{q}=0) \text{ for } i\neq k, \text{ and } E_L^k(\vec{q}\neq 0)\neq E_L^k(\vec{q}=0).$$

Thus, the difference between the $\vec{E}_L(\vec{q}=0)$ and $\vec{E}_L(\vec{q}\neq 0)$ occurs only in the component of the local field which is along $\vec{q}$'s direction.

The i^{th} component of the polarization of the material is defined as the sum of all the dipoles in a primitive cell divided by the

volume of the cell:

$$P^i = \Sigma_m \frac{p_m^i}{V_c}, \tag{3.10}$$

where the dipole moment p_m^i is proportional to the local field as calculated above. We also can write the linear polarization as:

$$P^i = \Sigma_j \chi_{ij} < E^j >, \tag{3.11}$$

where $< E^j >$ is the j^{th} component of macroscopic average field defined by Eq.(2.45). The linear susceptibility χ_{ij} is therefore defined by:

$$\chi_{ij} = \frac{\partial P^i}{\partial < E^j >}, \tag{3.12}$$

The dielectric constant is defined by:

$$\epsilon_{ij} = \delta_{ij} + 4\pi\chi_{ij}. \tag{3.13}$$

Considering the $\vec{q}\neq 0$ case, for ADM we use Eq.(3.1) in Eq.(3.10) where the local field is defined by Eq.(3.9a). Notice that the local field $E_L^k(\vec{q}\neq 0) \neq E_L^k(\vec{q}=0)$ for k along $\vec{q}$ direction and $\Sigma_m, S_{kk}(\vec{q},M,m) = (nL_{kk} - 4\pi)/V_c$. Then, from Eq.(3.12) even for $\vec{q}\neq 0$ case the susceptibility in ADM has the form

$$\chi_{ij} = \frac{N\alpha}{1 - L_{ij}N\alpha}. \tag{3.14}$$

Eq.(3.14) tells us that the susceptibility with $\vec{q}\neq 0$ is the same as with q=0 in ADM, i.e. $\chi_{ij}(\vec{q}\neq 0) = \chi_{ij}(\vec{q}=0)$ for small $\vec{q}$ and it is independent of $\vec{q}$'s direction. So in a crystal for $\vec{q}\neq 0$, the local fields are scaled by S_{ij} but the susceptibility is scaled by L_{ij}. If we are interested in how the dielectric property changes in a light scattering problem, then the L-factor is more important.

We also want to calculate the local field at an arbitrary position off the dipole's site $\vec{r}$, (i.e. $\vec{r} \neq \vec{r}_\ell$ or $\vec{r}_m$) in the unit cell. The local field at $\vec{r}$ is the external field plus the dipole fields at $\vec{r}$, where the dipole sums are over perfect lattices.

$$E_L^i(\vec{q},\vec{r}) = E_{ext}^i + \Sigma_{m,j}\, S_{ij}(\vec{q},\vec{r},m)p_m^j, \tag{3.15}$$

where $S_{ij}(\vec{q},\vec{r},m)$ was defined in (2.4) and p_m^j is the j component of the m^{th} basis dipole moment which is proportional to the local field at the dipole's site. We derived the solution to the local field at the dipole's site previously. For simplicity, we only consider the atomic dipole model, Eq.(3.15) then can be written as

$$\begin{aligned} E_L^i(\vec{q},\vec{r}) &= E_{ext}^i + \Sigma_{m,j}\alpha\cdot S_{ij}(\vec{q},\vec{r},m)E_L^j(\vec{q},m) \\ &= E_{ext}^i + \Sigma_{m,j}\alpha\cdot S_{ij}(\vec{q},\vec{r},m)\frac{E_{ext}^j}{(1 - \alpha\Sigma_{m'}S_{jj}(\vec{q},M,m'))}. \end{aligned} \tag{3.16}$$

We can choose $\vec{E}_{ext}$ to only have an i^{th} component, so we have:

$$E_L^i(\vec{q},\vec{r}) = E_{ext}^i \cdot \{\frac{1 - a\Sigma_m[S_{ii}(\vec{q},M,m) - S_{ii}(\vec{q},\vec{r},m)]}{1 - a\Sigma_m S_{ii}(\vec{q},M,m)}\},\ i=1..3. \quad (3.17)$$

We can use Eq.(3.17) to calculate the self consistent local field at an arbitrary position off the dipole's site $\vec{r}$ in the unit cell for ADM only.

3.3 Results and Discussions for the Cubic Tetrahedral Structure:

All of the following calculations are based on the long wave length assumption. For simplification, we always take the external field as a unit vector and the magnitude of the wave vector q in the crystal times the lattice constant a is about $q \cdot a \cong 4*10^{-3}$, which is dimensionless. From the discussion in Chapter II, we have already shown that the local field and the susceptibility calculation results are insensitive to the magnitude of q for $|\vec{q}| << |\vec{G}|$. Tables 3.1 through 3.5 list the calculated results for the diamond structure using ADM. Notice that the calculated results of the local fields at each atomic dipole's site are the same, and the macroscopic average field is equal to the external field because in the second term, Σ_m $\vec{q} \cdot \vec{p}_m$ is zero. Those tables can be reproduced exactly by using Eq.(3.9) where $L=4\pi/3$, n = 8 which corresponds to eight atoms per unit cell for diamond structure. This was done to check the validity of the computer program. In Table 3.1, we notice that the local field and the susceptibility become negative after the atomic polarizability a/a^3 reaches a certain value a_c/a^3. From the L-L relation, if we take the denominator $\{1 - (4\pi/3)Na\} > 0$, then we

Table 3.1 ADM in the diamond structure. $\vec{q}$ is along the [001] direction and $\vec{E}_{ext}$= (1,0,0). The self-consistent local fields at each dipole's site ($E_{Li}(m)$: m indicates the number of the dipoles) and the susceptibility. $\Sigma_m \hat{q}\cdot\vec{p}_m$ is part of the second term of the macroscopic average field and $\hat{q}$ is the unit wave vector.

a/a^3	$\Sigma_m \hat{q}\cdot\vec{p}_m$	$E_{Lx}(1)$ $E_{Lx}(2)$	$E_{Ly}(1)$ $E_{Ly}(2)$	$E_{Lz}(1)$ $E_{Lz}(2)$	χ
0.00	0.0000	1.0000 1.0000	0.0000 0.0000	0.0000 0.0000	0.0000
0.01	0.0000	1.5040 1.5040	0.0000 0.0000	0.0000 0.0000	0.1203
0.02	0.0000	3.0321 3.0321	0.0000 0.0000	0.0000 0.0000	0.4851
0.03	0.0000	-188.6792 -188.6792	0.0000 0.0000	0.0000 0.0000	-45.2830
0.04	0.0000	-2.9377 -2.9377	0.0000 0.0000	0.0000 0.0000	-0.9401
0.05	0.0000	-1.4803 -1.4803	0.0000 0.0000	0.0000 0.0000	-0.5922

Table 3.2 ADM in the diamond structure. $\vec{q}$ is along the [001] direction and $\vec{E}_{ext}$= $(1/\sqrt{2},1/\sqrt{2},0)$. The self-consistent local fields at each dipole's site ($E_{Li}(m)$: m indicates the number of the dipoles) and the susceptibility. $\Sigma_m \hat{q}\cdot\vec{p}_m$ is part of the second term of the macroscopic average field and $\hat{q}$ is the unit wave vector.

a/a^3	$\Sigma_m \hat{q}\cdot\vec{p}_m$	$E_{Lx}(1)$ $E_{Lx}(2)$	$E_{Ly}(1)$ $E_{Ly}(2)$	$E_{Lz}(1)$ $E_{Lz}(2)$	χ
0.00	0.0000	0.7071 0.7071	0.7071 0.7071	0.0000 0.0000	0.0000
0.01	0.0000	1.0635 1.0635	1.0635 1.0635	0.0000 0.0000	0.1203
0.02	0.0000	2.1440 2.1440	2.1440 2.1440	0.0000 0.0000	0.4851
0.025	0.0000	4.3581 4.3581	4.3581 4.3581	0.0000 0.0000	1.2327

Table 3.3 ADM in the diamond structure. $\vec{q}$ is along the $[1\bar{1}0]$ direction and $\vec{E}_{ext}$= $(1/\sqrt{3},1/\sqrt{3},1/\sqrt{3})$. The self-consistent local fields at each dipole's site and the susceptibility.

a/a^3	$\Sigma_m \hat{q}\cdot\vec{p}_m$	$E_{Lx}(1)$ $E_{Lx}(2)$	$E_{Ly}(1)$ $E_{Ly}(2)$	$E_{Lz}(1)$ $E_{Lz}(2)$	χ
0.00	0.0000	0.5774 0.5774	0.5774 0.5774	0.5774 0.5774	0.0000
0.01	0.0000	0.8683 0.8683	0.8683 0.8683	0.8683 0.8683	0.1203
0.02	0.0000	1.7507 1.7507	1.7507 1.7507	1.7507 1.7507	0.4851
0.025	0.0000	3.5587 3.5587	3.5587 3.5587	3.5587 3.5587	1.2327

Table 3.4 ADM in the diamond structure. $\vec{q}$ is along the [1$\bar{1}$0] direction and $\vec{E}_{ext}$= (1/$\sqrt{2}$,1/$\sqrt{2}$,0). The self-consistent local fields at each dipole's site ($E_{Li}(m)$: m indicates the number of the dipoles) and the susceptibility. $\Sigma_m \hat{q}\cdot\vec{p}_m$ is part of the second term of the macroscopic average field and $\hat{q}$ is the unit wave vector.

a/a^3	$\Sigma_m \hat{q}\cdot\vec{p}_m$	$E_{Lx}(1)$ $E_{Lx}(2)$	$E_{Ly}(1)$ $E_{Ly}(2)$	$E_{Lz}(1)$ $E_{Lz}(2)$	χ
0.00	0.0000	0.7071 0.7071	0.7071 0.7071	0.0000 0.0000	0.0000
0.01	0.0000	1.6035 1.6035	1.6035 1.6035	0.0000 0.0000	0.1203
0.02	0.0000	2.1441 2.1441	2.1441 2.1441	0.0000 0.0000	0.4852
0.025	0.0000	4.3585 4.3585	4.3585 4.3585	0.0000 0.0000	1.2328

Table 3.5 ADM in the diamond structure. $\vec{q}$ is along the [1$\bar{1}$0] direction and $\vec{E}_{ext}$= (0,0,1). The self-consistent local fields at each dipole's site and the susceptibility.

a/a^3	$\Sigma_m \hat{q}\cdot\vec{p}_m$	$E_{Lx}(1)$ $E_{Lx}(2)$	$E_{Ly}(1)$ $E_{Ly}(2)$	$E_{Lz}(1)$ $E_{Lz}(2)$	χ
0.00	0.0000	0.0000 0.0000	0.0000 0.0000	1.0000 1.0000	0.0000
0.01	0.0000	0.0000 0.0000	0.0000 0.0000	1.5040 1.5040	0.1203
0.02	0.0000	0.0000 0.0000	0.0000 0.0000	3.0322 3.0322	0.4852
0.05	0.0000	0.0000 0.0000	0.0000 0.0000	6.1636 6.1636	1.2327

have $\alpha/a^3 < 0.02984$, by taking n = 8. As mentioned above for $\alpha \geq \alpha_c$ we presume a phase transition of some kind and that the L-L relation is no longer valid. The susceptibility is independent of the direction of the polarization of the external field which is shown in all the tables, which can also be reproduced by Eq.(3.14) and taking $L=4\pi/3$ and n=8. Table 3.6 and 3.7 give the same calculations for the zinc blende structure using the ADM for which we have two kinds of atomic polarizabilities. We have also obtained the isotropic property of the linear dielectric constant for zincblende structure, and we have the same local fields at different atom's site. This is due to the assumption of the ADM which supposes that the medium is uniformly polarized. The calculated results satisfy the L-L formula by taking an average of the two polarizabilities $\alpha = (\alpha_1 + \alpha_2)/2$. The $S_{ij}(\vec{q},M,m')$ (at the M dipole's site) for the diamond and the zinc blende crystal for M=1 is listed in Appendix 0, from which we can see that $S_{ij}(\vec{q},M,m')$ are the same for different m'. Since for the ADM the local fields are the same at each dipole's site, we find for the the diamond and zinc blende structure the L-factor is $8L=\Sigma_{m'=1,2}S_{11}(\vec{q},M,m')$, where 8 is the number of atomic dipoles per unit cell and we find that L is exactly $4\pi/3$. Table 3.8 gives the comparison of the susceptibility from the self consistent calculation using ADM and from the L-L formula. In figure 3.4 the linear susceptibility as a function of the atomic polarizability for both the self-consistent calculation method and the L-L relation are shown.

Table 3.6 ADM in the zinc blende structure. $\vec{q}$ is along the [001] direction and $\vec{E}_{ext}$= $(1/\sqrt{2},1/\sqrt{2},0)$. The self-consistent local fields at each dipole's site ($E_{Li}(m)$: m indicates the number of the dipoles) and the susceptibility. There are two kinds of atomic polarizabilities, a_1 and a_2.

a_1/a^3	a_2/a^3	$\Sigma_m \hat{q}\cdot\vec{p}_m$	$E_{Lx}(1)$ $E_{Lx}(2)$	$E_{Ly}(1)$ $E_{Ly}(2)$	$E_{Lz}(1)$ $E_{Lz}(2)$	χ
0.005	0.006	0.0000	0.8669 0.8669	0.8669 0.8669	0.0000 0.0000	0.0539
0.015	0.011	0.0000	1.2529 1.2529	1.2529 1.2529	0.0000 0.0000	0.1843
0.020	0.016	0.0000	1.7819 1.7819	1.7819 1.7819	0.0000 0.0000	0.3629

Table 3.7 ADM in the zinc blende structure. $\vec{q}$ is along the $[1\bar{1}0]$ direction and $\vec{E}_{ext}$= (0,0,1). The self-consistent local fields at each dipole's site ($E_{Li}(m)$: m indicates the number of the dipoles) and the susceptibility. There are two kinds of atomic polarizabilities, a_1 and a_2.

a_1/a^3	a_2/a^3	$\Sigma_m \hat{q}\cdot\vec{p}_m$	$E_{Lx}(1)$ $E_{Lx}(2)$	$E_{Ly}(1)$ $E_{Ly}(2)$	$E_{Lz}(1)$ $E_{Lz}(2)$	χ
0.005	0.006	0.0000	0.0000 0.0000	0.0000 0.0000	1.2260 1.2260	0.0539
0.015	0.011	0.0000	0.0000 0.0000	0.0000 0.0000	1.7719 1.7719	0.1843
0.020	0.016	0.0000	0.0000 0.0000	0.0000 0.0000	2.5201 2.5201	0.3629

Table 3.8 ADM. Comparison of the susceptibility from the self-consistent local field calculation ($\chi_{sc\ell}$) and from the L-L relation (χ_{L-L}) for the diamond and zinc blende structure.

a/a^3	$\chi_{sc\ell}$	χ_{L-L}
0.000	0.0000	0.0000
0.005	0.0481	0.0481
0.010	0.1203	0.1203
0.015	0.2413	0.2413
0.020	0.4852	0.4852
0.025	1.2327	1.2327
0.030	-45.2830	-45.2830
0.040	-0.9401	-0.9401
0.050	-0.5922	-0.5922

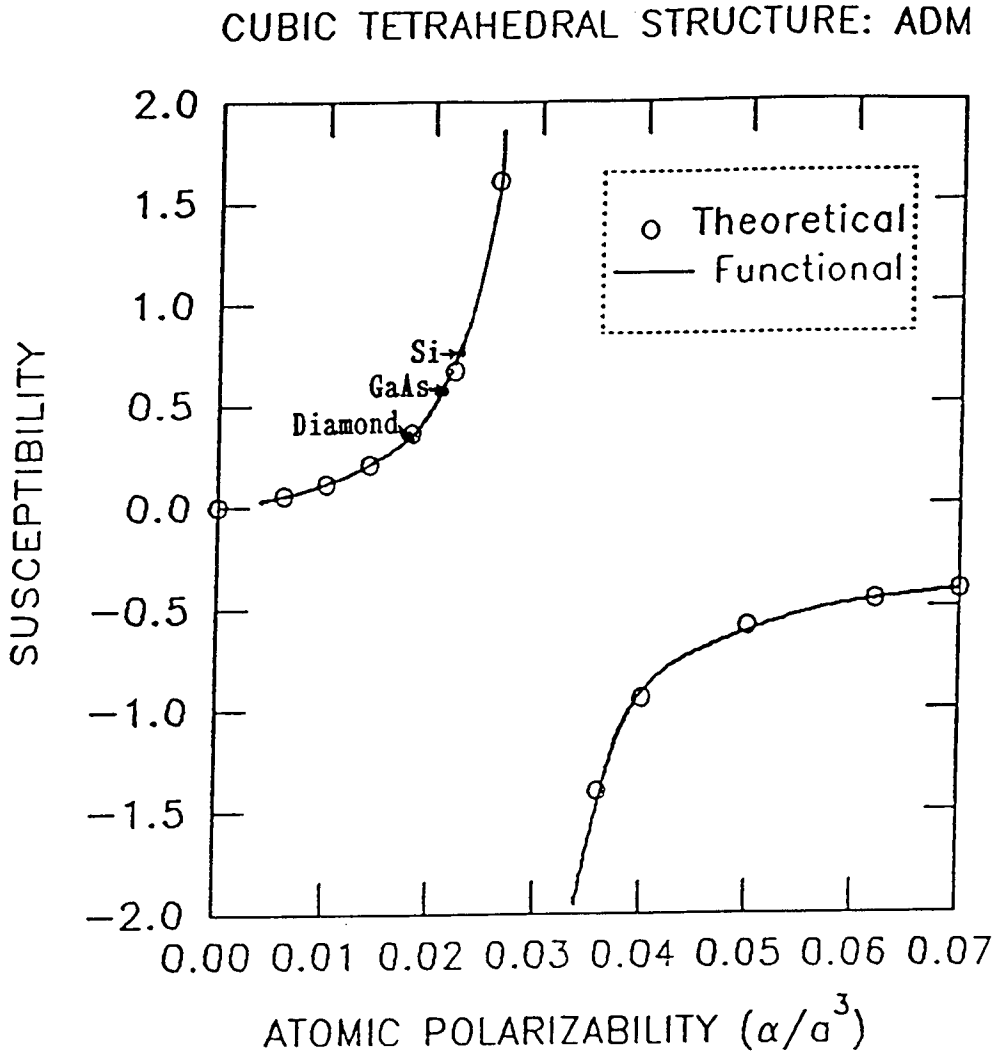

Figure 3.4 ADM. Plot of susceptibility vs atomic polarizability for the diamond and zinc blende structure from the self-consistent calculation and using the functional form.

Tables 3.9 through 3.13 list the self consistent calculations using the BDM. We can see the isotropic property of the susceptibility from those tables. However, in the BDM the local fields at each dipole's site are not the same, because the sp^3 bonds are very anisotropic. By studying the behavior of the susceptibility as a function of the bond polarizability, we found that the susceptibility vs bond polarizability has the following functional form:

$$\chi = \frac{n\ \alpha/a^3}{3(1 - 5.2515\ n\ \alpha/a^3)} \text{ (with } \sigma=0.0032), \qquad (3.18)$$

where σ is the standard deviation for $\chi > 0$ and n is the number of dipoles in one unit cell. For the diamond and zinc blende structure n=16. The factor 3 is a geometric average factor which comes from the bond orientation. We notice that the L-factor 5.2515 is not equal to $\frac{4\pi}{3}$ for BDM, even for cubic crystals. The dipole sums $S_{ij}(\vec{q},M,m)$ for M=1 using BDM is also listed in Appendix D. From these results we can see that if the local fields at the bond dipole's site were the same, then, we could have $16L=\Sigma_{m=1..4}S_{ij}(\vec{q},M,m)$ and still get $L = \frac{4\pi}{3}$. However, since the local fields are not the same at each bond dipole's site, we do not find the L-factor for the BDM so easily. It can be found by fitting the calculated data of the susceptibility. Therefore, we may not call the number 5.2515 a L-factor, since it is an empirical factor. Table 3.14 compares the results from the functional form Eq.(3.18)

Table 3.9 BDM in the cubic tetrahedral structure. $\vec{q}$ is along the [001] and $\vec{E}_{ext}$= (1,0,0). The self-consistent local fields at each dipole's site ($E_{Li}(m)$: m indicates the number of the dipoles) and the susceptibility. $\Sigma_m \hat{q}\cdot\vec{p}_m$ is part of the second term in the macroscopic average field, $\hat{q}$ is the unit wave vector.

a/a^3	$\Sigma_m \hat{q}\cdot\vec{p}_m$	$E_{Lx}(1)$ $E_{Lx}(2)$ $E_{Lx}(3)$ $E_{Lx}(4)$	$E_{Ly}(1)$ $E_{Ly}(2)$ $E_{Ly}(3)$ $E_{Ly}(4)$	$E_{Lz}(1)$ $E_{Lz}(2)$ $E_{Lz}(3)$ $E_{Lz}(4)$	χ
0.000	0.0000	1.0000 1.0000 1.0000 1.0000	0.0000 0.0000 0.0000 0.0000	0.0000 0.0000 0.0000 0.0000	0.0000
0.005	0.0000	1.5251 1.5251 1.5251 1.5251	0.0996 -0.0996 -0.0996 0.0996	0.0996 -0.0996 0.0996 -0.0996	0.0460
0.010	0.0000	4.8101 4.8101 4.8101 4.8101	0.7230 -0.7230 -0.7230 0.7230	0.7230 -0.7230 0.7230 -0.7230	0.3337
0.015	0.0000	-2.5104 -2.5104 -2.5104 -2.5104	-0.6661 0.6661 0.6661 -0.6661	-0.6661 0.6661 0.6661 0.6661	-0.3074
0.025	0.0000	-0.3836 -0.3836 -0.3836 -0.3836	-0.2626 0.2626 0.2626 -0.2626	-0.2626 0.2626 -0.2626 0.2626	-0.1212

Table 3.10 BDM in the cubic tetrahedral structure. $\vec{q}$ is along the [001] and $\vec{E}_{ext}$= $(1/\sqrt{2},1/\sqrt{2},0)$. The self-consistent local fields at each dipole's site ($E_{Li}(m)$: m indicates the number of the dipoles) and the susceptibility. $\Sigma_m \hat{q}\cdot\vec{p}_m$ is part of the second term in the macroscopic average field, $\hat{q}$ is the unit wave vector.

a/a^3	$\Sigma_m \hat{q}\cdot\vec{p}_m$	$E_{Lx}(1)$ $E_{Lx}(2)$ $E_{Lx}(3)$ $E_{Lx}(4)$	$E_{Ly}(1)$ $E_{Ly}(2)$ $E_{Ly}(3)$ $E_{Ly}(4)$	$E_{Lz}(1)$ $E_{Lz}(2)$ $E_{Lz}(3)$ $E_{Lz}(4)$	χ
0.000	0.0000	0.7071 0.7071 0.7071 0.7071	0.7071 0.7071 0.7071 0.7071	0.0000 0.0000 0.0000 0.0000	0.0000
0.005	0.0000	1.1489 1.0079 1.0079 1.1489	1.1489 1.0079 1.0079 1.1489	0.1409 0.0000 0.0000 -0.1409	0.0460
0.010	0.0000	3.9125 2.8900 2.8900 3.9125	3.9125 2.8900 2.8900 3.9125	1.0225 0.0000 0.0000 -1.0225	0.3337
0.015	0.0000	-2.2462 -1.3041 -1.3041 -2.2462	-2.2462 -1.3041 -1.3041 -2.2462	-0.9421 0.0000 0.0000 0.9421	-0.3074
0.025	0.0000	-0.4569 -0.0856 -0.0856 -0.4569	-0.4569 -0.0856 -0.0856 -0.4569	-0.3713 0.0000 0.0000 0.3713	-0.1212

Table 3.11 BDM in the cubic tetrahedral structure. $\vec{q}$ is along the $[1\bar{1}0]$ and $\vec{E}_{ext} = (1/\sqrt{3}, 1/\sqrt{3}, 1/\sqrt{3})$. The self-consistent local fields at each dipole's site ($E_{Li}(m)$: m indicates the number of the dipoles) and the susceptibility. $\Sigma_m \hat{q}\cdot\vec{p}_m$ is part of the second term in the macroscopic average field, $\hat{q}$ is the unit wave vector.

a/a^3	$\Sigma_m \hat{q}\cdot\vec{p}_m$	$E_{Lx}(1)$ $E_{Lx}(2)$ $E_{Lx}(3)$ $E_{Lx}(4)$	$E_{Ly}(1)$ $E_{Ly}(2)$ $E_{Ly}(3)$ $E_{Ly}(4)$	$E_{Lz}(1)$ $E_{Lz}(2)$ $E_{Lz}(3)$ $E_{Lz}(4)$	χ
0.000	0.0000	0.5774 0.5774 0.5774 0.5774	0.5774 0.5774 0.5774 0.5774	0.5774 0.5774 0.5774 0.5774	0.0000
0.005	0.0000	0.9956 0.7655 0.8805 0.8805	0.9956 0.8805 0.7655 0.8805	0.9956 0.8805 0.8805 0.7655	0.0460
0.010	0.0000	3.6120 1.9423 2.7772 2.7772	3.6120 2.7772 1.9423 2.7772	3.6120 2.7772 2.7772 1.9423	0.3337
0.015	0.0000	-2.2185 -0.6802 -1.4494 -1.4494	-2.2185 -1.4494 -0.6802 -1.4494	-2.2185 -1.4494 -1.4494 -0.6802	-0.3074
0.025	0.0000	-0.5247 0.0817 -0.2215 -0.2215	-0.5247 -0.2215 0.0817 -0.2215	-0.5247 -0.2215 -0.2215 0.0817	-0.1212

Table 3.12 BDM in the cubic tetrahedral structure. $\vec{q}$ is along the $[1\bar{1}0]$ and $\vec{E}_{ext} = (1/\sqrt{2}, 1/\sqrt{2}, 0)$. The self-consistent local fields at each dipole's site ($E_{Li}(m)$: m indicates the number of the dipoles) and the susceptibility. $\Sigma_m \hat{q}\cdot\vec{p}_m$ is part of the second term in the macroscopic average field, $\hat{q}$ is the unit wave vector.

a/a^3	$\Sigma_m \hat{q}\cdot\vec{p}_m$	$E_{Lx}(1)$ $E_{Lx}(2)$ $E_{Lx}(3)$ $E_{Lx}(4)$	$E_{Ly}(1)$ $E_{Ly}(2)$ $E_{Ly}(3)$ $E_{Ly}(4)$	$E_{Lz}(1)$ $E_{Lz}(2)$ $E_{Lz}(3)$ $E_{Lz}(4)$	χ
0.000	0.0000	0.7071 0.7071 0.7071 0.7071	0.7071 0.7071 0.7071 0.7071	0.0000 0.0000 0.0000 0.0000	0.0000
0.005	0.0000	1.1489 1.0079 1.0079 1.1489	1.1489 1.0079 1.0079 1.1489	0.1409 0.0000 0.0000 -0.1409	0.0460
0.010	0.0000	3.9126 2.8900 2.8900 3.9126	3.9126 2.8900 2.8900 3.9126	1.0225 0.0000 0.0000 -1.0225	0.3337
0.015	0.0000	-2.2461 -1.3041 -1.3041 -2.2461	-2.2461 -1.3041 -1.3041 -2.2461	-0.9421 0.0000 0.0000 0.9421	-0.3074
0.025	0.0000	-0.4569 -0.0856 -0.0856 -0.4569	-0.4569 -0.0856 -0.0856 -0.4569	-0.3713 0.0000 0.0000 0.3713	-0.1212

Table 3.13 BDM in the cubic tetrahedral structure. $\vec{q}$ is along the $[1\bar{1}0]$ and $\vec{E}_{ext}$= (0,0,1). The self-consistent local fields at each dipole's site ($E_{Li}(m)$: m indicates the number of the dipoles) and the susceptibility. $\Sigma_m \hat{q}\cdot\vec{p}_m$ is part of the second term in the macroscopic average field, $\hat{q}$ is the unit wave vector.

a/a^3	$\Sigma_m \hat{q}\cdot\vec{p}_m$	$E_{Lx}(1)$ $E_{Lx}(2)$ $E_{Lx}(3)$ $E_{Lx}(4)$	$E_{Ly}(1)$ $E_{Ly}(2)$ $E_{Ly}(3)$ $E_{Ly}(4)$	$E_{Lz}(1)$ $E_{Lz}(2)$ $E_{Lz}(3)$ $E_{Lz}(4)$	χ
0.000	0.0000	0.0000 0.0000 0.0000 0.0000	0.0000 0.0000 0.0000 0.0000	1.0000 1.0000 1.0000 1.0000	0.0000
0.005	0.0000	0.0996 -0.0996 0.0996 -0.0996	0.0996 0.0996 -0.0996 -0.0996	1.5251 1.5251 1.5251 1.5251	0.0460
0.010	0.0000	0.7230 -0.7230 0.7230 -0.7230	0.7230 0.7230 -0.7230 -0.7230	4.8101 4.8101 4.8101 4.8101	0.3337
0.015	0.0000	-0.6661 0.6661 -0.6661 0.6661	-0.6661 -0.6661 0.6661 0.6661	-2.5104 -2.5104 -2.5104 -2.5104	-0.3074
0.025	0.0000	-0.2626 0.2626 -0.2626 0.2626	-0.2626 -0.2626 0.2626 0.2626	-0.3836 -0.3836 -0.3836 -0.3836	-0.1212

Table 3.14 Comparison of the BDM self-consistent calculation of the susceptibility (χ_{sc}) with the results from function form (χ_{func}) and the ADM L-L's relation (χ_{L-L}) for the cubic tetrahedral structure.

a/a^3	χ_{sc}	χ_{func}	χ_{L-L}
0.000	0.0000	0.0000	0.0000
0.005	0.0460	0.0459	0.0481
0.006	0.0645	0.0645	0.0601
0.007	0.0906	0.0907	0.0732
0.008	0.1301	0.1302	0.0874
0.009	0.1968	0.1969	0.1031
0.010	0.3337	0.3338	0.1203
0.0115	1.8163	1.8187	0.1497
0.0120	-7.8144	-7.7220	0.1606
0.0125	-1.3281	-1.3253	0.1721
0.0150	-0.3074	-0.3073	0.2413

and from the self consistent calculations. Figure 3.5 is a plot of the linear susceptibility as a function of the input parameter of the polarizability per unit cell by using the self-consistent local field method and the functional form in Eq.(3.18) for BDM. Notice the similarity of Eq.(3.18) with the L-L relation (3.2) which was based on the atomic dipole model with Lorentz local fields. The similarity of the self-consistent BDM calculation and the L-L relation illustrates the utility of the L-L relation in this cases. As we have discussed in Chapter I, the L-L relation is of doubtful validity for a covalent crystal. Eq.(3.18) was based on the bond dipole model which is an attempt to extend the L-L description to to covalent crystals. Moreover, the self-consistent calculation we are presenting here gives a much clearer picture of how the local fields effect the dielectric property of solids. Table 3.15 compares the polarizability from the BDM and ADM which corresponds to the experimental high frequency dielectric constant for some selected tetrahedral compounds. Unfortunately, the polarizability is not a quantity accessible to experiment.

By using the ADM, in Table 3.16 we have also calculated the local field for a simple tetragonal (ST) crystal structure for $\vec{q}$ along the x direction but with different polarization of the external fields in (a) and (b) and $\vec{q}$ along z direction in (c), for lattice constant ratio c/a = 0.8. Since in a non-cubic crystal the wave vector is not necessarily perpendicular to the polarization of the

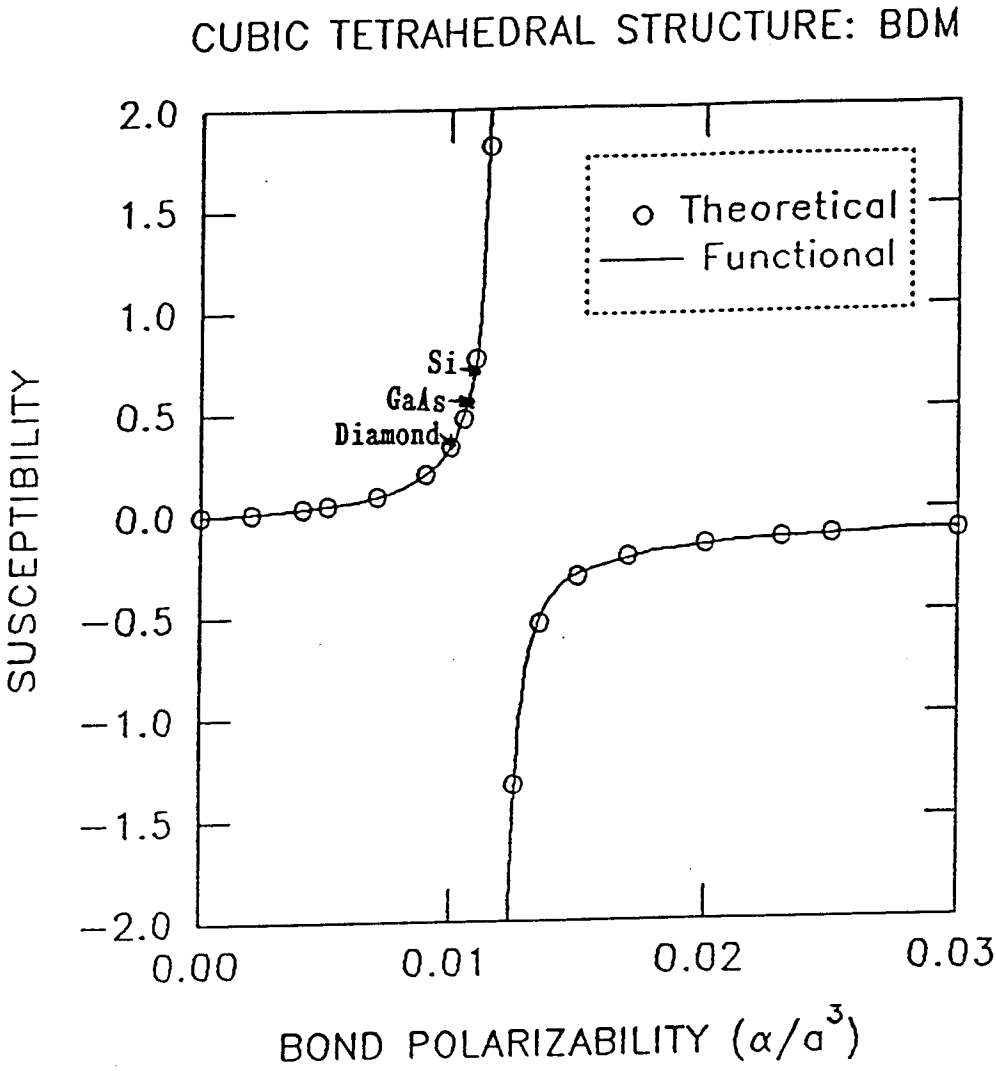

Figure 3.5 BDM. Plot of susceptibility vs bond polarizability for the diamond and zinc blende structure from the self-consistent calculation and using the functional form.

Table 3.15 The calculated bond polarizability (α_B/a^3) and atomic polarizability (α_A/a^3) for some cubic tetrahedral compounds.

semi-conductor compounds	dielectric constant ϵ_∞^*(exp.)	α_B/a^3 $\times 10^{-2}$	α_A/a^3 $\times 10^{-2}$
Diamond	5.7[1]	1.01746	1.82150
Ge	16.0[1]	1.13005	2.48680
GaAs	10.9[2]	1.10140	2.29017
GaP	9.1[3]	1.08345	2.17763
Si	12.0[1]	1.10967	2.34469
InP	9.6[2]	1.08912	2.21239
SiC	6.7[2]	1.04404	1.95514
InAs	12.2[2]	1.11101	2.35370

* Data from 1. N. A. Goryunova, "Chemistry of Diamond-like Semiconductors" (Chapman and Hall, London, 1965). 2. E. Burstein, H. M. Brodsky, and G. Lucousky, Int. J. Quant. Chem. **1s**, 759 (1967). 3. A. S. Barker, Phys. Rev. **165**, 917 (1968).

Table 3.16 ADM for the ST structure with the lattice ratio c/a =0.8. The self-consistent local fields at each dipole's site and the susceptibility. $\vec{q}$ is the wave vector in the crystal.
(a) $\vec{q}$ is along the [100], $\vec{E}_{ext}$= $(0,1/\sqrt{2},1/\sqrt{2})$.

a/a^3	$\Sigma_m \hat{q}\cdot\vec{p}_m$	E_{Lx}	E_{Ly}	E_{Lz}	$\chi_{11}=\chi_{22}$	χ_{33}
0.05	0.0000	0.0000	0.8452	1.3062	0.0747	0.1155
0.10	0.0000	0.0000	1.0503	8.5492	0.1857	1.5113
0.15	0.0000	0.0000	1.3868	-1.8809	0.3677	-0.4988
0.20	0.0000	0.0000	2.0407	-0.8473	0.7215	-0.2996

(b) $\vec{q}$ is along the [100], $\vec{E}_{ext}$= $(1/\sqrt{3},1/\sqrt{3},1/\sqrt{3})$.

a/a^3	$\Sigma_m \hat{q}\cdot\vec{p}_m$	E_{Lx}	E_{Ly}	E_{Lz}	$\chi_{11}=\chi_{22}$	χ_{33}
0.05	0.0222	0.3559	0.6901	1.0665	0.0747	0.1155
0.10	0.0322	0.2573	0.8576	6.9804	0.1857	1.5113
0.15	0.0378	0.2014	1.1323	-1.5358	0.3677	-0.4988
0.20	0.0414	0.1655	1.6662	-0.6918	0.7215	-0.2996

(c) $\vec{q}$ is along the [001], $\vec{E}_{ext}$= $(1/\sqrt{3},1/\sqrt{3},1/\sqrt{3})$.

a/a^3	$\Sigma_m \hat{q}\cdot\vec{p}_m$	E_{Lx}	E_{Ly}	E_{Lz}	$\chi_{11}=\chi_{22}$	χ_{33}
0.05	0.0272	0.6901	0.6901	0.4352	0.0747	0.1155
0.10	0.0436	0.8576	0.8576	0.3492	0.1857	1.5113
0.15	0.0547	1.1323	1.1323	0.2916	0.3677	-0.4988
0.20	0.0626	1.6662	1.6662	0.2503	0.7215	-0.2996

For ST structure(c/a=0.8), $\vec{q}$ along $\vec{x}$, S_{11}=-12.4404, $L_{xx}=L_{yy}$= 2.6140, L_{zz}=7.3383; $\vec{q}$ along $\vec{z}$, $S_{11}=S_{22}=L_{xx}/0.8$=3.2675, S_{33}= -6.5351.

external field, with $\vec{E}_{ext}$ polarized in different directions in Table 3.16, we can see that the susceptibility $\chi_{ij}(\vec{q}\neq 0) = \chi_{ij}(\vec{q}=0)$. The local fields along the x, y and z directions are determined by $E_L^i = E_{ext}^i/(1-S_{ii}a)$ for $\vec{q}\neq 0$ case. From Chapter II we have shown that dipole sum $S_{ii} = L_{ii}/V_c$ for i not in $\vec{q}$'s direction. For the case of i in $\vec{q}$'s direction, (from Table 3.16 case (a) and (b), it is S_{11} and in (c), it is S_{33}) it is not the L-factor but S_{11} that determines $E_L^1(\vec{q}\neq 0)$, which is different than $E_L^1(\vec{q}=0)$ for $\vec{q}$ along x direction, and S_{33} determines $E_L^3(\vec{q}\neq 0)$ which is different than $E_L^3(\vec{q}=0)$ for $\vec{q}$ has a component along the z direction. So if $\vec{q}$ is along the k direction, then $E_L^i(\vec{q}\neq 0) = E_L^i(\vec{q}=0)$ if $i\neq k$, but $E_L^k(\vec{q}\neq 0) \neq E_L^k(\vec{q}=0)$ if $i=k$. In Table 3.16(a) there is only the $i\neq k$ local field, so $\chi_{ij}(\vec{q}\neq 0)=\chi_{ij}(\vec{q}=0)$. However, in (b) and (c) there is an $i=k$ component and we still have $\chi_{ij}(\vec{q}\neq 0)=\chi_{ij}(\vec{q}=0)$. Notice that in (c) χ_{33} changes sign even though E_L^3 does not. The reason is that χ_{ij} is determined by L_{ij} but E_L^i is determined by S_{ij}. On the other hand, this is not surprising because the susceptibility is independent of the direction of the polarization of the external field in (a) and (b). From (a), (b) and (c) we also can see that the susceptibility is independent of the direction of $\vec{q}$ too, because $\vec{q}$ can be in any direction. The only quantity dependent on the direction of $\vec{q}$ is the local field along that direction. However, $\vec{E}_L(\vec{q}\neq 0)$ may be more meaningful for optical effects including light scattering which are really a $\vec{q}\neq 0$ case with $|\vec{q}| << |\vec{G}|$. In Table 3.17, we calculated a series of Lorentz factors for the ST structure with different c/a ratio. The L-factor in

Table 3.17 ADM for the simple tetragonal structure. The L-factor for different lattice ratio c/a. They all satisfy the sum rule, $L_{11}+L_{22}+L_{33}=4\pi$.

c/a	$L_{xx}= L_{yy}$	L_{zz}
0.4	-8.7424	30.0512
0.5	-3.3317	19.2298
0.6	-0.3853	13.3370
0.7	1.4112	9.7440
0.8	2.6140	7.3883
0.9	3.4926	5.5811
1.0	$4.1888(=\frac{4\pi}{3})$	$4.1888(=\frac{4\pi}{3})$
1.1	4.7808	3.0048
1.2	5.3150	1.9404
1.3	5.8108	0.9448
1.4	6.2888	-0.0113
1.5	6.7556	-0.9447
1.6	7.2158	-1.8652
1.8	8.1267	-3.6871
2.0	9.0325	-5.4986
2.5	11.2920	-10.0175
3.0	13.5504	-14.5344

Table 3.17 satisfies the L sum rule Eq.(2.54). The method by which we calculate the L-factor, is much simpler and easier as compared with Purvis and Taylor[2]'s method which take q=0 in the dipole sums, use a special crystal geometry to avoid the depolarization factor and very carefully deal with the summation orders. Figure 3.6 plots the L-factor as a function of the lattice ratio c/a. A negative L-factor corresponds to a reduced local field, and A positive L-factor corresponds to an enhanced local field.

In Table 3.18, we calculate $S_{ij}(\vec{q},\vec{r})$ using ADM for different $\vec{r}$ points in the unit cell for ST crystal with different c/a (the m dependence in S_{ij} is suppressed in the notation since we are examining the case m=1). By using Eq.(3.17), we can evaluate the strength of the local field in the unit cell for the ADM. Notice that even though the local fields at the atomic dipole's site are the same, the local fields still vary with in a unit cell. This may provide some useful information for a study of defects in solids. From Eq.(3.17), if $S_{ii}(\vec{q},\vec{r}) > L_{ii}$, then the local field at $\vec{r}$ is greater than the local field at the dipole's site. From Table 3.18 we see that in the center of a SC structure (i.e. c/a = 1), the S_{ii} (for $i \neq k$ which is the direction of $\vec{q}$) are the same as it is at the dipole's site ($\vec{r}$=0). Actually, this is true for any $\vec{r}$ along the diagonal line of the SC structure. So along the diagonal line of the cubic crystal, the three components of the local fields are the same and are the same as at the origin. But anywhere off the diagonal line and not at the origin point, or for $c/a \neq 1$, S_{ii} is different in

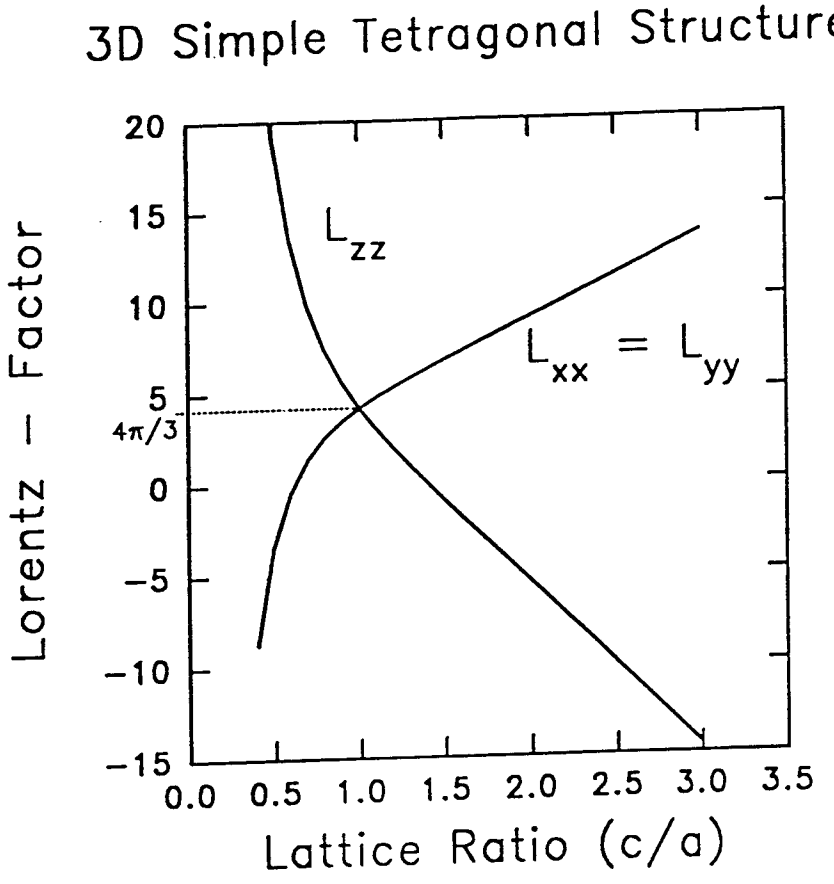

Figure 3.6 Plot of the L-factor with different lattice ratio c/a for the ST structure.

Table 3.18 ADM for the simple tetragonal structure. The dipole sum $S_{ij}(\vec{q},\vec{r})$ at different $\vec{r}$ in a unit cell (with different lattice ratio c/a). Wave vector $\vec{q}$ is along the [100]. $S_{11}+S_{22}+S_{33}=0$.

c/a	$\vec{r}_c$(0.5, 0.5, 0.5*c/a)		$\vec{r}$(0.0, 0.5, 0.0)	
	S_{22}	S_{33}	S_{22}	S_{33}
0.4	15.6804	0.0551	51.0430	-0.8450
0.5	12.4214	0.2899	42.7935	-2.3296
0.6	10.0694	0.8052	38.4996	-4.2422
0.7	8.1915	1.5689	36.2870	-6.2000
0.8	6.6213	2.4654	35.1525	-7.9892
0.9	5.2965	3.3697	34.5705	-9.5389
1.0	4.1888	4.1888	34.2708	-10.8522
c/a	$\vec{r}$(0.5, 0.0, 0.0)		$\vec{r}$(0.0, 0.25, 0.0)	
	S_{22}	S_{33}	S_{22}	S_{33}
0.4	-18.7821	-0.8450	139.0999	-31.6391
0.5	-15.3312	-2.3296	135.7859	-42.3498
0.6	-13.3135	-4.2422	134.9337	-49.3945
0.7	-12.1350	-6.2000	134.7117	-54.0170
0.8	-11.4554	-7.9892	134.6532	-57.1536
0.9	-11.0690	-9.5389	134.6377	-59.3798
1.0	-10.8522	-10.8522	134.6335	-61.0335

the three direction. This means a charge at any position along the diagonal line of the SC structure will be in a stable state. So if there is an interstitial, it would like to stay at any position along the diagonal line of the SC structure. Also when the atoms come together to form a crystal, the local field effects will make it easier to form a cubic crystal. At the center of ST structure, $E_{Ly}(\vec{q},\vec{r}_c)$ gets lager when the crystal is compressed, while $E_{Lz}(\vec{q},\vec{r}_c)$ gets smaller. Also look at the point $\vec{r}_1$=(0.0,0.5,0.0) and $\vec{r}_2$=(0.0,0.25,0.0), the local field gets lager at the point closer to the atom, i.e. $E_L(\vec{r}_2) > E_L(\vec{r}_1)$.

Chapter IV

BRILLOUIN SCATTERING IN SOLIDS

4.1 Introduction:

Light scattering is now a well established optical technique for investigating phonons in crystals[17,18,38,39,40,41]. Figure 4.1 shows a general spectrum of light scattered by phonons. There are two kinds of phonons. Light scattered by an acoustic phonon is called Brillouin scattering, and by an optical phonon is called Raman scattering[42,43,44,45]. Brillouin scattering is due to the density fluctuation in solids or liquids. Generally the Brillouin scattering spectrum consists of an intense incident line and two satellite lines, one shifted to lower frequency and the other shifted to higher frequency (see Fig. 4.1). The higher frequency (up-shifted) line corresponds, in a solid, to acoustic phonon absorption while the lower frequency (down-shifted) line corresponds to acoustic phonon emission. As is to be expected, the relative intensities of the shifted pair are temperature dependent since the number of phonons available for up-shifting depends on temperature. The frequency shifts can tell us about the small q acoustic phonon spectrum in the solid.

Equally important are the absolute intensities of the the scattered light components, for these are related to the coupling constant between the light and the acoustic phonons and involve the

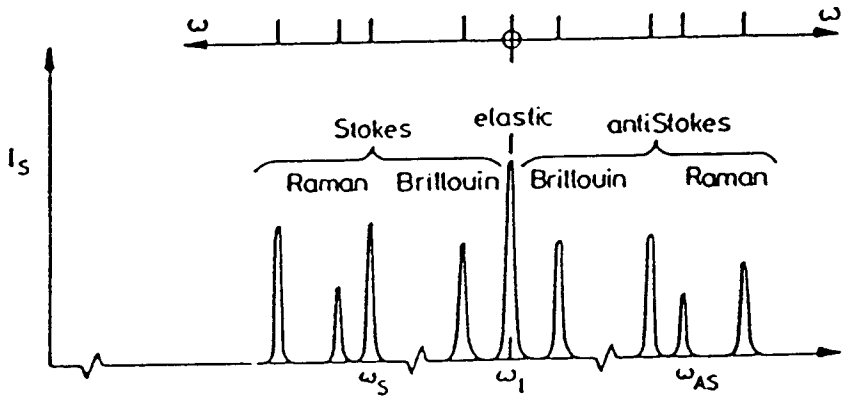

Figure 4.1 Schematic spectrum of scattered light.

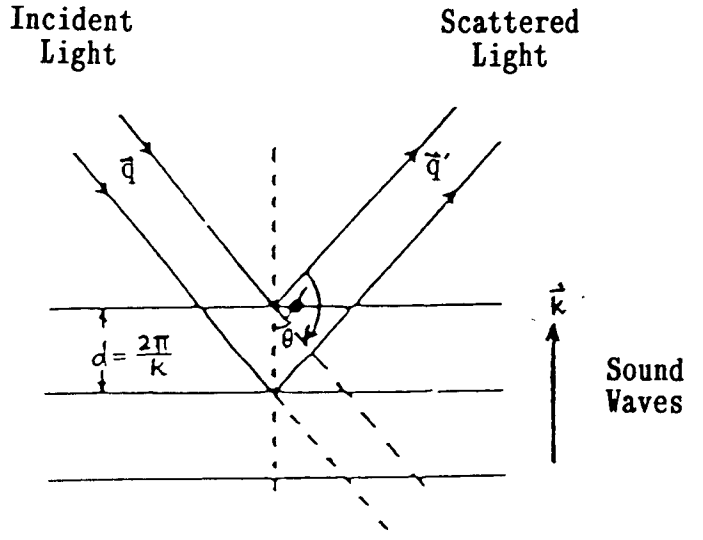

Figure 4.2 Schematic representation of the scattering of light by sound waves. The Bragg condition $m\lambda = 2d \sin\theta$ (m an integer), can be written as $mk = 2q \sin\theta$, or $mk = (\vec{q}' - \vec{q})\cdot\hat{k}$. Since Bragg reflection is specular (angle of incidence equals angle of reflection) and since the magnitude q′ equals the magnitude q, it follows that $(\vec{q}' - \vec{q})$ must be parallel to $\vec{k}$, and therefore $\vec{q}' - \vec{q} = m\vec{k}$.

elastic and elasto-optic materials parameters[46,47,48,49,50].

An elementary picture of the scattering process is given in Figure 4.2. If a beam of light passes through a medium, a small fraction of the incident light will be scattered in all directions by thermal fluctuations in the dielectric constant of the medium. Consider the incident and scattered light with angular frequencies ω_i and ω_s and wave vectors $\vec{q}_i$ and $\vec{q}_s$, interacting with a particular normal mode of the acoustic branch with angular frequency ω and wave vector $\vec{K}$. We assume that only this particular normal mode is excited; i.e. we consider the interaction of the light with one phonon at a time. Conservation of energy and crystal momentum in one phonon process requires

$$\omega_s = \omega_i \pm \omega(\vec{K}) \tag{4.1}$$

and

$$n\vec{q}_s = n\vec{q}_i \pm \vec{K}. \tag{4.2}$$

Here the upper sign refers to phonon absorption (anti-stokes), the lower sign refers to phonon emission (stokes), and n is the index of refraction of the medium. The scattered light follows Bragg's law. The spectrum of the scattered light is determined by the time dependence of the fluctuations in the dielectric constant, which is non-linear in general. Moreover, the light scattered from this fluctuation has a frequency changes $\pm\delta\omega$. Thus, Brillouin predicted a long time ago that thermally scattered light should show certain frequency changes $\pm\delta\omega$ which are functions of the scattering angle:

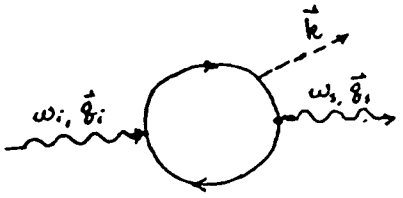

Figure 4.3 Feynman diagram of the photon-electron-phonon interaction.

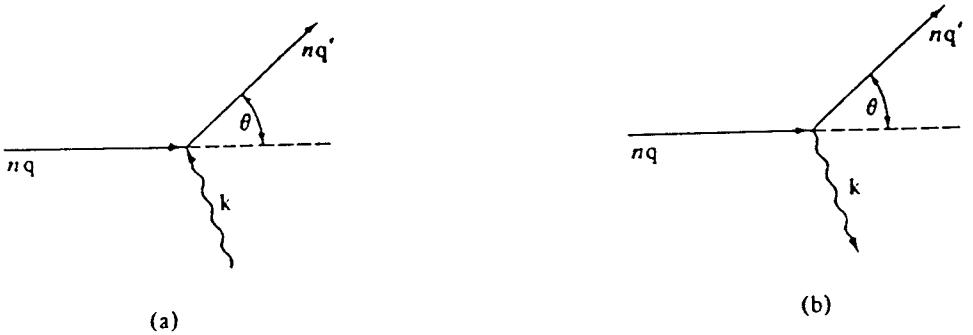

Figure 4.4. Schematic diagram of (a) anti-Stokes and (b) Stokes Brillouin Scattering. The scattering of a photon through an angle θ from free space wave vector $\vec{q}$ to free space wave vector $\vec{q}'$ with (a) absorption of a phonon of wave vector $\vec{k}$ and (b) the emission of a phonon of wave vector $\vec{k}$. The photon wave vectors in the crystal are $n\vec{q}$ and $n\vec{q}'$, where n is the index of refraction.

$$(\delta\omega/\omega_o) = 2(V/c)\ n\ \sin(\theta/2), \qquad (4.3)$$

where ω_o is the frequency of the incident light wave, and c is the velocity of light in vacuum, V is the velocity of the thermally excited sound wave. This formula was first obtained by Brillouin[51].

Viewed in more detail the scattering process is best described by the Figure 4.3. Here the incident photon (associated with the self-consistent local field at that point) excites an electron-hole pair followed by the electron (or hole) emitting (or absorbing) an acoustic phonon and then annihilating with the production of the scattered photon. Thus, in principle, the scattering intensity depends on the electron-phonon coupling constants as well as the electrodynamics coupling constant. In a simpler picture, which emphasis the macroscopic (long wavelength) character of the process, the interaction shrinks to a "dot" as shown in Figure 4.4. and the coupling is described by macroscopic parameter as discussed in section 4.2.

4.2 Brillouin Scattering Cross Section:

The calculation of the acoustic-phonon scattering cross section closely follows the quantum theory of the scattering cross section for photon-electron-phonon interactions[17]. The detailed derivation has been worked out by M. Born and K. Huang[18]. We give a basic picture here. Since the Hamiltonians of the interacting light and the scattering medium can be written as:

$$H = \frac{1}{2} \int d^3r \, \vec{D} \cdot \vec{E}$$

$$= \frac{1}{2} \int d^3r \, \epsilon \, \vec{E}_s \cdot \vec{E}_I, \qquad (4.4)$$

where the dielectric tensor ϵ to a first order approximation can be taken as a linear function of the elastic strain η, i.e

$$\epsilon \cong \epsilon_o + \frac{\partial \epsilon}{\partial \eta} \eta, \qquad (4.5)$$

where ϵ_o is the dielectric constant of the crystal without a strain and $\frac{\partial \epsilon}{\partial \eta}$, the change of the dielectric constant under a strain, which we will see in next section, is related to the elasto-optical (Pockels) constants. The differential cross section is determined by the Golden rule in quantum theory which gives us an expression in terms of a scattering tensor T, which is a combination of the Pockels constants. The standard formula for the Brillouin scattering cross section can be written as[38]:

$$\frac{d\sigma}{d\Omega} = \text{constant} \cdot \frac{[\vec{e}_s \cdot T \cdot \vec{e_I}]^2}{X} \qquad (4.6)$$

where the $\vec{e}_s$ and $\vec{e}_I$ are the unit polarization vectors of the scattered and incident light, T is the scattering tensor which is related to the Pockels constants, X is a combination of elastic constants corresponding to the normalization of wave function. Values of T and X for a cubic crystal have been tabulated for phonon

direction along [110] in Table 4.1[17]. For a cubic crystal, the only non-vanishing elasto-optic constants are the following:

$$p_{1111} = p_{2222} = p_{3333} = p_{11}$$
$$p_{1122} = p_{2211} = p_{2233} = p_{3322} = p_{3311} = p_{1133} = p_{12}$$
$$p_{1212} = p_{2121} = p_{1221} = p_{2112} = p_{2323} = p_{2332} = p_{3223}$$
$$= p_{3232} = p_{3131} = p_{3113} = p_{1331} = p_{1313} = p_{44}. \qquad (4.7)$$

Let us consider the incoming radiation along one cubic axis and the scattered radiation observed along another axis. The differential cross sections for the acoustic phonon traveling along [110] in the order shown Table 4.1 are:

$$\frac{d\sigma}{d\Omega} = \text{constant}\cdot\frac{2(p_{12}^2 + p_{44}^2)}{(c_{11} + c_{12} + 2c_{44})} \quad \text{(Longitudinal)}$$
$$= \text{constant}\cdot\left(\frac{p_{44}^2}{c_{44}}\right) \quad \text{(Transverse)} \qquad (4.8)$$
$$= 0, \quad \text{(Transverse)}$$

where the c_{ij} are the elastic constants of a cubic crystal, which have the same symmetry of the Pockels constants. If we know the elastic constants of a cubic crystal, then calculations of the differential cross sections for Brillouin scattering will become calculations of the Pockels constants.

Table 4.1 Scattering tensor T, X and the lattice displacement vector $\vec{u}$, for a phonon traveling in the direction [110] in a cubic crystal.

X	T	$\vec{u}$
$\frac{c_{11}+c_{12}+2c_4}{2}$	$\begin{bmatrix} p_{11}+p_{12} & 2p_{44} & 0 \\ 2p_{44} & p_{11}+p_{12} & 0 \\ 0 & 0 & 2p_{12} \end{bmatrix}$	[110]: Longitudinal
c_{44}	$\sqrt{2}\begin{bmatrix} 0 & 0 & p_{44} \\ 0 & 0 & p_{44} \\ p_{44} & p_{44} & 0 \end{bmatrix}$	[001]: Transverse
$\frac{c_{11}-c_{12}}{2}$	$\begin{bmatrix} p_{11}-p_{12} & 0 & 0 \\ 0 & p_{12}-p_{11} & 0 \\ 0 & 0 & 0 \end{bmatrix}$	[$\bar{1}$10]: Transverse

4.3 Pockels Constants and Their Calculations:

Pockels constants are dimensionless constants, which are a measure of the change in the inverse dielectric tensor with respect to deformations. They are defined as[18]:

$$\delta(\epsilon^{-1})_{ij} = (\epsilon^{-1})_{ij} - (\epsilon_o^{-1})_{ij} = \Sigma_{kl}\, p_{ijkl}\eta_{kl}, \tag{4.9}$$

where ϵ^{-1} denotes the inverse of the dielectric tensor and η is the elastic strain tensor,

$$\eta_{kl} \equiv \frac{1}{2}\left[\frac{\partial u_k}{\partial x_l} + \frac{\partial u_l}{\partial x_k}\right], \tag{4.10}$$

and u represents the elastic displacement. The symmetric coefficients

$$p_{ijkl} = p_{jikl} = p_{ijlk}, \tag{4.11}$$

are the elasto-optic constants in tensor notation.

There are two ways to calculate the Pockels constants. A formal procedure to calculate the elasto-optic coefficient is contained in the band theory of solids. The imaginary part of the dielectric response tensor in $\epsilon_{ij} = \epsilon_{1,ij} + i\epsilon_{2,ij}$ is related to the absorption coefficient which can be calculated by the Golden rule if we know the initial and final states of the electron wave functions. The real part of the dielectric function is given by a Kramers-Kronig

transformation,

$$\epsilon_{1,ij}(\omega) - 1 = \frac{2}{\pi} \int_{\omega_g}^{\infty} \frac{\omega' \epsilon_{2,ij}(\omega')}{(\omega'^2 - \omega^2)} d\omega'. \tag{4.12}$$

Here ω_g refers to the absorption threshold frequency. In the presence of strain, the wave functions and the energy bands will be modified slightly. From Eq.(4.12) changes in ϵ_1 and ϵ_2 are related by

$$\delta\epsilon_{1,ij}(\omega) = \frac{2}{\pi} \int_{\omega_g'}^{\infty} \frac{\omega' \delta\epsilon_{2,ij}(\omega')}{(\omega'^2 - \omega^2)} d\omega'. \tag{4.13}$$

where $\omega_g' = \omega_g + \delta\omega_g$, and $\delta\omega_g$ is the strain induced shift in the absorption threshold. Calculating $\delta\epsilon_{2,ij}$ for each strain component η_{kl} is certainly a difficult task.

Another way to calculate the Pockels constants is to use the classical Lorentz-Lorenz model of a solid, avoiding the more complex energy band problem[42,43]. The details of this approach were first worked out by Mueller[28], who calculated the Pockels constant for NaCl type of crystals. N.R. Werthamer[39] calculated the Pockels constants for rare gas crystals like Xenon with a form of L-L theory using non-self-consistent dipole sums and atomic polarizabilities.

Here we present a calculation of Pockels constants which uses the quantum dipoles in the classical limit and considers the local field self-consistently. In order to compare with Werthamer, we use

the atomic dipole model as well and calculate the Pockels constants for Xenon. We use a phenomenological parameter, the atomic and bond polarizability which is defined by the dielectric formula in chapter III. The calculations in this chapter use a strain or shear to the lattice to calculate the Pockels constants. We give different η_{kl} to find the linear relationship of $\delta(\epsilon^{-1})_{ij}$ vs η_{kl}. The slope, as shown for example in Figure 4.5, is the elasto-optic constant.

4.4 Results and Comparison:

In this calculation, we let the wave vector of the external field lay along one of the crystal axis (say z), and the polarization of the field along the plane which is perpendicular to that axis (say the x-y plane). This is equivalent to the experimental method of measuring Brillouin scattering.

Figures 4.6a and 4.6b give a schematic picture for a simple cubic crystal under a deformation δ (strain or shear) along the x direction. For diamond or zinc blende crystals under a strain δ along the x direction, in the ADM, the positions of the two basis atoms are: [0.0, 0.0, 0.0] and [0.25(1-δ), 0.25, 0.25]. In the BDM, the positions of the four basis bond dipoles are: [0.125(1-δ), 0.125, 0.125], [0.125(1-δ), 0.375, 0.375], [0.375(1-δ), 0.125, 0.375], [0.375(1-δ), 0.375, 0.125]. The change in primitive lattice vectors

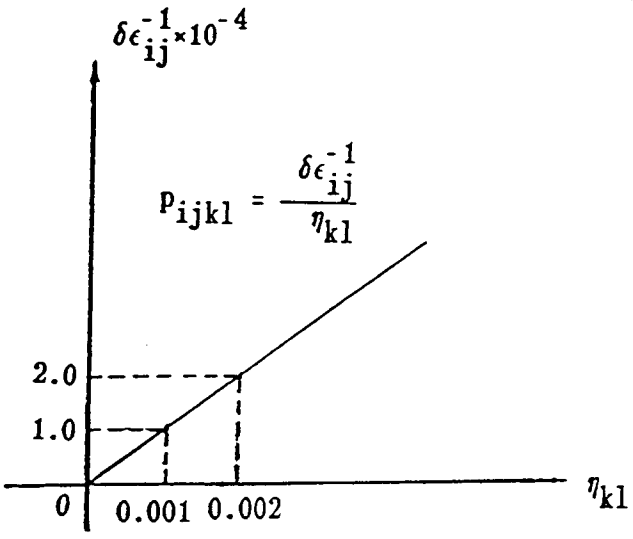

Figure 4.5 Schematic diagram of Pockels constant calculation. Showing the typical behavior of the Pockels constants. The shift in the inverse dielectric components $\delta\epsilon_{ij}^{-1}$ vs the crystal deformation η_{kl}. The slope is the Pockels constant p_{ijkl}.

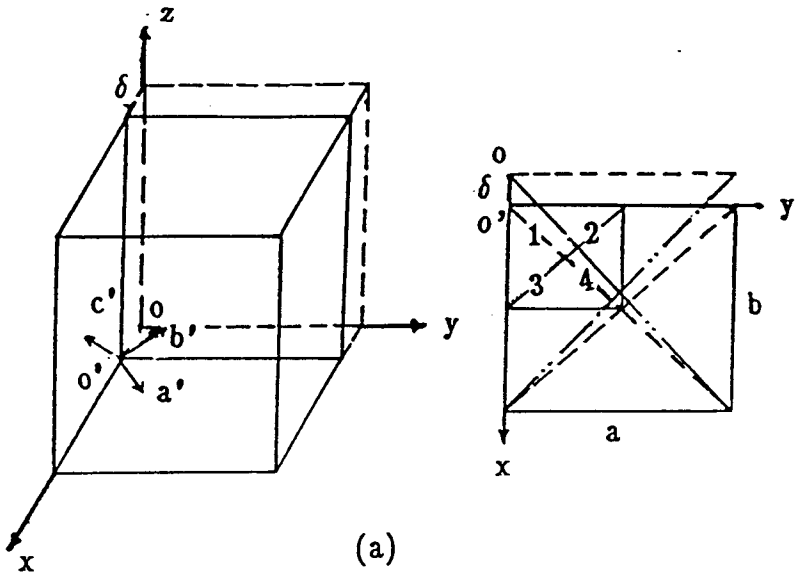

(a)

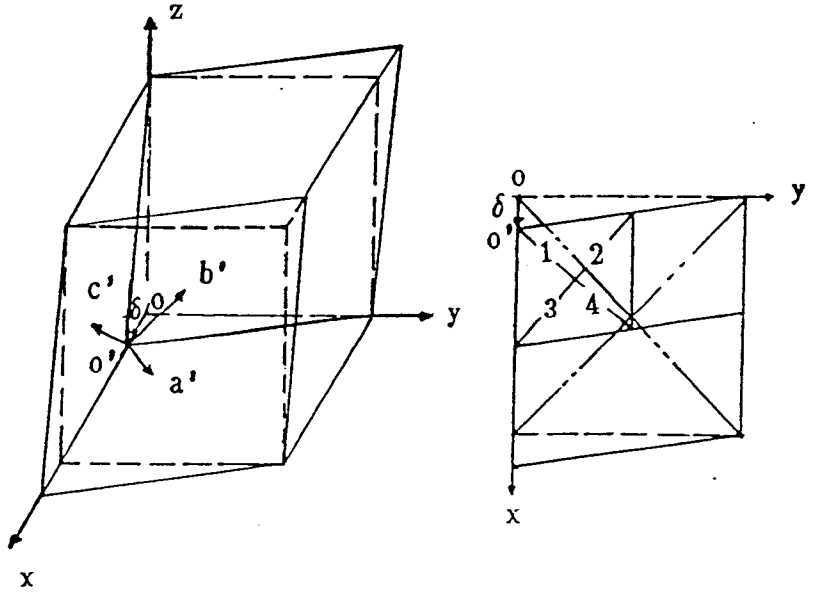

(b)

Figure 4.6 Schematic representation of a simple cubic crystal under (a) a strain δ (along x direction) and (b) a shear δ (along x direction).

for the cubic tetrahedral structure with strain δ along the x direction are:

$$\begin{aligned}
\vec{a}' &= \frac{a}{2}\,[(1-\delta)\hat{x} + \hat{y}\,] \\
\vec{b}' &= \frac{a}{2}\,[\hat{y} + \hat{z}\,] \\
\vec{c}' &= \frac{a}{2}\,[(1-\delta)\hat{x} + \hat{z}\,]
\end{aligned} \tag{4.14}$$

and the volume primitive cell is,

$$\begin{aligned}
V_c &= |\ \vec{a}'\cdot\vec{b}'x\vec{c}'\ | \\
&= \frac{a^3}{4}\,(1-\delta),
\end{aligned} \tag{4.15}$$

where a is the lattice constant of the crystal without strain and δ represents η_{11}. In the same way if the strain δ is oriented along the y direction, then it will represent η_{22}.

The reciprocal lattice vectors will also change due to the strain along the x direction. For the cubic tetrahedral structure, they now become:

$$\begin{aligned}
\vec{A} &= \frac{2\pi}{a}\,[\,\frac{1}{(1-\delta)}\,\hat{x} + \hat{y} - \hat{z}\,] \\
\vec{B} &= \frac{2\pi}{a}\,[\,\frac{-1}{(1-\delta)}\,\hat{x} + \hat{y} + \hat{z}\,] \\
\vec{C} &= \frac{2\pi}{a}\,[\,\frac{1}{(1-\delta)}\,\hat{x} - \hat{y} + \hat{z}\,].
\end{aligned} \tag{4.16}$$

For the crystal under a shear $\delta = \eta_{12}$, in the ADM, the positions of the two basis atoms are: $[(0.0-\delta),\ 0.0,\ 0.0]$ and $[(0.25-0.75\delta),\ 0.25,\ 0.25]$. In the BDM, the positions of the four basis bond

dipoles are: [(0.125+0.875δ), 0.125, 0.125], [(0.125+0.625δ), 0.375, 0.375], [(0.375+0.625δ), 0.125, 0.375], [(0.375+0.875δ), 0.375, 0.125]. The primitive lattice vectors for diamond and zinc blende structure are then changed to be:

$$\begin{aligned} \vec{a}' &= \frac{a}{2}\,[(1-\delta)\hat{x} + \hat{y}\,] \\ \vec{b}' &= \frac{a}{2}\,[-\delta\hat{x} + \hat{y} + \hat{z}\,] \\ \vec{c}' &= \frac{a}{2}\,[(1-\delta)\hat{x} + \hat{z}\,] \end{aligned} \tag{4.17}$$

and the volume primitive cell is,

$$V_c = \frac{a^3}{4}\,(1 - \frac{\delta}{2}). \tag{4.18}$$

The reciprocal lattice vectors for the crystal under a shear have changed to be:

$$\begin{aligned} \vec{A} &= \frac{2\pi}{a(1-\delta/2)}\,[\,\hat{x} + \hat{y} - (1-\delta)\hat{z}\,] \\ \vec{B} &= \frac{2\pi}{a(1-\delta/2)}\,[\,-\hat{x} + (1-\delta)\hat{y} + (1-\delta)\hat{z}\,] \\ \vec{C} &= \frac{2\pi}{a(1-\delta/2)}\,[\,\hat{x} - (1-\delta)\hat{y} + \hat{z}\,]. \end{aligned} \tag{4.19}$$

To calculate p_{11}, p_{12} and p_{44} for some tetrahedral compounds, we first use the polarizability listed in Table 3.15 which is the polarizability for the crystal without deformation. Using the ADM, Table 4.2 gives the calculated results for some selected tetrahedral crystals with the deformation $\delta = \pm\ 0.001$ along x direction. We can see immediately that although the dielectric constant changes with

Table 4.2 ADM self-consistent calculation of the Pockels constants for some selected compounds. The dielectric constant and the atomic polarizabilities used in calculations are listed in Table 3.15. ($\epsilon_\infty(\delta=0)$ is the undeformed high frequency dielectric constant. $\epsilon_{ij}^{\pm}$ and $p_{ij}^{\pm}$ corresponding to the deformation $\delta=\pm 0.001$).

Compounds	ϵ_{11}^{+}	ϵ_{22}^{+}	ϵ_{44}^{+}	p_{11}^{+}	p_{12}^{+}	p_{44}^{+}
$\epsilon_\infty(\delta=0)$	ϵ_{11}^{-}	ϵ_{22}^{-}	ϵ_{44}^{-}	p_{11}^{-}	p_{12}^{-}	p_{44}^{-}
Diamond	5.7024	5.7169	5.7110	-0.0748	-0.5190	-0.3366
5.7	5.6976	5.6832	5.6891	-0.0745	-0.5190	-0.3349
Ge	15.9918	16.1400	16.0955	0.0319	-0.5423	-0.3710
16.0	16.0082	15.8623	15.9062	0.0319	-0.5427	-0.3687
GaAs	10.8998	10.9642	10.9432	0.0014	-0.5375	-0.3624
10.9	10.9002	10.8365	10.8574	0.0018	-0.5375	-0.3601
GaP	9.1014	9.1444	9.1296	-0.0163	-0.5339	-0.3568
9.1	9.0987	9.0560	9.0707	-0.0162	-0.5342	-0.3549
Si	11.9984	12.0779	12.0526	0.0111	-0.5378	-0.3637
12.0	12.0013	11.9227	11.9478	0.0091	-0.5403	-0.3638
InP	9.6009	9.6495	9.6331	-0.0101	-0.5343	-0.3578
9.6	9.5990	9.5509	9.5672	-0.0113	-0.5360	-0.3573
SiC	6.7024	6.7237	6.7155	-0.0527	-0.5256	-0.3449
6.7	6.6977	6.6765	6.6846	-0.0522	-0.5253	-0.3429
InAs	12.1982	12.2807	12.2545	0.0120	-0.5385	-0.3647
12.2	12.2016	12.1202	12.1461	0.0110	-0.5400	-0.3637

For diamond and zinc blende crystals under (a) strain δ along x direction, the L-factors are: ($L^{\pm}$ corresponds to $\delta=\pm 0.001$)

$L_{xx}^{+}=V_c^{+}\cdot 16.7500$, $L_{yy}^{+}=L_{zz}^{+}=V_c^{+}\cdot 16.7828$;

$L_{xx}^{-}=V_c^{-}\cdot 16.7604$, $L_{yy}^{-}=L_{zz}^{-}=V_c^{-}\cdot 16.7276$; $V_c^{\pm} = (1\mp\delta)\cdot a^3/4$.

(b) under shear δ along x direction, the L-factors are:

$L_{xx}^{+}=V_c^{+}\cdot 16.7524$, $L_{yy}^{+}=L_{zz}^{+}=V_c^{+}\cdot 16.7692$;

$L_{xx}^{-}=V_c^{-}\cdot 16.7576$, $L_{yy}^{-}=L_{zz}^{-}=V_c^{-}\cdot 16.7412$; $V_c= (1\mp\delta/2)\cdot a^3/4$.

different deformation (+0.001 or -0.001), which corresponds to the changes in density, the Pockels constants are almost unchanged. This gives us a rough evaluation of the Pockels constants for the dielectric constants and crystal structures are known. Table 4.3 lists the experimental data of the Pockel's constants for some cubic tetrahedral compounds. Comparing the calculated results in Table 4.2 with the experimental data, they are not in agreement. However, if we consider that the atomic polarizability will be a tensor for a deformed crystal, which is more objective description of the real physical system, then our calculation has excellent agreement with the experimental data; this is also shown in Table 4.3. From Table 4.3 we notice that the calculation is very sensitive to the polarizability we used. This may tell us that the L-L relation is only good for a rough evaluation. In Table 4.4 we show our calculated results of the Pockels constants for the rare gas solid Xenon, obtained using the self-consistent method, and compared with Werthamer's calculation. By using the same value $\alpha/a^3 = 0.045$ as Werthamer used, our calculation did not give any better results. However, if we know the observed Pockels constants instead of only the ratio, we can find the atomic polarizabilities for the deformed crystal.

We are also interested in calculating the Pockels constants using the BDM. For a crystal under a strain or shear along the x direction the change in the four bond directions are:

Table 4.3 The experimental data of the Pockels constants for some tetrahedral crystals and the calculated Pockels constants from tensor atomic polarizabilities (a_o is the undeformed polarizability from Table 3.15).

Compounds	p_{11}^*	p_{11}	p_{12}^*	p_{12}	p_{44}^*	p_{44}
diamond	-0.43	-0.4290	0.19	0.1892	-0.16	-0.1591
Ge	0.27	0.2706	0.235	0.2351	0.125	0.1258
GaAs	-0.165	-0.1658	-0.140	-0.1397	-0.072	-0.0727
GaP	-0.151	-0.1508	-0.082	-0.0814	-0.074	-0.0741

* Data from D. A. Pinnow "Laser Handbook", V1, page 999 (1972)

Compounds	$(a_o/a^3)\times10^{-2}$	$(a_{11}/a^3)\times10^{-2}$	$(a_{22}/a^3)\times10^{-2}$	$(a_{44}/a^3)\times10^{-2}$
diamond	1.82150	1.82324	1.81803	1.82063
Ge	2.48680	2.48511	2.48131	2.48329
GaAs	2.29017	2.29124	2.28763	2.28832
GaP	2.17763	2.17844	2.17491	2.17593

Table 4.4 ADM self-consistent calculation of the Pockels constants for Xenon. Xenon has fcc structure, with deformation δ=0.001 along x direction and $\vec{q}$ is along the [001], $\vec{E}_{ext}$= $(1/\sqrt{2}, 1/\sqrt{2}, 0)$. The dielectric constant without crystal deformation ϵ_o is calculated by using the L-L relation.

(a) Crystal under strain δ along x, S_{11}=4.1938, S_{22}=4.1926.

a/a^3	E_{Lx}	E_{Ly}	E_{Lz}	p_{11}	p_{12}
0.045[1]	2.8847	2.8822	0.0000	-0.4114	-0.3354
0.01735[2]	0.9974	0.9973	0.0000	-0.3750	-0.3466

(b) Crystal under shear δ along x, S_{11}=4.1913, S_{22}= 4.1907.

a/a^3	E_{Lx}	E_{Ly}	E_{Lz}	p_{44}
0.045[1]	2.8834	2.8822	0.0004	-0.3524
0.01735[2]	0.9973	0.9972	0.0001	-0.3529

The observed elasto-optical constants for xenon[3] are
p_{12}/p_{11}=1.45, p_{44}/p_{11}= -0.10.

In Werthamer's calculation by using a/a^3=0.045, they are
$p_{12}/p_{11} \simeq$ 0.81, $p_{44}/p_{11} \simeq$ -0.063.

This work: (1) a/a^3 = 0.045, p_{12}/p_{11}= 0.815, p_{44}/p_{11}=0.856;
(2) a/a^3 =0.01735, p_{12}/p_{11}= 0.924, p_{44}/p_{11}=0.941.

Data from 1. N. R. Werthamer, Phys. Rev. B6, 4075 (1972).
2. From atomic optical calculation in Rare Gas Solids, p146 and p250. Ed. by M. L. Klein and J. A. Venables. Academic Press. (Harcourt Brace Jovanovich; London, 1976).
3. W. S. Gornall and B. P. Stoicheff, Phys. Rev. B4, 4518 (1971).

$$
\begin{aligned}
d^1 &= [(1-\delta),\ 1,\ 1] \ /\ \sqrt{2 + (1-\delta)^2} \\
d^2 &= [(1-\delta),\ \bar{1},\ \bar{1}] \ /\ \sqrt{2 + (1-\delta)^2} \\
d^3 &= [-(1-\delta),\ 1,\ \bar{1}] \ /\ \sqrt{2 + (1-\delta)^2} \\
d^4 &= [-(1-\delta),\ \bar{1},\ 1] \ /\ \sqrt{2 + (1-\delta)^2}.
\end{aligned}
\tag{4.20}
$$

If we take the strain or shear to be on the order of 10^{-3}, the effect of considering the change of bond directions yields a difference of about 10^{-3} in the results of the calculated Pockels constants or the polarizability.

By considering the bond polarizability to be a tensor for the crystal under deformation, we find that the new functional forms for the deformed crystal (with strain or shear δ = 0.001) can be approximately evaluated using the following three equations.

$$
\chi_{11} = \frac{n\,\tau_{11}/3}{(1 - 5.2633n\tau_{11})}, \quad \text{(strain)} \tag{4.21}
$$

$$
\chi_{22} = \frac{n\,\tau_{22}/3}{(1 - 5.2537n\tau_{22})}, \quad \text{(strain)} \tag{4.22}
$$

$$
\chi_{44} = \frac{n\,\tau_{44}/3}{(1 - 5.2583n\tau_{44})}, \quad \text{(shear)} \tag{4.23}
$$

where n is the number of the bond dipoles per unit cell (here n=16), and χ_{ij} is the susceptibility of the solid under deformation, τ_{ij} is the bond polarizability per unit cell, $\tau_{ij} = a_{ij}/a^3$, and the subscript i and j corresponding to the susceptibility tensor. Different values of τ may represent different compounds which have

Table 4.5 BDM. Comparison of the susceptibilities from the self-consistent calculation (χ_{11}, χ_{22} and χ_{44})$_t$ and from the functional forms (χ_{11}, χ_{22} and χ_{44})$_f$ for the diamond or zinc blende structure under deformation (strain or shear) δ=0.001 along the x direction.

a/a^3	$(\chi_{44})_t$	$(\chi_{44})_f$	$(\chi_{11})_t$	$(\chi_{11})_f$	$(\chi_{22})_t$	$(\chi_{22})_f$
0.0000	0.0000	0.0000	0.0000	0.0000	0.0000	0.0000
0.0070	0.0908	0.0908	0.0909	0.0909	0.0908	0.0907
0.0090	0.1977	0.1977	0.1982	0.1983	0.1974	0.1971
0.0100	0.3362	0.3361	0.3376	0.3378	0.3348	0.3346
0.0105	0.4803	0.4803	0.4837	0.4837	0.4772	0.4771
0.0110	0.7871	0.7871	0.7964	0.7964	0.7780	0.7786
0.0115	1.8884	1.8887	1.9446	1.9438	1.8331	1.8408
0.0120	-6.6850	-6.6711	-6.0484	-6.0643	-7.5355	-7.3475
0.0125	-1.2911	-1.2905	-1.2650	-1.2266	-1.3216	-1.3139
0.0150	-0.3054	-0.3054	-0.3038	-0.3039	-0.3075	-0.3066
0.0250	-0.1209	-0.1208	-0.1206	-0.1206	-0.1213	-0.1211

the same crystal structure. We can use $\epsilon_{ij} = 1 + 4\pi\chi_{ij}$ to get the deformed dielectric constant. In table 4.5 we compare the results from the self-consistent local field method and from the functional forms for the crystal under a strain or shear of 0.001, and they are in an excellent agreement with standard deviation $\sigma < 0.003$ in the positive range of χ. In Figure 4.7, we plot the results of Table 4.5 for χ_{11} vs a_{11} only. χ_{22} vs a_{22} and χ_{44} vs a_{44} show a similar plot.

Table 4.6 lists the calculated Pockels constants and the corresponding bond polarizabilities a_{11}, a_{22}, and a_{44} using the BDM from the self-consistent local field method for some selected compounds. Table 4.7 lists results of using the functional form to calculate the Pockels constants. Comparison of the experimental data in Table 4.3, the results from the functional form give a good estimation of the pockels constants. Furthermore, it gives the right sign of the Pockels constants with better than 0.01 percent accuracy.

A comparison of the bond polarizabilities of the deformed crystal with the ideal crystal of the diamond and zinc blend structure are difficult due to the limited availability of data. However, we can see that the relations $a_{11} < a_{44} < a_{22} < a_o$ hold for the diamond and zinc blende structure, where a_o is the undeformed bond polarizability from Chapter 3. If we could determine how a_{ii} changes with crystal structure, then we could predict the Pockels constants.

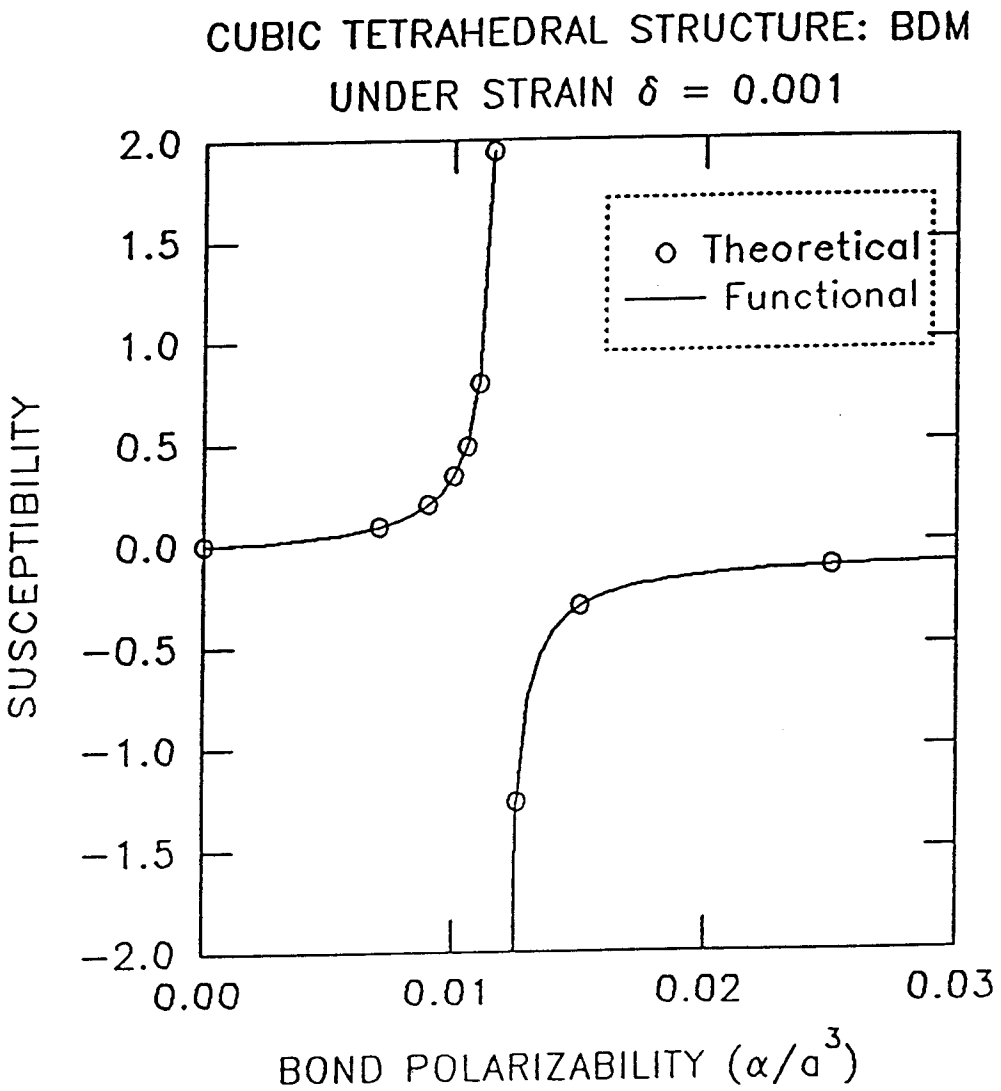

Figure 4.7 BDM in the diamond or zinc blende structure with strain δ=0.001. Plot of χ_{11} vs the bond polarizability from the self-consistent calculation and the functional form. χ_{22} and χ_{44} show a similar plot.

Table 4.6 BDM in the diamond and zinc blende structure under deformation δ = 0.001 along the x direction. The self consistent calculation of the Pockels constants for some compounds, using tensor bond polarizabilities.

Compounds	a_{11}/a^3 $\times 10^{-2}$	a_{22}/a^3 $\times 10^{-2}$	a_{44}/a^3 $\times 10^{-2}$	p_{11}	p_{12}	p_{44}
diamond	1.015977	1.016833	1.016486	-0.4299	0.1902	-0.1593
Ge	1.127371	1.129488	1.128539	0.2699	0.2345	0.1251
GaAs	1.099277	1.101176	1.100148	-0.1654	-0.1392	-0.0719
GaP	1.081392	1.083150	1.082239	-0.1514	-0.0817	-0.0742

Table 4.7 Using the BDM functional forms to calculate the Pockels constants.

Compounds	a_{11}/a^3 $\times 10^{-2}$	a_{22}/a^3 $\times 10^{-2}$	a_{44}/a^3 $\times 10^{-2}$	p_{11}	p_{12}	p_{44}
diamond	1.015977	1.016833	1.016486	-0.4576	0.2602	-0.1458
Ge	1.127371	1.129488	1.128539	0.2766	0.1108	0.1219
GaAs	1.099277	1.101176	1.100148	-0.1684	-0.2088	-0.0702
GaP	1.081392	1.083150	1.082239	-0.1602	-0.1187	-0.0700

CHAPTER V

SELF-CONSISTENT LOCAL FIELD CALCULATIONS ON A SURFACE

5.1 Introduction:

The last few decades have seen a growing interest in a wide range of surface optical phenomena. These include linear and non-linear properties of metal and dielectric surfaces, optical properties of surface absorbed atoms and molecules and the striking strongly enhanced Raman scattering at the surface of rough metals[52,53,54,55]. Each of these phenomena have the common element that local field effects are probably involved.

The importance of the local field effects is that at the surface the external field is modified by the presence of the electric dipoles on the solid surface. Each of these dipoles is induced by the external field and the dipole fields from the other dipoles on the surface. In the simple self consistent picture used here, as in the previous chapters, the local field at any point on a surface can be written as:

$$\vec{E}_L = \vec{E}_{ext} + \vec{E}_p. \qquad (5.1)$$

This dipolar effect modifies the absorption spectra, the intensity, and the resonant Raman cross section of absorbed molecules[56,57,58,59,60,61,63]. However in the case of a semi-infinite material — a real surface — the local fields vary

with each layer and a self consistent calculation becomes extremely difficult. Moreover, in a metal the effective polarizability cannot be treated in a simple way since a local dipole approximation is certainly incorrect. Moreover the frequency dependence and complex character of any model of an effective metallic polarizability are bound to be extremely important.

In the case of surface enhanced Raman scattering, a local field picture such as has been discussed here may have some relevance - however crudely - in interpreting this striking effect. If it is assumed that a local field can be calculated then, as we shall show, it will again display the L-L form observed for three-dimensional matter

$$\vec{E}_L = \frac{\vec{E}_{ext}}{1 - \alpha S}, \tag{5.2}$$

which leads to two interesting possibilities:

(1) If αS is negative, there will be a local suppression of the external field;

(2) If $0 < \alpha S < 1$, there will be a local enhancement of the external field.

Thus, even the approach taken here, if carried out in some realistic way, could provide an understanding of the surface enhanced Raman effect at metal surfaces. This, however, is beyond the intended scope of the present investigation. We will, however, explore the self consistent dipole sums with a constant local polarizability for

a model surface consisting of atoms and bonds in a two dimensional layer.

The two goals we have here are: (1) to calculate the self consistent local field at dipole's site, so that we can evaluate the dielectric constant of the surface, and (2) to calculate the self consistent local field at an arbitrary point off the dipole's site on the surface, this information may be very useful to study defects on a surface.

5.2 The Two Dimensional Dipole Summations:

As we have discussed in Chapter II, the two dimensional dipole sums at an arbitrary point $\vec{\rho}$ on a surface can be defined as:

$$S_3^{2D}(\vec{q},\vec{\rho},m) = \Sigma'_{\ell} \frac{\exp(i\vec{q}\cdot\vec{x}_{\ell m})}{|\vec{\rho}_{\ell m}|^3}, \tag{5.3}$$

and

$$S_5^{2Dij}(\vec{q},\vec{\rho},m) = \Sigma'_{\ell} \frac{\rho^i_{\ell m}\rho^j_{\ell m}\exp(i\vec{q}\cdot\vec{x}_{\ell m})}{|\vec{\rho}_{\ell m}|^5}. \tag{5.4}$$

The prime on the sum indicates that the point $\rho_{\ell m}= 0$ is excluded, $\vec{q}$ is the external wave vector which is a three dimensional quantity, $\vec{x}_{\ell m}=\vec{\rho}_{\ell m}+\vec{z}$ and at the surface z=0, i and j run from 1 to 2 and represent the two components of the two dimensional Cartesian coordinate, $\vec{\rho}_{\ell m}= \vec{\rho} - \vec{r}_{\ell} - \vec{r}_m$, and $\vec{\rho}$ is an arbitrary position in a surface unit cell. For a calculation of the local fields at the dipole's site, we take $\vec{\rho}$ at the dipole site. $\vec{r}_{\ell}$ is the two

dimensional lattice primitive vector and $\vec{r}_m$ is the position of the mth basis in the primitive cell. If we define the dipole sum $S_{ij}^{2D}(\vec{q},\vec{\rho},m)$,

$$S_{ij}^{2D}(\vec{q},\vec{\rho},m) = 3S_5^{2Dij}(\vec{q},\vec{\rho},m) - \delta_{ij}S_3^{2D}(\vec{q},\vec{\rho},m), \tag{5.5}$$

then, as we defined in chapter II and III, the i^{th} component of the dipole field at the $\vec{\rho}$ point can be written as:

$$E_p^i(\vec{q},\vec{\rho}) = \Sigma_{m,j} S_{ij}^{2D}(\vec{q},\vec{\rho},m)p_m^j. \tag{5.6}$$

The derivation of the two dimensional dipole summations closely follows the three dimensional dipole summation derivation in Chapter II. We use Euler's integral (2.6) and take the Fourier transform for a two dimensional system which gives (see Appendix A):

$$\Sigma_\ell \exp(i\vec{q}\cdot\vec{\rho}_{\ell m} - \rho_{\ell m}^2 t) = \Sigma_G \frac{\exp[i\vec{G}\cdot(\vec{\rho}-\vec{r}_m)]}{\sigma_c}\cdot\left(\frac{\pi}{t}\right)\exp\left(\frac{-G'^2}{4t}\right), \tag{5.7}$$

$$\Sigma_l \rho_{lm}^i\rho_{lm}^j\exp(i\vec{q}\cdot\vec{\rho}_{lm} - \rho_{lm}^2 t) = \Sigma_G \frac{\exp[i\vec{G}\cdot(\vec{\rho}-\vec{r}_m)]}{\sigma_c}\cdot\left(\frac{1}{2t}\delta_{ij} - \frac{G_i'G_j'}{4t^2}\right)\cdot\left(\frac{\pi}{t}\right)\exp\left(\frac{-G'^2}{4t}\right), \tag{5.8}$$

$\vec{G}$ is the two dimensional reciprocal lattice vector. Notice that for the $\vec{G} = 0$ term, $\vec{G}' \neq 0$, where $\vec{G}' = \vec{G} - \vec{q}$, and $\vec{q}$ is the external wave vector, These two equations are called the two dimensional theta

function transformations. We will use them to derive the two dimensional dipole summations and they will be used to prove that the final results of the two dimensional dipole sums are independent of the Ewald parameter.

As in three dimensions, we may now write the n^{th} order dipole sum as:

$$S_n^{2D}(\vec{\rho},m) = \frac{1}{\Gamma(n/2)} \int_0^{\infty} t^{(\frac{n}{2} - 1)} \Sigma'_{\ell m} \exp(i\vec{q}\cdot\vec{x}_{\ell m} - \rho_{\ell m}^2 t)\, dt. \qquad (5.9)$$

We break the integral into two parts, one from 0 to η and the other from η to ∞. Notice that the perfect lattice and the imperfect lattice sums are related by

$$\Sigma_{\ell} \exp(i\vec{q}\cdot\vec{\rho}_{\ell m} - \rho_{\ell m}^2 t) = \Sigma'_{\ell} \exp(i\vec{q}\cdot\vec{\rho}_{\ell m} - \rho_{\ell m}^2 t) - 1. \qquad (5.10)$$

We can substitute the two dimensional theta function transformation into the first part and make it look like the incomplete gamma function. Then, using the recurrence formula of the incomplete gamma function introduced in Chapter II, we can derive the following equation:

$$\Gamma(-\tfrac{1}{2}, x) = 2[x^{-1/2} \exp(-x) - \Gamma(\tfrac{1}{2}, x)]. \qquad (5.11)$$

The final results for the two dimensional dipole sums at the dipole's site are:

$$S_3^{2D}(\vec{q},M,m') = \frac{4\sqrt{\pi}}{\sigma_c}\Sigma_G \exp[i\vec{G}\cdot(\vec{\rho}-\vec{r}_{m'})]\{\sqrt{\eta}\exp(\frac{-G'^2}{4\eta}) - \frac{|\vec{G}'|}{2}\sqrt{\pi}[1-F(\frac{|\vec{G}'|}{2\sqrt{\eta}})]\} - \delta_{m,m'}\frac{4\eta^{3/2}}{3\sqrt{\pi}} + \Sigma'_\ell \frac{\exp(i\vec{q}\cdot\vec{\rho}_{\ell m'})}{|\vec{\rho}_{\ell m'}|^3}\{[1-F(\sqrt{\eta}\cdot\rho_{\ell m'})] + \frac{2}{\sqrt{\pi}}\sqrt{\eta}\cdot\rho_{\ell m'}\exp(-\eta\rho_{\ell m'}^2)\}, \quad (5.12)$$

and,

$$S_5^{2Dij}(\vec{q},M,m') = \frac{4\sqrt{\pi}}{3\sigma_c}\Sigma_G \exp[i\vec{G}\cdot(\vec{\rho}-\vec{r}_{m'})]\{[\sqrt{\eta}\exp(\frac{-G'^2}{4\eta}) - \frac{|\vec{G}'|}{2}\sqrt{\pi}(1-F(\frac{|\vec{G}'|}{2\sqrt{\eta}}))]\delta_{ij} - \frac{G'_iG'_j}{|G'|}\frac{\sqrt{\pi}}{2}[1-F(\frac{|\vec{G}'|}{2\sqrt{\eta}})]\} + \Sigma'_\ell \frac{\rho^i_{\ell m'}\rho^j_{\ell m'}\exp(i\vec{q}\cdot\vec{\rho}_{\ell m'})}{|\vec{\rho}_{\ell m'}|^5}\{[1-F(\sqrt{\eta}\cdot\rho_{\ell m'})] + \frac{2}{\sqrt{\pi}}\sqrt{\eta}\cdot\rho_{\ell m'}\exp(-\eta\rho_{\ell m'}^2) + \frac{4}{3\sqrt{\pi}}(\eta\rho_{\ell m'}^2)^{3/2}\exp(-\eta\rho_{\ell m'}^2)\}. \quad (5.13)$$

where η is the Ewald parameter and F(x) is the error function introduced in Chapter II. For a calculation of the dipole sum off the dipole's site (i.e. at $\vec{\rho} \neq \vec{r}_\ell$ or $\vec{r}_m$), the dipole sums are over a perfect lattice, so that the term $\frac{4\eta^{3/2}}{3\sqrt{\pi}}$ in Eq.(5.12), which comes from the exclusion of the dipole's self contribution, is vanishing.

Now we prove that the two dimensional dipole sums are independent of the Ewald parameter η. For convenience, we set $\eta = \sqrt{\xi}$, and take the partial derivative of the dipole sums with respect the parameter ξ.

$$\frac{\partial S_3^{2D}}{\partial \xi} = \frac{4\sqrt{\pi}}{\sigma_c} \Sigma_G \exp[i\vec{G}\cdot(\vec{\rho} - \vec{r}_m)] \{ \exp(\frac{-G'^2}{4\xi^2}) + \frac{G'^2}{2\xi^2}\exp(\frac{-G'^2}{4\xi^2}) - \frac{G'^2}{4\xi^2}\sqrt{\pi}\frac{\partial F(x_G)}{\partial x_G} - \frac{4\xi^2}{\sqrt{\pi}} + \Sigma'_\ell \frac{\exp(i\vec{q}\cdot\vec{\rho}_{\ell m})}{|\vec{\rho}_{\ell m}|^3}\{-\rho_{\ell m}\frac{\partial F(x_r)}{\partial x_r} + \frac{2}{\sqrt{\pi}}\rho_{\ell m}\exp(-\xi^2\rho_{\ell m}^2) - \frac{4}{\sqrt{\pi}}\xi^2\rho_{\ell m}^3\exp(-\xi^2\rho_{\ell m}^2)\}, \quad (5.14)$$

where, $x_G = \frac{|G'|}{2\xi}$, and $x_r = \xi\rho_{\ell m}$. Using the following formula:

$$\frac{\partial F(x)}{\partial x} = \frac{2}{\sqrt{\pi}}\exp(-x^2), \quad (5.15)$$

the two dimensional theta function transformation and Equation (5.6), we immediately get:

$$\frac{\partial S_3^{2D}}{\partial \xi} = 0. \quad (5.16)$$

In the same way we can prove:

$$\frac{\partial S_5^{2Dij}}{\partial \xi} = 0. \quad (5.17)$$

Therefore, the two dimensional dipole sums are independent of the Ewald parameter η just like the three dimensional dipole sums. The convergence and the independence of the Ewald parameter η is shown in Table 5.1 and 5.2.

Table 5.1 The convergence of the two dimensional dipole sums for simple square surface lattice. External wave vector $\vec{q}$ is along the z direction and $q \cdot a = 4.1931 \times 10^{-2}$, where a is the lattice constant. The Ewald parameter $\eta = 1.75$ and N is the number of terms taken in the dipole sums in both real and wave vector space.

N	S_3^{2D}	S_5^{2D11}	$S_5^{2D12} = S_5^{2D21}$	S_5^{2D22}
3	9.0073	4.5080	0.0000	4.5080
6	9.0073	4.5080	0.0000	4.5080
9	9.0073	4.5080	0.0000	4.5080

Table 5.2 The independence of the Ewald parameter of the two dimensional dipole sums. For a simple square surface structure with different Ewald parameter η. N = 3, all other conditions are the same as in Table 5.1.

η	S_3^{2D}	S_5^{2D11}	$S_5^{2D12} = S_5^{2D21}$	S_5^{2D22}
1.25	9.0073	4.5080	0.0000	4.5080
1.50	9.0073	4.5080	0.0000	4.5080
1.75	9.0073	4.5080	0.0000	4.5080
2.00	9.0073	4.5080	0.0000	4.5080

5.3 Two Dimensional Macroscopic Average Field:

The macroscopic average field for the two dimensional system can be calculated by averaging the local fields over a unit cell on the surface, which is just the zero order Fourier component of the local field. The i^{th} component of the macroscopic average field can be written as follows:

$$< E_i(\vec{q}) >_{2D} = \frac{1}{\sigma_c} \int_{cell} E_L^i(\vec{q},\vec{\rho})\ d^2\rho. \tag{5.18}$$

The local field is due to the external field plus the contribution of the fields from all the dipoles on the surface, except the self contribution if $\vec{\rho}$ is taken at a dipole's site. We can rewrite the equation above as

$$< E_i(\vec{q}) >_{2D} = E_{ext}^i + \frac{1}{\sigma_c} \int_{cell} E_p^i(\vec{q},\vec{\rho})\ d^2\rho, \tag{5.19}$$

where $E_p^i(\vec{q},\vec{\rho})$ is the interactive dipole's field. At a point on the surface which is not a dipole then $\vec{E}_p$ is the sum over a perfect dipole lattice. If the point is a dipole's site, then the self contribution must be excluded and the sum is over an imperfect lattice. By using the dipole sums defined in section 5.1, we can rewrite the macroscopic average field as

$$< E_i >_{2D} = E_{ext}^i + \Sigma_{m,j} S_{ij}^{2D}(\vec{q},m)|_{G=0} p_m^i. \tag{5.20}$$

$S_{ij}^{2D}(\vec{q},m)|_{G=0}$ is the zero order Fourier component of the dipole sum of the m^{th} sublattice (it is not dependent on $\vec{\rho}$, so we did not write out the variable $\vec{\rho}$ in S_{ij}^{2D} for simplification), and it can be obtained by directly applying Euler's integral and the two dimensional theta function transformations. Notice that there are two kinds of dipole sums at the surface, one is due to the perfect lattice, i.e when we take $\vec{\rho} \neq \vec{r}_\ell$ or $\vec{r}_m$. Another is due to an imperfect lattice, when we take $\vec{\rho}$ at the dipole's site. Using the same method we used for the three dimension case in Chapter II, the zero order Fourier component for both kinds of dipole sums can be written as:

$$S_3^{2D}(\vec{q},m)|_{G=0} = \lim_{\mu\to o} \frac{2\sqrt{\pi}}{\sigma_c} \int_\mu^\infty \frac{\exp(-\frac{q^2}{4t})}{\sqrt{t}}\, dt$$
$$= \frac{4\pi}{\sigma_c q}, \qquad (5.21)$$

and

$$S_5^{2Dij}(\vec{q},m) = \lim_{\mu\to o} \frac{2\sqrt{\pi}}{3\sigma_c} \int_\mu^\infty \left[\frac{\exp(-\frac{q^2}{4t})}{\sqrt{t}}\,\delta_{ij} - \frac{q_i q_j}{2}\,\frac{\exp(-\frac{q^2}{4t})}{t^{3/2}}\right] dt$$
$$= \frac{4\pi}{3\sigma_c q}\left[\delta_{ij} - \frac{q_i q_j}{2}\right], \qquad (5.22)$$

where, we use:

$$\int_o^\infty \frac{\exp(-\frac{q^2}{4t})}{\sqrt{t}}\, dt = \frac{2\sqrt{\pi}}{q}. \qquad (5.23)$$

Then $S_{ij}^{2D}(\vec{q},m)|_{G=0}$ can be written as

$$S_{ij}^{2D}(\vec{q},m)|_{G=0} = -\frac{2\pi}{\sigma_c}\cdot\frac{q_i q_j}{q}, \tag{5.24}$$

and the two dimensional macroscopic average field can be written as:

$$< \vec{E} >_{2D} = \vec{E}_{ext} - \frac{2\pi}{\sigma_c}\cdot\frac{\vec{q}}{q}\Sigma_m(\vec{q}\cdot\vec{p}_m). \tag{5.25}$$

If the surface is the x-y plane, and the external field wave vector $\vec{q}$ is along the z direction, then the second term will vanish since from Eq.(5.24) we have $S_{ij}^{2D}=0$. So $S_{ij}^{2D}|_{\text{all G}} = S_{ij}^{2D}|_{G\neq 0}$ for i and j =1,2 on the surface. Then, for the ADM with a surface structure has m identical atoms per primitive cell, the L-factor can be calculated from $nL_{ij}=\Sigma_{m'}\sigma_c\cdot S_{ij}^{2D}(\vec{q},M,m')|_{\text{all G}}$ for $\vec{q}$ along z direction, where $S_{ij}^{2D}(\vec{q},M,m')$ is the dipole sum due to the m'^{th} sublattice at the dipole M which is on the sublattice m. If the atoms per primitive cell are not identical, or if using the BDM, then the L-factor can not be obtained so easily because the local fields at each dipole's site may be different. Also we have that the local field on the surface $\vec{E}_L(\vec{q}\neq 0)=\vec{E}_L(\vec{q}=0)$ for $\vec{q}$ not on the surface since S_{ij}^{2D} is directly related to the L-factor which is a q=0 case. This leads to the conclusion that the dielectric constant of the surface $\epsilon(\vec{q}\neq 0) = \epsilon(\vec{q}=0)$. For the case of $\vec{q}$ along i on the surface, we have $E_L^i(\vec{q}\neq 0)\neq E_L^i(\vec{q}=0)$ and $E_L^j(\vec{q}\neq 0)=E_L^j(\vec{q}=0)$ for $j\neq i$, because $\vec{E}_L(\vec{q}\neq 0)$ is determined by S_{ij}^{2D} which is different from L_{ij} along $\vec{q}$'s direction. However, ϵ_{ij} is still determined by L_{ij}, just as in three dimensions. So $\epsilon(\vec{q}\neq 0) = \epsilon(\vec{q}=0)$ always holds and it is independent of the

direction of the $\vec{q}$. From Eq.(2.24) we notice that when $\vec{q}$ has components on the surface, $S_{ij}^{2D}|_{G=0}$ depends on $q_i q_j/q$. The dielectric constant, however, is determined by the L-factor which is related to $S_{ij}^{2D}|_{G\neq 0}$ which, is regular at $\vec{q}$=0. Also because q is very small and the dipole sum converges very quickly, $\mathrm{Re}[\exp(i\vec{q}\cdot\vec{\rho}_l)$ is approximately equal to 1 and therefore $S_{ij}^{2D}|_{G\neq 0}$ is insensitive to q. This is shown in Table 5.3 (a) and (b). This leads to another conclusion that in two dimension there is NO sum rule for S_{ij}^{2D} since $S_{ij}^{2D}|_{G=0}$ is function of $\vec{q}$.

5.4 Self-Consistent Calculations Using Two Types of Dipole Models:

In this calculation we set the external field wave vector $\vec{q}$ along the z direction. The polarization of the external field lays on the x-y plane and we always take it to be a unit vector. So the second term in Eq.(5.25) is always zero and the dipole sums only depend on the surface structure and are directly related to the surface L-factor. Following the self-consistent approach the local field at a site M can be written as the sum of the external field E_{ext} plus the dipole fields $E_p(\vec{q},M,m')$. The equations of the coupled local fields can be expressed in the same way as in Chapter III. The dipole field E_p depends on the different dipole models and the crystal structure.

Let's consider a center rectangular surface structure with identical atoms per primitive cell, as shown in figure 5.1(a), where

Table 5.3 The insensitivity of the two dimensional dipole sum to the different magnitude of q·a for the simple square structure. The Ewald parameter η =1.75 and the number of unit cell N = 3. S^{2D12}_{5} = S^{2D21}_{5} = 0.0000 is not listed in the Table. $S^{2D}_{ij} = 3S^{2Dij}_{5} - \delta_{ij}S^{2D}_{3}$.

(a) $\vec{q}$ along the z direction: $S^{2D}_{ii}|_{\text{all G}} = S^{2D}_{ii}|_{G\neq 0}$.

q·a= 4.1931×	S^{2D}_{3}	S^{2D11}_{5}	S^{2D22}_{5}	$S^{2D}_{11} = S^{2D}_{22}$
10^{-2}	8.7719	4.4296	4.4296	4.5169
10^{-3}	9.0073	4.5080	4.5080	4.5168
10^{-4}	9.0310	4.5159	4.5159	4.5168
10^{-6}	9.0336	4.5168	4.5168	4.5168

(b)$\vec{q}$ along the [101] direction: $q_1a=q_3a=qa/\sqrt{2}$, $S^{2D}_{11}|_{G=0} = -\frac{2\pi}{\sigma_c}\cdot\frac{q_1^2}{q}$.

q·a= $\sqrt{2}$·4.1931×	$S^{2D}_{11}|_{\text{all G}}$	$S^{2D}_{11}|_{G\neq 0}$	$S^{2D}_{22}|_{G\neq 0} = S^{2D}_{22}|_{\text{all G}}$
10^{-3}	4.4982	4.5168	4.5168
10^{-6}	4.5168	4.5168	4.5168

$S^{2D}_{11}|_{G=0}$ = 0.0186 for $qa=10^{-3}$, $S^{2D}_{11}|_{G=0} \cong$ 0.0000 for $qa=10^{-6}$.

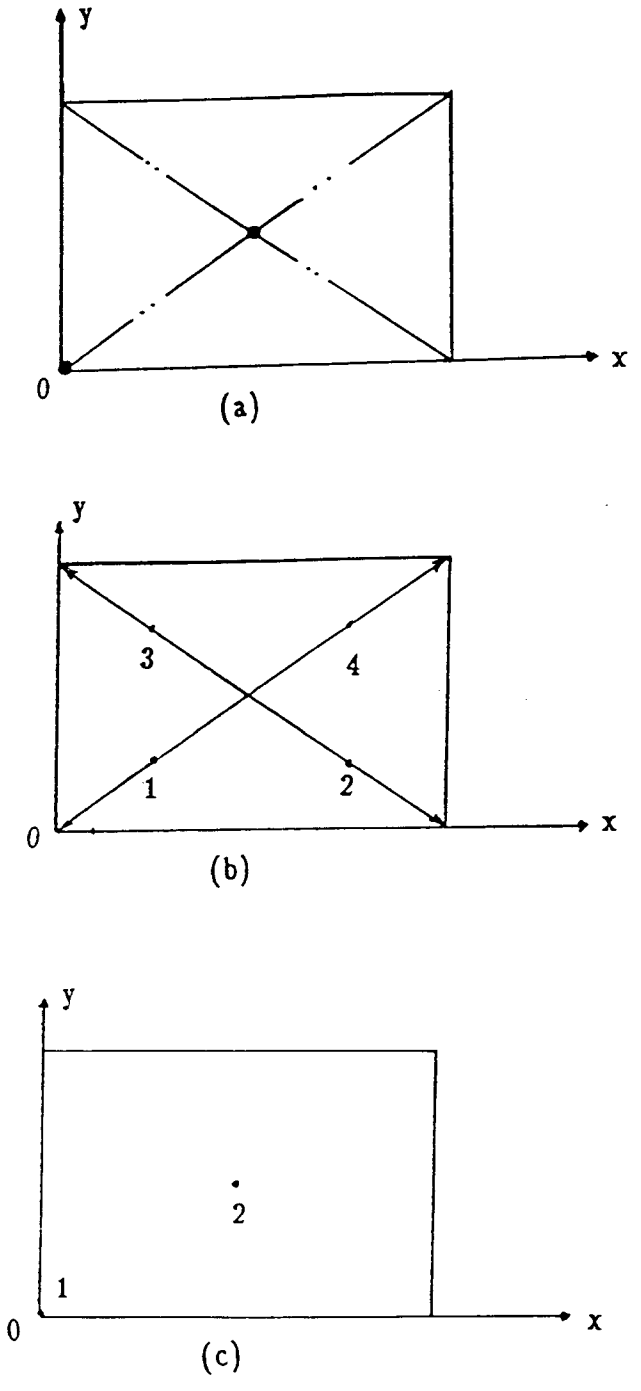

Figure 5.1 (a) Two dimensional centered rectangular structure, (b) lattice of the bond dipoles, and (c) lattice of the atomic dipoles.

a and b are the lattice constants. The ratio γ=b/a, and when γ = 1 the structure is a center square structure.

Consider the atomic dipole model (ADM). There are two atoms per unit cell for the center rectangular structure on a surface (Figure. 5.1(c)). We can use the rectangular Bravais lattice with two basis atoms to represent its structure. Tables 5.4 and 5.5 list the local field at the two dipole sites for a center square surface structure under different polarizations of the external field. For the two atoms are identical, the ADM results shown that the local fields at the two dipole sites that are exactly the same. However, if the two atoms are different, then the ADM results will give the local fields at the two dipole sites are different since the dipole sums $S_{ii}^{2D}(\vec{q},M,m')$ are different for different M and m'. However, for the system with identical atoms, we see that for the two dimensional system the local field and the local field affected linear susceptibility still have the Lorentz form. The Lorentz factor is different from three the dimensional problem, i.e.

$$E_L^i(\vec{q}) = \frac{E_{ext}^i}{1 - \alpha \cdot \Sigma_m S_{ii}^{2D}(\vec{q},m)} \text{ (in the principle axis)}, \qquad (5.26)$$

where the variable M in S_{ii}^{2D} and E_L^i is suppressed since local fields

Table 5.4 2D ADM for center square structure. $\vec{q}$ is along the [001] and $\vec{E}_{ext}=(1,0)$. The self-consistent local fields at each dipole's site and the susceptibility ($E_{Li}(m)$: m indicates the number of the dipoles).

a/a^2	$E_{lx}(1)$	$E_{Ly}(1)$	$E_{Lx}(2)$	$E_{Ly}(2)$	χ
0.00	1.0000	0.0000	1.0000	0.0000	0.0000
0.01	1.1465	0.0000	1.1465	0.0000	0.0229
0.05	2.7684	0.0000	2.7684	0.0000	0.2768
0.07	9.4588	0.0000	9.4588	0.0000	1.3242
0.10	-3.6031	0.0000	-3.6031	0.0000	-0.7206
0.13	-1.5133	0.0000	-1.5133	0.0000	-0.3935
0.25	-0.4558	0.0000	-0.4558	0.0000	-0.2279

Table 5.5 2D ADM for center square structure. $\vec{q}$ is along the [001] and $\vec{E}_{ext}=(1/\sqrt{2},1/\sqrt{2})$. The self-consistent local fields at each dipole's site and the susceptibility ($E_{Li}(m)$: m indicates the number of the dipoles).

a/a^2	$E_{lx}(1)$	$E_{Ly}(1)$	$E_{Lx}(2)$	$E_{Ly}(2)$	χ
0.00	0.7071	0.7071	0.7071	0.7071	0.0000
0.01	0.8107	0.8107	0.8107	0.8107	0.0229
0.05	1.9575	1.9575	1.9575	1.9575	0.2768
0.07	6.6884	6.6884	6.6884	6.6884	1.3242
0.10	-2.5478	-2.5478	-2.5478	-2.5478	-0.7206
0.13	-1.0701	-1.0701	-1.0701	-1.0701	-0.3935
0.25	-0.3223	-0.3223	-0.3223	-0.3223	-0.2279

$S_{11}^{2D}(\vec{q},1,1) = 4.5168$, $S_{22}^{2D}(\vec{q},1,1) = 4.5168$;

$S_{11}^{2D}(\vec{q},1,2) = 8.2587$, $S_{22}^{2D}(\vec{q},1,2) = 8.2587$.

$2L = \Sigma_m S_{ii}^{2D}(q,1,m)$, $L = 6.3878$ for center square surface..

at each identical atom's site are the same. The susceptibility is determined by:

$$\chi_{ij} = \frac{n\alpha/ab}{1 - L_{ij}n\alpha/ab}, \quad (i \& j = 1,2) \tag{5.27}$$

where the L factor for a center square lattice is: L = 6.3878, a and b are the lattice constant, and n is the number of atomic dipoles per unit cell (n = 2 in this case). Notice that for a two dimensional system with identical atoms, the simple square structure and the center square structure have different L-factors (from Table 5.3, for a simple square surface, L = 4.5168), which is not like the three dimensional system where for cubic symmetry L is always $4\pi/3$ even if we have different values of n for different cubic systems. In Table 5.5 we also list the values $S_{ij}^{2D}(\vec{q},M,m')$ at M=1 for m'=1 and 2, we can see that they are different. However, since the two atoms are identical, we still have the local fields at each atom's site are the same, we have $2L=\Sigma_m S_{ij}^{2D}(\vec{q},M,m')$, and get L= 6.3878. Table 5.6 list the results of local field and linear susceptibility using these functional forms for the case of an external field along (10) direction. We can see the excellent agreement with table 5.4. Table 5.7 lists the L-factor for a simple rectangular surface structure with different lattice ratio b/a. Table 5.8 lists the L-factor for

Table 5.6 2D ADM for center square structure. Using the functional form to repeat the calculation in Table 5.4

a/a^2	$E_{lx}(1)$	$E_{Ly}(1)$	$E_{Lx}(2)$	$E_{Ly}(2)$	χ
0.00	1.0000	0.0000	1.0000	0.0000	0.0000
0.01	1.1465	0.0000	1.1465	0.0000	0.0229
0.05	2.7684	0.0000	2.7684	0.0000	0.2768
0.07	9.4600	0.0000	9.4600	0.0000	1.3244
0.10	-3.6028	0.0000	-3.6028	0.0000	-0.7206
0.13	-1.5133	0.0000	-1.5133	0.0000	-0.3934
0.25	-0.4558	0.0000	-0.4558	0.0000	-0.2279

Table 5.7 2D ADM for simple rectangular structure. Calculated L-factor for different lattice ratio γ = b/a. $\vec{q}$ is along the [001].

γ	$L_{xx}=\sigma_c \cdot S_{11}^{2D}$	$L_{yy}=\sigma_c \cdot S_{22}^{2D}$
0.4	-8.4459	30.0513
0.5	-3.0350	19.2314
0.6	-0.0879	13.3467
0.7	1.7110	9.7791
0.8	2.9192	7.4283
0.9	3.8072	5.7666
1.0	4.5168	4.5168
1.1	5.1262	3.5250
1.2	5.6792	2.7017
1.5	7.1969	0.7975
1.7	8.1693	-0.2114
2.0	9.6157	-1.5175
2.5	12.0205	-3.3783
3.0	14.4247	-5.0190

Table 5.8 2D ADM for center rectangular structure. Calculated L-factor for different lattice ratio γ = b/a. ($\vec{q}$ is along the [001], $\vec{q}$ and M=1 did not write out in $S_{ii}^{2D}(\vec{q},M,m)$).

γ	$S_{11}^{2D}(1)$	$S_{22}^{2D}(1)$	$S_{11}^{2D}(2)$	$S_{22}^{2D}(2)$	L_{xx}	L_{yy}
1.0	4.5168	4.5168	8.2587	8.2587	6.3878	6.3878
1.2	4.7327	2.2514	4.2748	8.1121	5.4044	6.2180
1.4	4.7883	0.9752	2.1846	7.3257	4.8810	5.8107
1.6	4.8029	0.1720	1.1114	6.3547	4.7315	5.2214
1.8	4.8068	-0.3718	0.5652	5.4181	4.8348	4.5418
2.0	4.8078	-0.7587	0.2879	4.5974	5.0957	3.8387

center rectangular structure (i.e. the simple rectangular lattice with two basis atoms) with a different ratio b/a. Figure 5.2 shows the L-factor vs b/a for simple rectangular structure. For the anisotropic structure, the Lorentz factor is a tensor, corresponding to the susceptibly tensor. In principle axis, we have $S^{2D}_{i\neq j} = 0$ and there are only two independent elements (L_{xx} and L_{yy}) for the two dimensional problem, corresponding to $L_{xx} = \sigma_c \cdot S^{2D}_{11}$ and $L_{yy} = \sigma_c \cdot S^{2D}_{22}$, where S^{2D}_{ii} are at the dipole's site (for a simple rectangular structure with only one atom per primitive cell).

Notice that if we exchange the x and y axis, even if we maintain a constant a·b, L_{xx} does not have symmetry with L_{yy}. This is because the lattice constant a in the old coordinate system is a constant. In the new coordinate system the lattice constant along the x direction is b, which is not a constant. However, if we multiple the ratio of b/a by their L-factors (L_{xx} and L_{yy}), then we obtain the symmetry of the L-factor. For example from Table 5.7, taking L-factors for b/a=2 and multiplying by 2, is the same as exchanging the two L-factors for b/a=0.5.

Figure 5.3 shows the results of χ_{ij} vs a/ab for the center rectangular structure using the ADM. For $\gamma = 1$, the functional form of the self-consistent calculation for the atomic dipole model has the same form as we obtained in the three dimensional calculations. The only difference is the Lorentz factor. However, for the center square structure the linear susceptibility is a scalar and it will

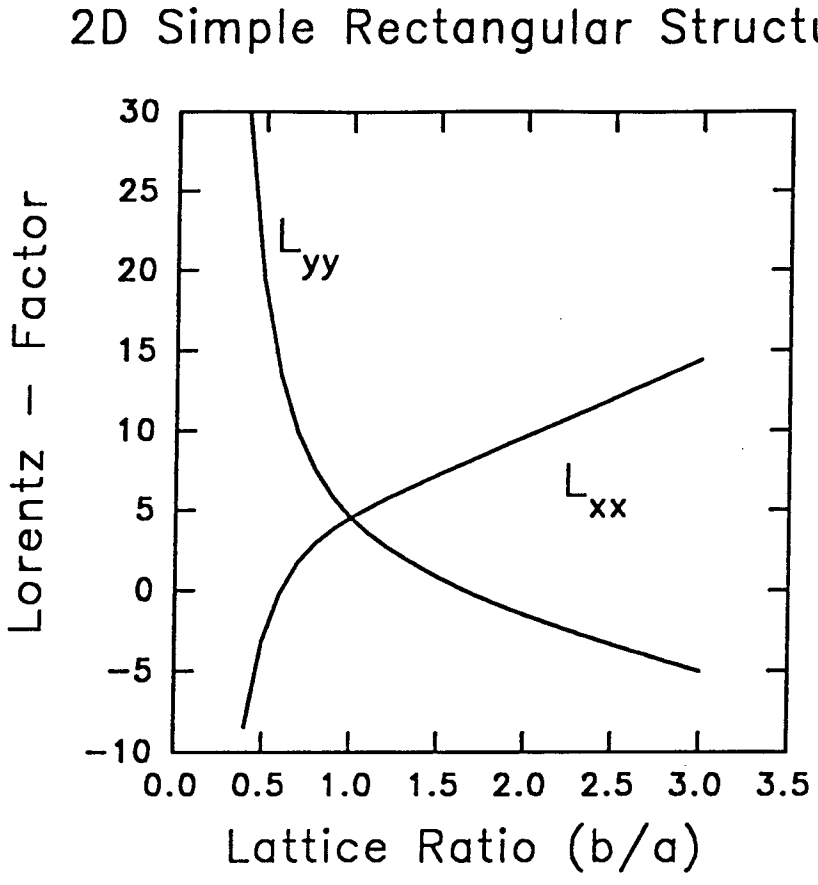

Figure 5.2 Plot of the L-factor vs lattice ratio b/a.

2D CENTER RECTANGULAR STRUCTURE: ADM

(a)

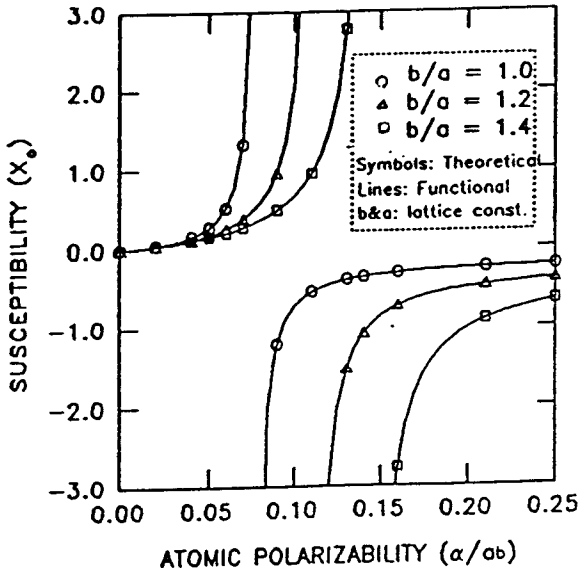

(b)

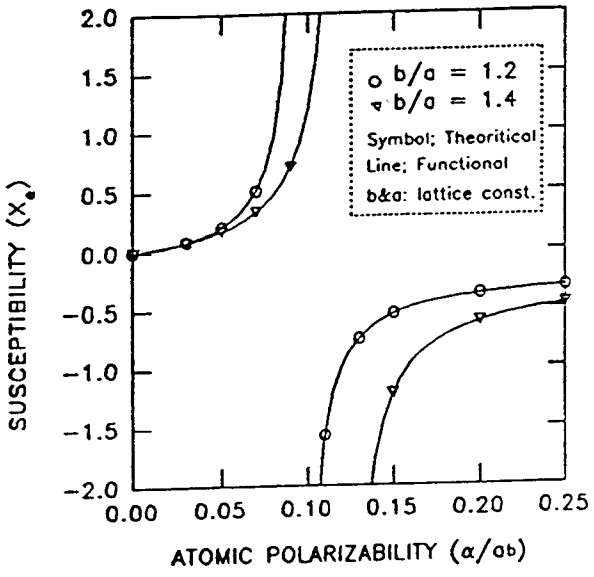

Figure 5.3 2D ADM in the center rectangular structure: (a) the ordinary susceptibility (χ_{11}) and (b) the extraordinary susceptibility (χ_{22}) for different lattice ratio b/a. Plot of the susceptibility vs the atomic polarizability (α/ab).

not change it's value for different polarizations of the external fields, which we can see from tables 5.4 and 5.5. For the center rectangular structure ($\gamma > 1$), the linear susceptibility is a second order tensor and the material is birefringence. In principle axis we have $\chi_{12} = \chi_{21} = 0$, and χ_{11} and χ_{22} are two independent numbers. They are related to the ordinary and extra-ordinary refractive index n_o and n_e by $n_o = \sqrt{\epsilon_o}$, and $n_e = \sqrt{\epsilon_e}$, where $\epsilon_o = 1 + 4\pi\chi_{11}$, and $\epsilon_e = 1 + 4\pi\chi_{22}$.

To evaluate the local field off the dipole's site (i.e. at $\vec{\rho} \neq \vec{r}_\ell$ or $\vec{r}_m$), we need to calculate $S_{ij}^{2D}(\vec{q},\vec{\rho},m)$. As we obtained in chapter III, we can use Eq.(3.17) to evaluate $\vec{E}_L(\vec{q},\vec{\rho})$ for the two dimensional systems. Table 5.9 lists $S_{ij}^{2D}(\vec{q},\vec{\rho})$ (m=1 did not write out in $S_{ij}^{2D}(\vec{q},\vec{\rho},m)$) at different points $\vec{\rho}$ for a simple rectangle structure with a different lattice ratio b/a. By using Eq.(3.17) we can immediately see that at the center of the simple rectangular structure $S_{ii}^{2D}(\vec{q},\vec{\rho}) > L_{ii}$. Hence, the local field at the center is larger than the local field at the atom's site. Also if $\vec{\rho}_1$ is closer to the atom's site than $\vec{\rho}_2$, then, $E_L(\vec{\rho}_1) > E_L(\vec{\rho}_2)$.

In the bond dipole model (BDM) calculation, the center rectangular structure can be represented as a simple rectangular Bravais lattice with four basis dipoles as we have shown in Figure 5.1(b). The primitive lattice vector $\vec{r}_\ell$ is defined to be $a(\ell_1\hat{x} + \gamma\ell_2\hat{y})$, where ℓ_1 and ℓ_2 are integers and γ=b/a. If we take a dipole's site as the origin, then the coordinates of the four bond

Table 5.9 2D ADM for simple rectangular structure. Calculated dipole sum $S_{ij}^{2D}(\vec{q},\vec{\rho})$ at different point $\vec{\rho} = (\rho_x, \rho_y)$, with different lattice ratio γ=b/a. $\vec{q}$ is along the [001].

γ	(0.5, 0.5*γ)		(0.5, 0.0)	
	S_{11}^{2D}	S_{22}^{2D}	S_{11}^{2D}	S_{22}^{2D}
0.4	48.3909	0.8430	50.3071	-0.8449
0.5	36.7790	2.3036	42.2046	-2.3282
0.6	27.9292	4.1066	38.0077	-4.2334
0.7	20.9653	5.7838	35.8621	-6.1684
0.8	15.5328	7.0648	34.7743	-7.9097
0.9	11.3770	7.8755	34.2242	-9.3815
1.0	8.2587	8.2587	33.9459	-10.5869

γ	(0.0, 0.5*γ)		(0.25, 0.0)	
	S_{11}^{2D}	S_{22}^{2D}	S_{11}^{2D}	S_{22}^{2D}
0.4	-246.5008	525.9001	139.0971	-31.6389
0.5	-121.4742	269.2638	135.7837	-42.3476
0.6	-66.9623	155.8380	134.9318	-49.3821
0.7	-39.7176	98.1751	134.7100	-53.9764
0.8	-24.7637	65.8429	134.6516	-57.0578
0.9	-15.9901	46.3569	134.6361	-59.1983
1.0	-10.5869	33.9459	134.6319	-60.7371

dipoles are: $(0,0)$, $\frac{a}{2}(1,0)$, $\frac{a}{2}(0,\gamma)$, $\frac{a}{2}(1,\gamma)$. The four bond directions are:

$$\begin{aligned}
\hat{d}_1 &= (-1,-\gamma)/\sqrt{(1+\gamma^2)} \\
\hat{d}_2 &= (1,-\gamma)/\sqrt{(1+\gamma^2)} \\
\hat{d}_3 &= (-1,\gamma)/\sqrt{(1+\gamma^2)} \\
\hat{d}_4 &= (1,\gamma)/\sqrt{(1+\gamma^2)}.
\end{aligned} \tag{5.28}$$

For $\gamma=1$, i.e. the centered square structure, the local field equations are composed of eight coupled equations. Not only is there the coupling between the four dipoles, but also the coupling between each of the components of the local field. The coefficients of each component of the local fields are the sixteen different $S_{ij}^{2D}(q,M,m')$ for m=1..4, with different M (M=1..4) as the origin.

Because of the different bond orientations, the surface calculations using the bond dipole model will give us different pictures of the local fields than the ADM. Tables 5.10 and 5.11 list for polarization of the external field along different directions on the surface, the results of the self-consistent local fields at the four dipole positions and the linear susceptibility, for the center square surface structure. By comparing table 5.10 and 5.11, we can immediately see that local field effects do not change the isotropic property of the linear dielectric constant. However, the local

Table 5.10 2D BDM for center square structure. $\vec{q}$ is along the [001] and $\vec{E}_{ext}$ = (1,0). The self-consistent local fields at each dipole's site and the susceptibility ($E_{Li}(m)$: m indicates the number of the dipoles).

a/a^2	$E_{Lx}(1)$ $E_{Lx}(3)$	$E_{Ly}(1)$ $E_{Ly}(3)$	$E_{Lx}(2)$ $E_{Lx}(4)$	$E_{Ly}(2)$ $E_{Ly}(4)$	χ
0.00	1.0000 1.0000	0.0000 0.0000	1.0000 1.0000	0.0000 0.0000	0.0000
0.03	1.8788 1.8788	-0.2574 0.2574	1.8788 1.8788	0.2574 -0.2574	0.0973
0.05	3.5008 3.5009	-0.7325 0.7325	3.5009 3.5009	0.7325 -0.7325	0.2768
0.07	12.9626 12.9626	-3.5038 3.5038	12.9626 12.9626	3.5038 -3.5038	1.3242
0.08	-64.6037 -64.6037	19.2151 -19.2151	-64.6037 -64.6037	-19.2151 19.2151	-7.2622
0.10	-5.5098 -5.5098	1.9067 -1.9067	-5.5098 -5.5098	-1.9067 1.9067	-0.7206
0.15	-1.9576 -1.9576	0.8663 -0.8663	-1.9576 -1.9576	-0.8663 0.8663	-0.3274
0.25	-1.0589 -1.0589	0.6030 -0.6030	-1.0589 -1.0589	-0.6030 0.6030	-0.2279

Table 5.11 2D BDM for center square structure. $\vec{q}$ is along the [001] and $\vec{E}_{ext} = (1/\sqrt{2}, 1/\sqrt{2})$. The self-consistent local fields at each dipole's site and the susceptibility ($E_{Li}(m)$: m indicates the number of the dipoles).

a/a^2	$E_{Lx}(1)$ $E_{Lx}(3)$	$E_{Ly}(1)$ $E_{Ly}(3)$	$E_{Lx}(2)$ $E_{Lx}(4)$	$E_{Ly}(2)$ $E_{Ly}(4)$	χ
0.00	0.7071 0.7071	0.7071 0.7071	0.7071 0.7071	0.7071 0.7071	0.0000
0.03	1.1465 1.5106	1.1465 1.5106	1.5106 1.1465	1.5106 1.1465	0.0973
0.05	1.9575 2.9934	1.9575 2.9934	2.9934 1.9575	2.9934 1.9575	0.2768
0.07	6.6884 11.6435	6.6884 11.6435	11.6435 6.6884	11.6435 6.6884	1.3242
0.08	-32.0945 -59.2689	-32.0945 -59.2689	-59.2689 -32.0945	-59.2689 -32.0945	-7.2622
0.10	-2.5478 -5.2442	-2.5478 -5.2442	-5.2442 -2.5478	-5.2442 -2.5478	-0.7206
0.15	-0.7717 -1.9968	-0.7717 -1.9968	-1.9968 -0.7717	-1.9968 -0.7717	-0.3274
0.25	-0.3223 -1.1751	-0.3223 -1.1751	-1.1751 -0.3223	-1.1751 -0.3223	-0.2279

fields at each bond dipole's site are different. Table 5.12 lists the linear susceptibilities for a center rectangle structure with different lattice ratios γ. Notice that for $\gamma \neq 1$, there is birefringence. As an example for $\gamma = 1.2$, χ_{22} changes sign much slower than χ_{11} when the bond polarizability increase, because the y components of the local field at each dipole's site change very slowly. This is shown in Table 5.13.

Figure 5.4 shows the results of the linear susceptibility as a function of the bond polarizabilities for different values of γ. A general functional formula of the self-consistent local field calculations of the linear susceptibility is of the form,

$$\chi_{ij}(\text{BDM}) = \frac{n\,\tau/(1+\gamma^2)}{1 - L_{ij} n\,\tau}, \tag{5.26}$$

where $\tau = a/ab = \gamma a/a^2$ which is the bond polarizability per area ab, and n is the number of bond dipoles per unit cell, n = 4 in this case. For a lattice ratio $\gamma = 1$, the tensor becomes a scalar, and we have $L(\gamma=1) = 3.1939$, which gives exactly the same form as we have obtained for the ADM (see Eq. (5.26)). This is not surprising and in fact it is a good check for using the BDM and occurs because of the character of the two dimensional bond orientation. For example, when the external field is polarized along the [11] direction, the bond orientation of the center square structure (γ=1) has two dipoles

Table 5.12 2D BDM for center rectangular structure. The self-consistent calculation of susceptibility for different lattice ratio γ.

a/a^2	$\chi(\gamma=1.0)$	$\chi_{11}(\gamma=1.2)$	$\chi_{22}(\gamma=1.2)$	$\chi_{11}(\gamma=1.4)$	$\chi_{22}(\gamma=1.4)$
0.00	0.0000	0.0000	0.0000	0.0000	0.0000
0.02	0.0537	0.0415	0.0414	0.0309	0.0357
0.04	0.1636	0.1734	0.0874	0.1549	0.0674
0.06	0.5140	-3.0145	0.1388	-0.4592	0.0959
0.07	1.3242	-0.4820	0.1669	-0.2153	0.1090
0.09	-1.2017	-0.2274	0.2283	-0.1261	0.1335
0.11	-0.5428	-0.1701	0.2983	-0.0997	0.1556
0.15	-0.3274	-0.1307	0.4716	-0.0798	0.1944
0.20	-0.2572	-0.1127	0.7855	-0.0701	0.2346
0.25	-0.2279	-0.1041	1.3077	-0.0654	0.2678

Table 5.13 2D BDM for center rectangular structure (γ = 1.2). $\vec{q}$ is along the [001] and $\vec{E}_{ext}=(1/\sqrt{2},1/\sqrt{2})$. The self-consistent local fields at each dipole's site and the susceptibility ($E_{Li}(m)$: m indicates the number of the dipoles).

a/a^2	$E_{Lx}(1)$ $E_{Lx}(3)$	$E_{Ly}(1)$ $E_{Ly}(3)$	$E_{Lx}(2)$ $E_{Lx}(4)$	$E_{Ly}(2)$ $E_{Ly}(4)$	χ_{11}	χ_{22}
0.00	0.7071 0.7071	0.7071 0.7071	0.7071 0.7071	0.7071 0.7071	0.0000	0.0000
0.05	4.1224 4.9109	1.4644 0.8086	4.9109 4.1224	0.8086 1.4644	0.4743	0.1124
0.11	-1.7059 0.3870	1.7291 1.9644	0.3870 -1.7059	1.9644 1.7291	-0.1701	0.2983
0.35	-19.1557 19.0313	21.4341 21.5666	19.0313 -19.1557	21.5666 21.4341	-0.0958	5.4422
0.45	25.2101 -25.2689	-26.8427 -26.7159	-25.2689 25.2101	-26.7159 -26.8427	-0.0917	-7.1941
0.50	13.9054 -13.9426	-14.5189 -14.3940	-13.9426 13.9054	-14.3940 -14.5189	-0.0904	-3.9669

2D CENTER RECTANGULAR STRUCTURE: BDM

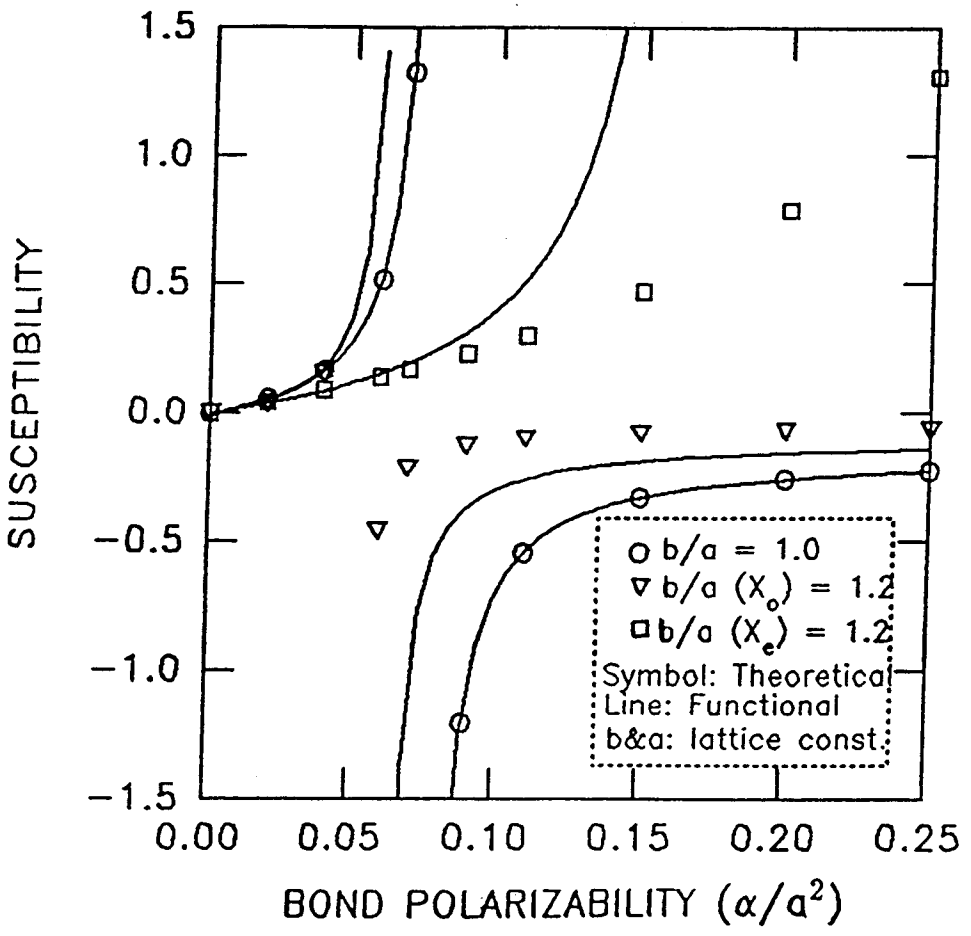

Figure 5.4 2D BDM in the center rectangular structure: the ordinary and the extraordinary susceptibilities for different lattice ratios b/a.

polarized the same as in the ADM. The other two are perpendicular to the external field, so they give no contribution. However, for the $\gamma \neq 1$ case, the bond orientations make a big difference between using the two different kinds of dipole models. The L-factor remains a tensor however, since the local fields at each bond dipole's site are different, the L-factor cannot be obtained easily as in the ADM. By fitting the self consistent calculated data for the case of $\gamma = 1.2$ in principle axis, we have $L_{11}(\gamma=1.2) = 3.875$ and $L_{22}(\gamma=1.2) = 1.525$. The results of the susceptibility calculated using the functional form are listed in Table 5.14, It gives a good approximation in the positive range of the susceptibility.

Table 5.14 2D BDM for center rectangular structure. The calculated susceptibility using the functional form.

a/a^2	$\chi(\gamma=1.0)$	$\chi_{11}(\gamma=1.2)$	$\chi_{22}(\gamma=1.2)$
0.00	0.0000	0.0000	0.0000
0.02	0.0537	0.0475	0.0373
0.04	0.1636	0.1726	0.0867
0.06	0.5140	1.4052	0.1551
0.07	1.3244	-1.3500	0.2003
0.09	-1.2016	-0.3735	0.3271
0.11	-0.5428	-0.2558	0.5481
0.15	-0.3274	-0.1856	2.8929
0.20	-0.2572	-0.1561	-1.4903
0.25	-0.2279	-0.1426	-0.7806

L_{xx}=3.8751 with standard deviation σ=0.0043 in $\chi_{11} > 0$ range.
L_{yy}=1.525 with standard deviation σ=0.029 in $\chi_{11} > 0$ range.

CHAPTER VI

CONCLUSIONS AND FUTURE DEVELOPMENTS

Local field effects on the dielectric properties of semiconductor solids have been investigated using the classical Lorentz-Lorenz (L-L) approach in both its original form with polarizable dipoles located at atomic sites (ADM) and in a modified form with polarizable charge distributions placed along bond directions (BDM). The bond dipole model naturally comes from taking a classical limit of the overlap of quantum sp^3 hybrids orbitals, and it is intended to remedy some of the obvious L-L deficiencies for covalent crystals. In both models the local fields and dielectric constants can be expressed in terms of the familiar L-L formula

$$\epsilon = 1 + \frac{4\pi N\alpha}{1 - LN\alpha}, \tag{6.1}$$

where L is the Lorentz factor (constant) determined by the lattice structure only. The dielectric constant is independent of the magnitude of $|\vec{q}|$ and the direction of the $\vec{q}$. Also $\epsilon(\vec{q}\neq 0) = \epsilon(\vec{q}=0)$ for small q, while the local field $E_L^k(\vec{q}\neq 0) \neq E_L^k(\vec{q}=0)$ for $\vec{q}$ along the k direction and $E_L^i(\vec{q}\neq 0) = E_L^i(q=0)$ for $i\neq k$. In the ADM the Lorentz factor has a value which is familiar from other calculations, in particular it is $\frac{4\pi}{3}$ for cubic crystals. However, in the BDM this constant assumes values different from the ADM values, even for cubic crystal.

The L-L form implies the possibility of strong enhancements or

reductions of the macroscopic average and the local electric fields and even suggests the onset of structural (ferroelectric) phase transitions. Thus because of its qualitative richness it is of some interest to study the range of applicability and possible modifications to this venerable formula.

The calculations have been extended to a two-dimensional crystal where the cubic lattice sum cancellations, important for the original Lorentz derivation, fail. Here too the ADM and the BDM are studied and the variations of local field strength over the two-dimensional surface are studied with an eye towards understanding possible local field related light absorption or light scattering enhancements.

We have also calculated the L-factor using the ADM in three dimensions for a simple tetragonal structure with different lattice ratios c/a, and in two dimension for a simple rectangular and centered rectangular structure with different lattice ratios b/a, with small $\vec{q}\neq 0$ in the dipole sums. For three dimensions the L-factor satisfies a sum rule but for two dimensions there is no sum rule. Even for the same lattice with a different basis (for example, the centered rectangular structure is the same lattice as simple rectangular but with two basis atoms), it has a different L-factor. The method we used here can be compared with Purvis and Taylor[2] who use q=0 in dipole sums and have to impose a special summation order, which corresponds to a certain shape of the crystal in order to avoid the depolarization factor in obtaining the L-factor. This method seems to be a much simpler calculation of the L-factor. Also, the method and the formulas we have obtained here can be easily extended

to quadrupole or even higher multipole calculations. The dipole sum formulas have been used to determine the local field strength at interstitial sites in three-dimensional crystals as well as in two-dimensional crystals with an eye towards understanding crystal defect problems.

We have also noticed that the BDM as a more objective description of dipoles in covalent crystals gives the non-uniform local fields at each bond dipole site even for the system has identical atoms. However, this model has its limitations. The BDM should be used only for semiconductors or insulators with strong bond orientation, such as covalent crystals.

It is difficult to conceive of direct experimental tests for the L-L theory since local polarizabilities and local fields in a solid are not experimentally accessible quantities. On the other hand, certain derivatives of the dielectric function are experimentally accessible. The numerical dipole sums have been applied to strained crystals and we have investigated elasto-optic (Pockels) constants using both the ADM and the BDM. In particular for some tetrahedral compounds and for the rare gas crystal Xenon, which probably fulfills the L-L criterion as well as any other solid, the results of the isotropic atomic polarizability do not compare very well with the observed value. However, using an anisotropic atomic polarizability assumption the fitting is possible in excellent agreement with the observed value. The value of the anisotropic atomic polarizabilities are very close to the isotropic value and the calculations are very sensitive to a small change of the polarizability. This leads us to

conclude that the L-L is a qualitatively important result which gives a good approximation of the scale of polarizability.

Assuming that the L-L result has largely qualitative significance, it would be interesting to extend it to cases where the local polarizability is non-linear in the local field. There we can possibly obtain at least a qualitative picture of local field effects on non-linear optical processes, especially at surfaces.

BIBLIOGRAPHY

1. C. Kittle, Introduction to Solid State Physics, (Wiley, New York) Chapters 10, 11 & 13, 5^{th} edition, 1976.
2. C. K. Purvis and P. L. Taylor, Phys. Rev. **B26**, 4547 (1982).
3. S. L. Adler, Phys. Rev. **126**, 413 (1962).
4. N. Wiser, Phys. Rev. **129**, 62 (1963).
5. S. K. Sinha, R. P. Gupta and D. L. Price, Phys. Rev. Lett., **26**, 1324 (1971).
6. S. K. Sinha, R. P. Gupta and D. L. Price, Phys. Rev. **B9**, 2573 (1974).
7. J. H. P. Colpa, Physica **56**, 185 and 205 (1971).
8. Y. Onodera, Prog. of Theor. Phys. **49**. 37 (1973).
9. J. A. Van Vechten and R. M. Martin, Phys. Rev. Let. **28**, 446 (1972).
10. S. G. Louie, J. R. Chelikowsky and M. L. Cohen, Phys. Rev. Let. **34**, 155 (1975).
11. W. Hanke and L. J. Sham, Phys. Rev. Let. **33**, 582 (1974).
12. W. Hanke and L. J. Sham, Phys. Rev. **B12**, 4501 (1975), and Phys. Rev. **B21**, 4656 (1980).
13. W. Hanke and L. J. Sham, Phys. Rev. Let. **43**, 387 (1979).
14. W. Hanke, Adv. Phys., **27**, 287 (1978).
15. G. D. Mahan, Electronic Structure of Polymer and Molecular Crystal **B9**, 79 (1974).
16. P. P. Ewald, Ann Physik 64, 253 (1921).

17. W. Hayes and R. Loudon, Scattering of Light by Crystals, (Wiley, New York) Chapter 8, 1978.

18. M. Born and K. Huang, Dynamical Theory of Crystal Lattice, Oxford University Press, 1954.

19. M. H. Cohen and F. Keffer, Phys. Rev. **99**, 1128 (1955).

20. R. D. Misra, Proc. Cambridge Phil. Soc. **36**, 173 (1940).

21 M. Born and M. Bradburn, Proc. Cambridge Phil. Soc. **39**, 113 (1943).

22. M. P. Tosi, Solid State Physics, edited by F. Seitz and D. Turhbull. Acadmic Press, **Vol.16**, 1 (1964).

23. S. Aung and H. L. Strauss, J. Chem. Phys. **58**, 2737 (1973).

24. M. S. Duesbery and R. Taylor, J. Phys. **F7**, 47 (1977).

25. A. P. Smith and N. W. Ashcroft, Phys. Rev. **B38**, 12942 (1988).

26. B. R. A. Nijboer and F. W. De Wette, Physica **23**, 309 (1957); **24**, 442 (1958).

27. J. A. Osborn, Phys. Rev. **67**, 351 (1945)

28. H. Mueller, Phy. Rev. **47**, 947 (1935).

29. J. C. Phillips, Bonds and Bands in Semiconductors, Academic Press, 1973.

30. B. F. Levine, J. of Chem. Phys. **59**, 1463 (1973)

31. J. C. Phillips and J. A. Van Vechten, Phys. Rev. **183**, 709 (1969).

32. J. C. Phillips, Phys. Rev. Lett. **20**, 550 (1968); Rev. Mod. Phys. **42**, 317 (1970); Covalent Bonding in Crystals, Molecules, and Polymers, Univ. of Chicago Press. 1969.

33. G. D. Mahan, Phys. Rev. **153**, 983 (1967).

34. G. D. Mahan and R. M. Mazo, Phys. Rev. **175**, 1191 (1968).

35. J. N. Decarpigny and M. Lannoo. Phys. Rev. **B14**, 538 (1976).

36. R. M. Martin, Phys. Rev. **186**, 871 (1969).

37. R. M. Pick, M. H. Cohen and R. M. Martin, Phys. Rev. **B1**, 910 (1970).

38. A. S. Pine, Phys. Rev. **B5**, 3003 (1972); in M. Cardona, Ed., Light Scattering in Solids, (Springer-Verlag, New York)p253 (1975).

39. N. R. Werthamer, Phys. Rev. **185**, 348 (1969); Phys. Rev. **B6**, 4075 (1972), and Rare Gas Solid **V1**, 265 (1976).

40. R. L. Abrams and D. A. Pinnow, J. Appl. Phys. **41**, 2765 (1970).

41. D. W. Oxtoby and V. Chandrasekharan, Phys. Rev. **B16**, 1706 (1977).

42. A. A. Maradudin and E. Burstein, Phys. Rev. **164**, 1081 (1967).

43. S. Efrima and H. Metiu, Israel J. of Chem. **18**, 17 (1979).

44. L. N. Ovander and N. S. Tyu, Phys. Stat. Sol. (b) **91**, 763 (1979).

45. R. Loudon, Proc. Roy. Soc. (London) **A275**, 218 (1963).

46 M. H. Grimsditch and A. K. Ramdas, Phys. Rev. **B11**, 3139 (1975); Phys. Rev. **B14**, 1670 (1976).

47. Y. Kato and B. P. Stoicheff, Phys. Rev. **B11**, 3984 (1975).

48. H. Z. Cummins and P. E. Schoen, Laser Handbook, (North-Holland, Amsterdam), 1029 (1972).

49. D. Landheer, H. E. Jackson, R. A. McLaren, and B. P. Stoicheff, Phys. Rev. **B13**, 888 (1976).

50. G. B. Benedek and K. Fritsch, Phys. Rev. **149**, 647 (1967).

51. L. Brillouin, Compt. Rend. **158**, 1331 (1914); Ann. Phys. (Paris) **17**, 88 (1922).

52. A. Vokaun, Solid State Phys., edited by F. Seitz and D. Turhbull. Acadmic Press, **Vol.38**, 223 (1984).

53. S. S. Jha, J. R. Kirtley, and J. C. Tsang, Phys. Rev. **B22**, 3973 (1980).

54. S. Efrima and H. Metiu, Surface Science **92**, 417 (1980); J. Chem. Phy. **70**, 1603 & 1939 (1979), **70**, 2297 (1979).

55. H. Metiu, Surface-Enhanced Raman Scattering, edited by R. K. Chang and T. E. Furtak, Plenum Press (New York), 1 (1982).

56. S. S. Jha, Surface-Enhanced Raman Scattering, edited by R. K. Chang and T. E. Furtak, Plenum Press (New York), 129 (1982).

57. T. K. Lee and J. L. Birman, Surface-Enhanced Raman Scattering, edited by R. K. Chang and T. E. Furtak, Plenum Press (New York), 51(1982).

58. G. C. Schatz and R. P. Van Duyne, Surf. Sci. **101**, 425 (1980).

59. P. R. Hilton and D. W. Oxtoby, J. Chem. Phys. **72**, 6346 (1980).

60. W. E. Palke, Surf. Sci. **97**, L331 (1980).

61. F. W. King, R. P. Van Duyne, and G. C. Schatz, J. Chem. Phys. **69**, 4472 (1978).

62. F. W. De Wette and G. E. Schacher, Phys. Rev. **137**, A78 (1965).

63. W. H. Press, B. P. Flannery, S. A. Teukolsky and W. T. Vetterling, Numerical Recipes , Cambridge Univ. Press, 1986.

APPENDICES

Appendix A. 3D and 2D FOURIER TRANSFORM

We want to perform the Fourier transform of the following two equations for a three dimensional systems:

$$\Sigma_\ell \exp(-x_{\ell m}^2 t + i\vec{q}\cdot\vec{x}_{\ell m}) = \Sigma_G C_G \exp(i\vec{G}\cdot\vec{r}), \qquad (A\text{-}1)$$

and

$$\Sigma_\ell x_{\ell m}^i \cdot x_{\ell m}^j \exp(-x_{\ell m}^2 t + i\vec{q}\cdot\vec{x}_{\ell m}) = \Sigma_G D_G^{ij} \exp(i\vec{G}\cdot\vec{r}). \qquad (A\text{-}2)$$

Notice that,

$$D_G^{ij} = -\frac{\partial^2 C_G}{\partial q_i \, \partial q_j}. \qquad (A\text{-}3)$$

An expression for C_G is obtained first by taking the Fourier transform of Eq.(A-1) which gives,

$$C_G = \frac{1}{V_c} \int_{cell} \exp(-i\vec{G}\cdot\vec{r}) \{ \Sigma_\ell \exp(-x_{\ell m}^2 t + i\vec{q}\cdot\vec{x}_{\ell m}) \} \, d^3\vec{r}. \qquad (A\text{-}4)$$

Interchanging the order of integral and the summation and changing the variable from $\vec{r}$ to $\vec{x}_{\ell m} = \vec{r} - \vec{r}_\ell - \vec{r}_m$ in the exponential factor then gives:

$$C_G = \frac{1}{V_c} \Sigma_\ell \int_{cell} \exp(-i\vec{G}\cdot\vec{r}_m) \cdot \exp[-x_{\ell m}^2 t - i(\vec{G} - \vec{q})\cdot\vec{x}_{\ell m}] d^3\vec{x}_{\ell m}, \qquad (A\text{-}5)$$

where we use the fact that $\exp(i\vec{G}\cdot\vec{r}_\ell)$ is equal to unity. This integral is equivalent to the integral over all space,

$$C_G = \frac{1}{V_c}\int_{\text{space}} \exp(-i\vec{G}\cdot\vec{r}_m)\cdot\exp[-x_{\ell m}^2 t - i(\vec{G}-\vec{q})\cdot\vec{x}_{\ell m}]\, d^3\vec{x}_{\ell m}$$

$$= \frac{2\pi}{V_c}\int_0^\infty\int_{-1}^{1} \exp(-i\vec{G}\cdot\vec{r}_m)\cdot\exp[-x_{\ell m}^2 t - i|\vec{G}-\vec{q}|x_{\ell m}\cos\theta]\, x_{\ell m}^2 dx_{\ell m} d\cos\theta$$

$$= \frac{2\pi}{V_c}\int_0^\infty \exp(-i\vec{G}\cdot\vec{r}_m)\cdot\frac{1}{G}\exp(-x_{\ell m}^2 t)\sin(|\vec{G}-\vec{q}|x_{\ell m})\, dx_{\ell m}^2$$

$$= \frac{2\pi}{V_c t}\int_0^\infty \exp(-i\vec{G}\cdot\vec{r}_m)\cdot\exp(-x_{\ell m}^2 t)\cos(|\vec{G}-\vec{q}|x_{\ell m})\, dx_{\ell m}. \qquad \text{(A-6)}$$

Using the table of integrals by H. B. Dwight (4^{th} edition) 861.20:

$$\int_0^\infty \exp(-a^2x^2)\cos(mx)\, dx = \frac{1}{2a}\sqrt{\pi}\exp[-m^2/(4a^2)], \qquad \text{(A-7)}$$

we then have,

$$C_G = \frac{1}{V_c}\left(\frac{\pi}{t}\right)^{3/2}\exp\left[-i\vec{G}\cdot\vec{r}_m - \frac{(\vec{G}-\vec{q})^2}{4t}\right], \qquad \text{(A-8)}$$

which is Eq.(2.12). By using Eq.(A-3), we can easily get D_G^{ij}, which is Eq.(2.16).

For a two dimensional system, we have an integral over all surface,

$$C_G^{2D} = \frac{1}{\sigma_c} \prod_{i=1}^{2} \int_{-\infty}^{\infty} \exp(-i\vec{G}\cdot\vec{r}_m)\cdot\exp[-(\rho_{\ell m}^i)^2 t - i(G_i - q_i)\rho_{\ell m}^i]\, d\rho_{\ell m}^i$$

$$= \frac{4}{\sigma_c} \prod_{i=1}^{2} \int_{o}^{\infty} \exp(-i\vec{G}\cdot\vec{r}_m)\cdot\exp[-(\rho_{\ell m}^i)^2 t)]\cos(G_i - q_i)\rho_{\ell m}^i]\, d\rho_{\ell m}^i, \qquad (A\text{-}9)$$

using Eq.(A-7) again we have

$$C_G^{2D} = \frac{1}{\sigma_c} \exp(-iG\cdot r_m)\ (\frac{\pi}{t})\ \exp[-\frac{(\vec{G} - \vec{q})}{4\,t}], \qquad (A\text{-}10)$$

which is Eq.(5.7). Using the same arguments as for the three dimensional system we have

$$D_G^{2Dij} = -\frac{\partial^2 C_G^{2D}}{\partial q_i\ \partial q_j}$$

$$= \frac{1}{\sigma_c}\exp(-iG\cdot r_m)(\frac{\pi}{t})\exp[-\frac{(\vec{G} - \vec{q})}{4\,t}]$$

$$\cdot(\frac{1}{2t}\,\delta_{ij} - \frac{(G_i - q_i)(G_j - q_j)}{4\,t^2}), \qquad (A\text{-}11)$$

which is Eq.(5.8).

Appendix B. PROOF THE 3D DIPOLE SUMS ARE INDEPENDENT ON THE EWALD PARAMETER η

The partial derivatives of $S_3(\vec{q},M,m)$ and the $S_5^{ij}(\vec{q},M,m)$ (i.e. Eq.(2.29) and Eq.(2.30)) can be written as the following:

$$\frac{\partial S_3(\vec{q},M,m)}{\partial \eta} = \frac{2\pi}{V_c} \Sigma_G \exp[-i\vec{G}\cdot(\vec{r}-\vec{r}_m)\frac{\partial E1}{\partial x_G}\frac{\partial x_G}{\partial \eta} - \frac{4\eta^2}{\sqrt{\pi}}$$
$$+ \Sigma'_\ell \frac{1}{x_{\ell m}^3}\exp(i\vec{q}\cdot\vec{x}_{\ell m})\cdot[\frac{-\partial F}{\partial x_r} + \frac{2}{\sqrt{\pi}}\exp(-x_r^2)\cdot(1 - 2x_r^2)]\frac{\partial x_r}{\partial \eta}, \quad (B-1)$$

where $x_G = (\vec{G}-\vec{q})/4\eta^2$ and $x_r = \eta\, x_{\ell m}$. From the Handbook of Mathematical functions, edited by M. Abramowitz and I. A. Stegun, equations (7.2.8) and (6.5.26) we have

$$\frac{d\,E1(x)}{d\,x} = -\frac{\exp(-x)}{x} \quad (B-2)$$

and

$$\frac{d\,F(x)}{d\,x} = \frac{2}{\sqrt{\pi}}\exp(-x^2). \quad (B-3)$$

Therefore, we can rewrite (B-1) as:

$$\frac{\partial S_3(\vec{q},M,m)}{\partial \eta} = \frac{2\pi}{V_c}\Sigma_G \exp[-i\vec{G}\cdot(\vec{r}-\vec{r}_m)[\frac{2}{\eta}\exp(-x_G)]$$
$$- \frac{4\eta^2}{\sqrt{\pi}}[1 + \Sigma'_\ell \exp(i\vec{q}\cdot\vec{x}_{\ell m})\cdot\exp(-x_r^2)]. \quad (B-4)$$

Substituting Eq.(2.8) where $t = \eta^2$, and Eq.(2.13) into (B-4), we then have,

$$\frac{\partial S_3(\vec{q},\mathbf{M},m)}{\partial \eta} = \frac{4\pi}{V_c}\Sigma_G \exp[-i\vec{G}\cdot(\vec{r}-\vec{r}_m)][\frac{1}{\eta}\exp(-x_G)]$$

$$- \frac{4\pi}{V_c}\Sigma_G \frac{1}{\eta}\exp[-i\vec{G}\cdot(\vec{r}-\vec{r}_m)\exp(-x_G) = 0. \qquad (B\text{-}5)$$

Similarly we have,

$$\frac{\partial S_5^{ij}(\vec{q},\mathbf{M},m)}{\partial \eta} = \frac{2\pi}{3V_c}\Sigma_G\exp[-i\vec{G}\cdot(\vec{r}-\vec{r}_m)][\frac{2}{\eta}\delta_{ij} - \frac{(G_i-q_i)(G_j-q_j)}{\eta^3}]\exp(-x_G)$$

$$+ \Sigma'_\ell \frac{x_1^i x_1^j}{x_{\ell m}^5}\exp(i\vec{q}\cdot\vec{x}_{\ell m})[-\frac{8\eta^4}{3\sqrt{\pi}}x_{\ell m}^5\exp(-x_r^2)]. \qquad (B\text{-}6)$$

Substituting Eq.(2.9) and Eq.(2.17) into Eq.(B-6), we then have,

$$\frac{\partial S_5^{ij}(\vec{q},\mathbf{M},m)}{\partial \eta} = \frac{4\pi}{3V_c}\Sigma_G\exp[-i\vec{G}\cdot(\vec{r}-\vec{r}_m)][\frac{1}{\eta}\delta_{ij} - \frac{(G_i-q_i)(G_j-q_j)}{2\eta^3}]\exp(-x_G)$$

$$- \frac{8\pi}{3V_c}\Sigma_G\exp[-i\vec{G}\cdot(\vec{r}-\vec{r}_m)][\frac{1}{2\eta}\delta_{ij} - \frac{(G_i-q_i)(G_j-q_j)}{4\eta^3}]\exp(-x_G)$$

$$= 0. \qquad (B\text{-}7)$$

In the same way we can prove that

$$\frac{\partial S_3(\vec{q},\vec{r},m)}{\partial \eta} = 0, \text{ and } \frac{\partial S_5^{ij}(\vec{q},\vec{r},m)}{\partial \eta} = 0. \ (\vec{r}\neq\vec{r}_\ell,\vec{r}_m) \qquad (B\text{-}8)$$

Therefore, the three dimensional dipole sums are independent of the Ewald parameter η.

Appendix C. PROGRAM DIPSM

```
      PROGRAM DIPSM
c Written by Lingzhou L.Canfield, as part of thesis.
c This program use the Ewald method to calculate the dipole
c sums for the diamond or zinc blende structure with or without a
c strain, for the BDM and the ADM.
     implicit real*8 (a-b,d-h,o-z)
      implicit complex*16 (c)
      dimension sum5(10,10), sumk5(3,3),sumr5(3,3),s5(3,3),
     & s5ij(16,6), s3m(16),  rm(16,3),dke(3)
      ci=cmplx(0.0d0,1.0d0)
      pi=dacos(-1.0d0)
      dke(1)=0.d0
      dke(2)=0.d0
      dke(3)=4.1931d-3
c dke(i) are the wave vector q times a, a is lattice constants
         mb=175
         b=mb/100.d0
         max=3
      delt=0.001d0
      rc=1.d0-delt
       open(unit=6, file='s3p001x.out', status='new')
       open(unit=8, file='s5p001x.out', status='new')
       open(unit=4, file='brps.inp', status='old')
c open brps for the BDM; arps for the ADM.
        do 11 i1=1,m
c m = 16 for the BDM; m = 4 for the ADM
          read(4,*)(rm(i1,j1),j1=1,3)
          rmx=rm(i1,1)*rc
          rmy=rm(i1,2)
          rmz=rm(i1,3)
c rm= r-rp, for r run over all rps. rp is the position of the
c dipoles as the basis in one unit cell.
        do 20 i=1,3
           do 10 j=1,3
      if (j .le.i)then
       call subk(max,rc,i,j,b,pi,ci,rmx,rmy,rmz,
     & dke,csmk3,csmk51,csmk52)
       sumk3=2*pi*real(csmk3)
       smk51=real(csmk51)
       smk52=real(csmk52)
             if (j .eq. i)then
                sumk5(i,j)=2*pi*(smk51-2*smk52)/3.0d0
             else
                sumk5(i,j)=-4*pi*smk52/3.0d0
             endif
       call subr(max,rc,i,j,b,pi,ci,rmx,rmy,rmz,csmr3,csmr5)
               sumr3=real(csmr3)
               sumr5(i,j)=real(smr5)
             if (dabs(rmx)+dabs(rmy)+dabs(rmz) .eq. 0.d0)then
```

```
              sum3=(4*sumk3/rc)+sumr3-(4*b*b*b)/(3*dsqrt(pi))
            else
              sum3=(4*sumk3/rc)+sumr3
            endif
c the term -(4*b*b*b)/(3*dsqrt(pi)) is from excluded the self
c contribution
            sum5(i,j)=(4*sumk5(i,j)/rc)+sumr5(i,j)
       endif
 10     continue
 20   continue
         s3m(i1)=sum3
         s5ij(i1,1)=sum5(1,1)
         s5ij(i1,2)=sum5(2,1)
         s5ij(i1,3)=sum5(2,2)
         s5ij(i1,4)=sum5(3,1)
         s5ij(i1,5)=sum5(3,2)
         s5ij(i1,6)=sum5(3,3)
      write(6,56)s3m(i1)
      write(8,55)(s5ij(i1,j2),j2=1,6)
 55     format(6f12.4)
 56     format(f12.4)
 11     continue
       close(4)
       close(6)
       close(8)
      stop
      end

      subroutine subk(max,rc,i,j,b,pi,ci,rmx,rmy,rmz,dke,
     &     csmk3,csmk51,csmk52)
       implicit real*8(a-b,d-h,o-z)
       implicit complex*16 (c)
      dimension  dkm(3), dke(3),gm(3)
       csmk3=(0.0d0,0.0d0)
       csmk51=(0.0d0,0.0d0)
       csmk52=(0.0d0,0.0d0)
c loops in k space
      do 60 m3=-max,max
         do 50 m2=-max,max
            do 40 m1=-max,max
c where m1,m2,m3 are the integers of the reciprocal lattice vector
c Km=m1A+m2B+m3C
      gm(1)=2*pi*(m1-m2+m3)/rc
      gm(2)=2*pi*(m1+m2-m3)
      gm(3)=2*pi*(-m1+m2+m3)
      dkm(1)=gm(1)-dke(1)
      dkm(2)=gm(2)-dke(2)
      dkm(3)=gm(3)-dke(3)
      sqakm=dkm(1)**2+dkm(2)**2+dkm(3)**2
      akm=dsqrt(sqakm)
      x=akm/(2*b)
      sqx=x*x
```

```
      cexpgrm=cexp(-ci*cmplx(gm(1)*rmx+gm(2)*rmy+gm(3)*rmz))
      if (sqx .lt. 0.9d0)then
         call sube1(sqx,dei)
      else
           if (sqx .lt. 29.d0)then
c when sqx=29,e1(x)=8.4837e-15, which is apprx. eq 0
              call qromo(63)(0.0d0,1.0d0/sqx,ss)
              dei=ss
           else
             dei=0.0d0
           endif
        endif
      if (sqx .lt. 36.d0)then
         sk52=(dkm(i)*dkm(j)*dexp(-sqx))/sqakm
      else
        sk52=0.0d0
      endif
      sk3=dei
      sk51=dei
      csmk3=csmk3+cexpgrm*cmplx(sk3)
      csmk51=csmk51+cexpgrm*cmplx(sk51)
      csmk52=csmk52+cexpgrm*cmplx(sk52)
 40         continue
 50       continue
 60     continue
      return
      end

     subroutine subr(max,rc,i,j,b,pi,ci,rmx,rmy,rmz,csmr3,csmr5)
     implicit real*8(a-h,o-z)
     implicit complex*16(c)
     dimension rla(10)
      csmr3=(0.0d0,0.0d0)
      csmr5=(0.0d0,0.0d0)
c loops in r space
      do 60 l3=-max,max
         do 50 l2=-max,max
            do 40 l1=-max,max
c the primitive vector is t=l1*a+l2*b+l3*c.
        rla(1)=rmx-0.5d0*(l1+l3)*rc
        rla(2)=rmy-0.5d0*(l1+l2)
        rla(3)=rmz-0.5d0*(l2+l3)
        drl=rla(1)**2+rla(2)**2+rla(3)**2
        rl=dsqrt(drl)
        x=b*rl
     cexpker=cexp(ci*cmplx((dke(1)*rla(1)+dke(2)*rla(2)
      & +dke(3)*rla(3))))
      if (x .lt. 6.0d0)then
        sr31=1.0d0-erf(x)(63)
        sr32=(2*x*dexp(-x*x))/dsqrt(pi)
        sr53=(4*x*x*x*dexp(-x*x))/(3*dsqrt(pi))
```

```
      else
        sr31=0.0d0
        sr32=0.0d0
        sr53=0.0d0
        endif
      if (rl .eq. 0.0d0) then
         sr3=0.0d0
         sr5=0.0d0
      else
        sr3=(sr31+sr32)/rl**3
        sr5=rla(i)*rla(j)*(sr31+sr32+sr53)/rl**5
      endif
      csmr3=csmr3+cmplx(sr3)*cexpker
      csmr5=csmr5+cmplx(sr5)*cexpker
40          continue
50        continue
60      continue
       return
       end

      subroutine sube1(sqx,dei)
      implicit real*8(a-h,o-z)
      xm=sqx
      sn=0.0d0
      do 11 n=1,10
      CALL SUB(N,M1)
      s1=((-xm)**n)/(n*m1*1.0D0)
      sn=sn+s1
11    CONTINUE
      E1=-.5772156649d0-dLOG(XM)-SN
      dei=e1
      return
      end

      SUBROUTINE SUB(N,M1)
      IMPLICIT REAL*8(A-H,O-Z)
       m1=1
       i=1
5      m1=m1*i
       I=I+1
      if (i.le.n)then
         GOTO 5
       endif
       RETURN
       END
```

Appendix D. PROGRAM DMBRPS

```
      program dmbrps
c Written by Lingzhou L.Canfield, as part of thesis.
c this is a main program to create the rps for BOND DIPOLES in ONE
c primitive cell of the Diamond or Zinc Blende structure with or
c without deformation.
c This is the MAIN program
      implicit real*8(a-h,o-z)
      dimension rpu(8,3),rmp(16,3),rdm(16,16,3)
      call dmbr44x(rpu)
c call dmbr44x(rpu) for crystal under a shear along the x dir.,
c call dmbr(rpu) for crystal with or without a strain.
      do 22 m=1,4
          do 21 i=1,4
             do 20 j=1,3
       rdm(m,i,j)=rpu(i,j)-rpu(m,j)
 20          continue
 21        continue
      do 33 i=1,4
      write(16,44)(rdm(m,i,j),j=1,3)
 44   format(3f18.6)
 33   continue
 22   continue
      close(16)
      stop
      end

      subroutine dmbr44x(rpu)
      implicit real*8(a-h,o-z)
      dimension rpu(8,3)
      delt=0.002d0
      open(unit=16, file='r44p002x.inp', status='new')
       rpu(1,1)=0.125d0+0.875*delt
       rpu(1,2)=0.125d0
       rpu(1,3)=0.125d0
       rpu(2,1)=0.125d0+0.625d0*delt
       rpu(2,2)=0.375d0
       rpu(2,3)=0.375d0
       rpu(3,1)=0.375d0+0.625*delt
       rpu(3,2)=0.125d0
       rpu(3,3)=0.375d0
       rpu(4,1)=0.375d0+0.875*delt
       rpu(4,2)=0.375d0
       rpu(4,3)=0.125d0
       return
       end

      subroutine dmbr(rpu)
      implicit real*8(a-h,o-z)
      dimension rpu(8,3)
      open(unit=16, file='dmbr.inp', status='new')
       rpu(1,1)=0.d0
```

```
      rpu(1,2)=0.d0
      rpu(1,3)=0.d0
      rpu(2,1)=0.d0
      rpu(2,2)=0.25d0
      rpu(2,3)=0.25d0
      rpu(3,1)=0.25d0
      rpu(3,2)=0.d0
      rpu(3,3)=0.25d0
      rpu(4,1)=0.25d0
      rpu(4,2)=0.25d0
      rpu(4,3)=0.d0
    return
    end
```

Appendix E. PROGRAM ADMRPS

```
      program admrps
c Written by Lingzhou L.Canfield, as part of thesis.
c this is a program to create the rps for ATOMIC DIPOLES in ONE
c primitive cell of the Diamond or Zinc blende structure.
      implicit real*8(a-h,o-z)
      dimension rpu(8,3),ram(8,8,3)
       rpu(1,1)=0.d0
       rpu(1,2)=0.d0
       rpu(1,3)=0.d0
       rpu(2,1)=0.25d0
       rpu(2,2)=0.25d0
       rpu(2,3)=0.25d0
    do 22 m=1,2
       do 21 i=1,2
          do 20 j=1,3
       ram(m,i,j)=rpu(i,j)-rpu(m,j)
 20       continue
 21    continue
      open(unit=16, file='dmar.inp', status='new')
      do 33 i=1,2
      write(16,44)(ram(m,i,j),j=1,3)
  44   format(3f18.6)
 33    continue
 22    continue
       close(16)
       stop
       end
```

Appendix F. PROGRAM 2DBDMRPS

```
      program 2dbdmrps
c Written by Lingzhou L.Canfield, as part of thesis.
c this is a program to create the rps for Bond DIPOLES in ONE unit
c cell of the 2 Dimensional centered rectangular structure.
      implicit real*8(a-h,o-z)
      dimension rpu(8,3),rmp(16,3),rbm(16,16,3)
       rpu(1,1)=0.d0
       rpu(1,2)=0.d0
       rpu(2,1)=0.5d0
       rpu(2,2)=0.d0
       rpu(3,1)=0.d0
       rpu(3,2)=0.5d0
       rpu(4,1)=0.5d0
       rpu(4,2)=0.5d0
       do 22 m=1,4
           do 21 i=1,4
              do 20 j=1,2
        rbm(m,i,j)=rpu(i,j)-rpu(m,j)
 20           continue
 21        continue
       open(unit=16, file='2dbrps.inp', status='new')
       do 33 i=1,4
       write(16,44)(rbm(m,i,j),j=1,2)
 44   format(2f18.6)
 33   continue
 22   continue
      close(16)
      stop
      end
```

Appendix G. PROGRAM DIPSM44X

```
      program dipsm44x
c Written by Lingzhou L.Canfield, as part of thesis.
c this is a program using Ewald method to calculate the dipole sums
c for cubic tetrahedral structure under a shear.
c this is a MAIN program
      implicit real*8 (a-b,d-h,o-z)
      implicit complex*16 (c)
      dimension sum5(10,10), sumk5(3,3),sumr5(3,3),s5(3,3),
     & s5ij(16,6), s3m(16),  rm(16,3),dke(3)
      ci=cmplx(0.0d0,1.0d0)
      pi=dacos(-1.0d0)
      dke(1)=0.d0
      dke(2)=0.d0
      dke(3)=4.1931d-3
         mb=175
         b=mb/100.0d0
         max=3
     open(unit=4, file='r44p002x.inp', status='old')
     open(unit=6, file='s3p002x.44z', status='new')
     open(unit=8, file='s5p002x.44z', status='new')
     delt=0.002d0
     rc=1.d0
     dtn=1.d0-delt
     dnh=1.d0-delt/2.d0
c rc is the rate of c/a, where c and a are the lattice constants.
      do 11 i1=1,16
        read(4,*)(rm(i1,j1),j1=1,3)
        rmx=rm(i1,1)*rc
        rmy=rm(i1,2)
        rmz=rm(i1,3)
        do 20 i=1,3
             do 10 j=1,3
             if (j .le.i)then
      call subk44(max,rc,dnh,dtn,i,j,b,pi,ci,rmx,rmy,rmz,dke,
     &   csmk3,csmk51,csmk52)
         sumk3=2*pi*real(csmk3)
         smk51=real(csmk51)
         smk52=real(csmk52)
             if (j .eq. i)then
             sumk5(i,j)=2*pi*(smk51-2*smk52)/3.0d0
             else
             sumk5(i,j)=-4*pi*smk52/3.0d0
             endif
      call subr44(max,rc,dtn,i,j,b,pi,rmx,rmy,rmz,csmr3,csmr5)
             sumr3=real(smr3)
             sumr5(i,j)=real(smr5)
      if (dabs(rmx)+dabs(rmy)+dabs(rmz) .eq. 0.d0)then
             sum3=(4*sumk3/rc*dnh)+sumr3-(4*b*b*b)/(3*dsqrt(pi))
      else
             sum3=(4*sumk3/rc*dnh)+sumr3
      endif
```

```
            sum5(i,j)=(4*sumk5(i,j)/rc*dnh)+sumr5(i,j)
       endif
 10          continue
 20        continue
           s3m(i1)=sum3
           s5ij(i1,1)=sum5(1,1)
           s5ij(i1,2)=sum5(2,1)
           s5ij(i1,3)=sum5(2,2)
           s5ij(i1,4)=sum5(3,1)
           s5ij(i1,5)=sum5(3,2)
           s5ij(i1,6)=sum5(3,3)
           write(6,56)s3m(i1)
           write(8,55)(s5ij(i1,j2),j2=1,6)
 55      format(6f12.4)
 56      format(f12.4)
 11      continue
         close(4)
         close(6)
         close(8)
         stop
         end

       subroutine subk44(max,rc,dnh,dtn,i,j,b,pi,ci,rmx,rmy,rmz,dke,
      &   csmk3,csmk51,csmk52)
       implicit real*8(a-b,d-h,o-z)
       implicit complex*16 (c)
       dimension  dkm(3), dke(3),gm(3)
        csmk3=(0.0d0,0.0d0)
        csmk51=(0.0d0,0.0d0)
        csmk52=(0.0d0,0.0d0)
c loops in k space
       do 60 m3=-max,max
           do 50 m2=-max,max
              do 40 m1=-max,max
       gm(1)=2*pi*(m1-m2+m3)/(rc*dnh)
       gm(2)=2*pi*(m1+m2*dtn-m3*dtn)/dnh
       gm(3)=2*pi*(-m1*dtn+m2*dtn+m3)/dnh
       dkm(1)=gm(1)-dke(1)
       dkm(2)=gm(2)-dke(2)
       dkm(3)=gm(3)-dke(3)
       dakm=dkm(1)**2+dkm(2)**2+dkm(3)**2
       akm=dsqrt(dakm)
       sqakm=akm*akm
       x=akm/(2*b)
       sqx=x*x
       cexpgrm=cexp(-ci*cmplx(gm(1)*rmx+gm(2)*rmy+gm(3)*rmz))
      if (sqx .lt. .9d0)then
          call sube1(sqx,dei)
      else
         if (sqx .lt. 29.d0)then
         call qromo(63)(0.0d0,1.0d0/sqx,ss)
         dei=ss
```

```
          else
          dei=0.0d0
          endif
        endif
        if (sqx .lt. 36.d0)then
           sk52=(dkm(i)*dkm(j)*dexp(-sqx))/sqakm
        else
           sk52=0.0d0
        endif
           sk3=dei
           sk51=dei
           csmk3=csmk3+cexpgrm*cmplx(sk3)
           csmk51=csmk51+cexpgrm*cmplx(sk51)
           csmk52=csmk52+cexpgrm*cmplx(sk52)
  40         continue
  50       continue
  60     continue
       return
       end

       subroutine subr44(max,rc,dtn,i,j,b,pi,rmx,rmy,rmz,csmr3,csmr5)
       implicit real*8(a-h,o-z)
       implicit complex*16(c)
       dimension rla(10)
       csmr3=(0.0d0, 0.0d0)
       csmr5=(0.0d0, 0.0d0)
c loops in r space
        do 60 l3=-max,max
           do 50 l2=-max,max
              do 40 l1=-max,max
        rla(1)=rmx-0.5d0*((l1+l3)*dtn-l2*(1.d0-dtn))*rc
        rla(2)=rmy-0.5d0*(l1+l2)
        rla(3)=rmz-0.5d0*(l2+l3)
        drl=rla(1)**2+rla(2)**2+rla(3)**2
        rl=dsqrt(drl)
        x=b*rl
        cexpker=cexp(ci*cmplx((dke(1)*rla(1)+dke(2)*rla(2)
       &  +dke(3)*rla(3))))
       if (x .lt. 6.0d0)then
          sr31=1.0d0-erf(x)(63)
          sr32=(2*x*dexp(-x*x))/dsqrt(pi)
          sr53=(4*x*x*x*dexp(-x*x))/(3*dsqrt(pi))
       else
         sr31=0.0d0
         sr32=0.0d0
         sr53=0.0d0
       endif
       if (rl .eq. 0.0d0) then
          sr3=0.0d0
          sr5=0.0d0
       else
          sr3=(sr31+sr32)/rl**3
```

```
         sr5=rla(i)*rla(j)*(sr31+sr32+sr53)/rl**5
      endif
         csmr3=csmr3+cmplx(sr3)*cexpker
         csmr5=csmr5+cmplx(sr5)*cexpker
40         continue
50       continue
60     continue
      return
      end
```

Appendix H. PROGRAM 2DDIPSM

```
      Program 2ddipsm
c Written by Lingzhou L.Canfield, as part of thesis.
c this is a program calculating 2D dipole sums for center rectangular
c structure, by using the BDM and the ADM
c this is a MAIN program
      implicit real*8 (a-b,d-h,o-z)
      implicit complex*16 (c)
      dimension sum5(10,10), sumk5(2,2),sumr5(2,2),s5(2,2),
     &  s5ij(256,3), s3m(256), rm(256,3),dke(3)
      do 557 mrc=10,20,2
         rc=mrc/10.d0
c rc is the lattice ratio b/a
         mb=175
         b=mb/100.0d0
         max=3
         ci=cmplx(0.0d0,1.0d0)
         pi=dacos(-1.0d0)
         dke(1)=0.d0
         dke(2)=0.d0
         dke(3)=4.1931d-3
      open(unit=6, file='2ds3rctl.out', status='new')
      open(unit=8, file='2ds5rctl.out', status='new')
      open(unit=4, file='2dbrps.inp', status='old')
c BDM call 2dbrps; ADM call 2darps.
      do 11 i1=1,m
c m = 16 for BDM; m = 4 for ADM.
        read(4,*)(rm(i1,j1),j1=1,2)
        rmx=rm(i1,1)
        rmy=rm(i1,2)*rc
        do 20 i=1,2
           do 10 j=1,2
        if (j .le.i)then
        call subk(max,i,j,rc,b,pi,ci,rmx,rmy,dke,csmk3,csmk52)
     &  sumk3=4*dsqrt(pi)*real(csmk3)
         smk51=real(csmk3)
         smk52=real(csmk52)
         if (j .eq. i)then
           sumk5(i,j)=4*dsqrt(pi)*(smk51-smk52)/3.0d0
         else
           sumk5(i,j)=-4*dsqrt(pi)*smk52/3.0d0
         endif
         call subr(max,i,j,rc,b,pi,ci,dke,rmx,rmy,csmr3,csmr5)
         sumr3=real(csmr3)
         sumr5(i,j)=real(csmr5)
         if (dabs(rmx)+dabs(rmy) .eq. 0.d0)then
           sum3=sumk3/rc+sumr3-(4*b*b*b)/(3*dsqrt(pi))
         else
           sum3=sumk3/rc+sumr3
         endif
         sum5(i,j)=sumk5(i,j)/rc+sumr5(i,j)
```

```
        endif
 10       continue
 20     continue
        s3m(i1)=sum3
        s5ij(i1,1)=sum5(1,1)
        s5ij(i1,2)=sum5(2,1)
        s5ij(i1,3)=sum5(2,2)
        write(6,56)s3m(i1)
        write(8,55)(s5ij(i1,j2),j2=1,3)
 55     format(3f12.4)
 56     format(f12.4)
 11     continue
 557    continue
        close(4)
        close(6)
        close(8)
        stop
        end

      subroutine subk2d(max,i,j,rc,b,pi,ci,rmx,rmy,dke,csmk3,csmk52)
      implicit real*8(a-b,d-h,o-z)
      implicit complex*16 (c)
      dimension  dkm(3), dke(3),gm(3)
       csmk3=(0.0d0,0.0d0)
       csmk52=(0.0d0,0.0d0)
c loops in k space
       do 50 m2=-max,max
          do 40 m1=-max,max
        gm(1)=2*pi*m1
        gm(2)=(2*pi*m2)/rc
        dkm(1)=gm(1)-dke(1)
        dkm(2)=gm(2)-dke(2)
        dkm(3)=-dke(3)
        sqakm=dkm(1)**2+dkm(2)**2+dke(3)**2
        akm=dsqrt(sqakm)
        xg=akm/(2*b)
        sqx=xg*xg
        cexpgrm=cexp(-ci*cmplx(gm(1)*rmx+gm(2)*rmy))
        if (sqx .lt. 36.d0)then
          sk31=b*dexp(-sqx)
          sk32=dsqrt(pi)*akm*(1.d0-erf(xg)(64))/2.d0
        else
          sk31=0.0d0
          sk32=0.d0
        endif
        sk3=sk31-sk32
        sk52=dkm(i)*dkm(j)*sk32/sqakm
        csmk3=csmk3+cexpgrm*cmplx(sk3)
        csmk52=csmk52+cexpgrm*cmplx(sk52)
 40        continue
 50     continue
      return
```

```
      end

      subroutine subr2d(max,i,j,rc,b,pi,ci,dke,rmx,rmy,csmr3,csmr5)
      implicit real*8(a-b,d-h,o-z)
      implicit complex*16(c)
      dimension rla(10),dke(3)
      csmr3=(0.0d0,0.0d0)
      csmr5=(0.0d0,0.0d0)
c loops in r space
       do 50 l2=-max,max
          do 40 l1=-max,max
           rla(1)=rmx-l1
           rla(2)=rmy-rc*l2
           drl=rla(1)**2+rla(2)**2
           rl=dsqrt(drl)
           x=b*rl
           if (x .lt. 6.0d0)then
             sr31=1.0d0-erf(x)(63)
             sr32=(2*x*dexp(-x*x))/dsqrt(pi)
             sr53=(4*x*x*x*dexp(-x*x))/(3*dsqrt(pi))
           else
             sr31=0.0d0
             sr32=0.0d0
             sr53=0.0d0
           endif
           if (rl .eq. 0.0d0) then
             sr3=0.0d0
             sr5=0.0d0
           else
             sr3=(sr31+sr32)/rl**3
             sr5=rla(i)*rla(j)*(sr31+sr32+sr53)/rl**5
           endif
      cexprla=cexp(ci*(dke(1)*rla(1)+dke(2)*rla(2)))
      csmr3=csmr3+cmplx(sr3)*cexprla
      csmr5=csmr5+cmplx(sr5)*cexprla
  40      continue
  50    continue
        return
        end
```

Appendix I. PROGRAM SPBP

```
      program spbp
c Written by Lingzhou L.Canfield, as part of thesis.
c this is a program searching the parameter of c, i.e bond
c polarizability which fit the experimental data for cubic tetrahedral
c structure.
      implicit real*8 (a-h,o-z)
       data c/0.045d0/,xi/0.001d0/
       ftol=1.d-4
     open( unit=9,file='gapp2x.dt1', status='new')
     call powell(63)(c,xi,1,1,ftol,iter,fret)
      write(9,*)c,fret,iter
      close (9)
       stop
       end

        real*8 function func(c)
        implicit real*8 (a-h,o-z)
      dimension el(12), a(12,12), a1(12,12),b(12),s3(16),eld3(3),
     &  s5ij(16,6),s5(16,3,3),d(4,3),si(16,3),p(3),ext(3),q(3),
     &  eljdj1(3),indx(12),ave(3)
     data pijkl/-0.151d0/,epcer0/9.1d0/
c print 'input the data of which looking for c parameter'
      dudx=0.001d0
      delt=0.002d0
      rc=1.d0-delt
      dnh=1.d0-dudx/2.d0
      drc=1.d0-dudx
c for crystal under shear, rc=1.d0, for crystal under a strain,
c dnh=1.d0,
      pi=dacos(-1.d0)
      Ext(1)=1.d0/dsqrt(2.d0)
      Ext(2)=1.d0/dsqrt(2.d0)
      Ext(3)=0.d0
c Ext(i) is the ith component of the external field
      q(1)=0.d0
      q(2)=0.d0
      q(3)=1.d0
c q is the unit wave vector.
      c1=c
c c1 is the bond polarizability per a**3, a is the lattice constant
      if(c1.le.0.d0)then
      func=1.d10*dexp(dabs(c1))
      goto 1
      else
         if(c1.gt.1.d0)then
         func=1.d10*dexp(dabs(c1))
         goto 1
         else
      dnij=1.d0/(pijkl*dudx+(1.d0/epcer0))
      open(unit=5, file='s3p002x.out', status='old')
```

```
      open(unit=6, file='s5p002x.out', status='old')
      open(unit=7,file='dijins.inp',status='old')
      do 10 i=1,16
      read(5,*)s3(i)
      read (6,*)(s5ij(i,j),j=1,6)
         s5(i,1,1)=s5ij(i,1)
         s5(i,2,1)=s5ij(i,2)
         s5(i,2,2)=s5ij(i,3)
         s5(i,3,1)=s5ij(i,4)
         s5(i,3,2)=s5ij(i,5)
         s5(i,3,3)=s5ij(i,6)
         s5(i,1,2)=s5(i,2,1)
         s5(i,1,3)=s5(i,3,1)
         s5(i,2,3)=s5(i,3,2)
10    continue
      do 11 j0=1,4
        read(7,*)(d(j0,i0),i0=1,3)
        d(j0,1)=d(j0,1)*rc/dsqrt(2.d0+drc**2)
        d(j0,2)=d(j0,2)/dsqrt(2.d0+drc**2)
        d(j0,3)=d(j0,3)/dsqrt(2.d0+drc**2)
 11   continue
      close(5)
      close(6)
      close(7)
      do 15 m=1,13,4
         do 14 i1=1,3
         si(m,i1)=3.d0*(s5(m,i1,1)*d(1,1)+s5(m,i1,2)*d(1,2)+
     &       s5(m,i1,3)*d(1,3))-s3(m)*d(1,i1)
         si(m+1,i1)=3.d0*(s5(m+1,i1,1)*d(2,1)+s5(m+1,i1,2)*d(2,2)+
     &       s5(m+1,i1,3)*d(2,3))-s3(m+1)*d(2,i1)
         si(m+2,i1)=3.d0*(s5(m+2,i1,1)*d(3,1)+s5(m+2,i1,2)*d(3,2)+
     &       s5(m+2,i1,3)*d(3,3))-s3(m+2)*d(3,i1)
          si(m+3,i1)=3.d0*(s5(m+3,i1,1)*d(4,1)+s5(m+3,i1,2)*d(4,2)+
     &        s5(m+3,i1,3)*d(4,3))-s3(m+3)*d(4,i1)
 14       continue
 15    continue
       m1=0
       do 111 i=1,10,3
          do 114 k=1,3
       a1(i,k)=c1*d(1,k)*si(1+m1,1)
       a1(i+1,k)=c1*d(1,k)*si(1+m1,2)
       a1(i+2,k)=c1*d(1,k)*si(1+m1,3)
 114      continue
          do 115 k=4,6
        i2=k-3
        a1(i,k)=c1*d(2,i2)*si(2+m1,1)
        a1(i+1,k)=c1*d(2,i2)*si(2+m1,2)
        a1(i+2,k)=c1*d(2,i2)*si(2+m1,3)
 115      continue
          do 116 k=7,9
        i3=k-6
        a1(i,k)=c1*d(3,i3)*si(3+m1,1)
```

```
          a1(i+1,k)=c1*d(3,i3)*si(3+m1,2)
          a1(i+2,k)=c1*d(3,i3)*si(3+m1,3)
 116        continue
            do 117 k=10,12
          i4=k-9
          a1(i,k)=c1*d(4,i4)*si(4+m1,1)
          a1(i+1,k)=c1*d(4,i4)*si(4+m1,2)
          a1(i+2,k)=c1*d(4,i4)*si(4+m1,3)
 117        continue
          m1=m1+4
 111    continue
        do 100 i=1,12
          do 101 j=1,12
          if(j .eq. i)then
          A(i,i)=1.d0-A1(i,i)
          else
          A(i,j)=-A1(i,j)
          endif
 101      continue
 100    continue
        do 200 j1=1,10,3
        b(j1)=Ext(1)
200     continue
        do 201 j2=2,11,3
        b(j2)=Ext(2)
201     continue
        do 202 j3=3,12,3
        b(j3)=Ext(3)
202     continue
        call ludcmp(63)(a,12,12,indx,de)
        call lubksb(63)(a,12,12,indx,b)
        do 300 j=1,10,3
        el(j)=b(j)
        el(j+1)=b(j+1)
        el(j+2)=b(j+2)
300     continue
        e1d1=el(1)*d(1,1)+el(2)*d(1,2)+el(3)*d(1,3)
        e1d2=el(4)*d(2,1)+el(5)*d(2,2)+el(6)*d(2,3)
        e1d3=el(7)*d(3,1)+el(8)*d(3,2)+el(9)*d(3,3)
        e1d4=el(10)*d(4,1)+el(11)*d(4,2)+el(12)*d(4,3)
        do 310 i=1,3
        eljdj1(i)=e1d1*d(1,i)+e1d2*d(2,i)+e1d3*d(3,i)+e1d4*d(4,i)
        p(i)=4.d0*c1*eljdj1(i)/rc*dnh
310     continue
        qp=q(1)*eljdj1(1)+q(2)*eljdj1(2)+q(3)*eljdj1(3)
        do 311 i=1,3
        ave(i)=Ext(i)-16.d0*pi*c1*q(i)*qp
311     continue
        dkai11=p(1)/ave(1)
        dkai22=p(2)/ave(2)
        dkai12=p(1)/ave(2)
```

```
          dkai21=p(2)/ave(1)
          fe11=(1.d0+4.d0*pi*dkai11)
          fe22=(1.d0+4.d0*pi*dkai11)
          fe44=(1.d0+4.d0*pi*(dkai12+dkai21)/2)
            endif
          endif
 1        continue
          p11=((1.d0/fe11)-(1.d0/epcer0))/dudx
          p12=((1.d0/fe22)-(1.d0/epcer0))/dudx
          p44=((1.d0/fe44)-(1.d0/epcer0))/dudx
          func=(feij-dnij)**2
c print 'input the ij in 'feij' each time when you calculate'.
        return
        end
```

Appendix J. PROGRAM ADMLF

```
      program ADMLF
c Written by Lingzhou L.Canfield, as part of thesis.
c this is a program to evaluate the local field effect on the
c susceptibility in cubic tetrahedral structure, for ADM in cubic
c tetrahedral structure.  However, for 2D ADM problem, just change
c this 3D to 2D.
c this is a MAIN program
      implicit real*8(a-h,o-z)
      dimension el(6), a(6,6), a1(6,6),b(6),s3(4),ave(3),q(3),
     &  s5ij(4,6),s5(4,3,3),d(3,3),si(4,3,3),p(3),idex(6),ext(3)
      pi=dacos(-1.d0)
      Ext(1)=1.d0/dsqrt(2.d0)
      Ext(2)=1.d0/dsqrt(2.d0)
      Ext(3)=0.d0
      q(1)=0.d0
      q(2)=0.d0
      q(3)=1.d0
c q(i) is the unit wave vector
      dudx=0.0d0
      rc=1.d0-dudx
      open(unit=5, file='a3dmz.out', status='old')
      open(unit=6, file='a5dmz.out', status='old')
      open(unit=7, file='dit.inp', status='old')
      open(unit=9,file='a0qzexy.dat', status='new')
      do 10 i=1,4
        read(5,*)s3(i)
        read (6,*)(s5ij(i,j),j=1,6)
        s5(i,1,1)=s5ij(i,1)
        s5(i,2,1)=s5ij(i,2)
        s5(i,2,2)=s5ij(i,3)
        s5(i,3,1)=s5ij(i,4)
        s5(i,3,2)=s5ij(i,5)
        s5(i,3,3)=s5ij(i,6)
        s5(i,1,2)=s5(i,2,1)
        s5(i,1,3)=s5(i,3,1)
        s5(i,2,3)=s5(i,3,2)
 10   continue
      do 11 i=1,3
         read (7,*)(d(i,j),j=1,3)
 11   continue
      close(5)
      close(6)
      close(7)
      do 15 m=1,4
         do 14 i=1,3
            do 13 j=1,3
      si(m,i,j)=3*s5(m,i,j)-d(i,j)*s3(m)
 13         continue
 14      continue
 15    continue
```

```
      do 400 mc1=0,25,5
         c1=mc1/1.d2
c c1 is the atomic polarizability per a**3, a is the lattice const.
         m1=0
      do 111 i=1,4,3
         do 114 k=1,3
      a1(i,k)=c1*si(1+m1,1,k)
      a1(i+1,k)=c1*si(1+m1,2,k)
      a1(i+2,k)=c1*si(1+m1,3,k)
 114      continue
          do 115 k=4,6
       i2=k-3
       a1(i,k)=c1*si(2+m1,1,i2)
       a1(i+1,k)=c1*si(2+m1,2,i2)
       a1(i+2,k)=c1*si(2+m1,3,i2)
 115      continue
       m1=m1+2
 111    continue
        do 100 i=1,6
           do 101 j=1,6
           if(j .eq. i)then
           A(i,i)=1.d0-A1(i,i)
           else
           A(i,j)=-A1(i,j)
           endif
 101       continue
 100    continue
        do 200 j1=1,4,3
        b(j1)=Ext(1)
200     continue
        do 201 j2=2,5,3
        b(j2)=Ext(2)
201     continue
        do 202 j3=3,6,3
        b(j3)=Ext(3)
202     continue
     call ludcmp(63)(a,6,6,indx,det)
     call lubksb(63)(a,6,6,indx,b)
      do 300 j=1,4,3
      el(j)=b(j)
      el(j+1)=b(j+1)
      el(j+2)=b(j+2)
300   continue
      p(1)=4.d0*c1*(el(1)+el(4))/rc
      p(2)=4.d0*c1*(el(2)+el(5))/rc
      p(3)=4.d0*c1*(el(3)+el(6))/rc
      qpa=q(1)*p(1)+q(2)*p(2)+q(3)*p(3)
      do 310 i=1,3
      ave(i)=Ext(i)-4.d0*pi*q(i)*qpa
310   continue
      if(ext(3) .eq. 0.d0)then
```

```
      dkai11=p(1)/ave(1)
      dkai12=p(1)/ave(2)
      dkai21=p(2)/ave(1)
      dkai22=p(2)/ave(2)
      else
      dkai33=p(3)/ave(3)
      dkai13=p(1)/ave(3)
      dkai23=p(2)/ave(3)
      endif
      write(9,62)c1,dkai11,dkai22,dkai12,dkai21
 62   format(7f8.4)
400   continue
      close(9)
      stop
      end
```

Appendix K. PROGRAM BDMLF2D

```
      program BDMlf2D
c Written by Lingzhou L.Canfield, as part of thesis.
c this is a program to evaluate the local field effect on the
c susceptibility in 2D center rectangular structure, for the BDM.
c However, if change the external field to be 3D, and open the files
c of the 3D's dipole sums, then it can be used for calculating 3D's
c problem.
c this is a MAIN program
      implicit real*8(a-h,o-z)
      dimension el(8),a(8,8),a1(8,8),b(8),s3(96),eld3(3),
     &   s5ij(96,6),s5(96,3,3),d(24,2),si(96,3),p(3),ext(3),
     &   eljdj1(3),indx(12),ave(3),eld2(3),q(3)
      open(unit=5, file='2ds3rctl.out', status='old')
      open(unit=6, file='2ds5rctl.out', status='old')
      open(unit=7,file='2ddins.inp',status='old')
      open(unit=9, file='b2drct.dat', status='new')
      delt = 0.d0
      rc=1.0d0-delt
      pi=dacos(-1.d0)
      Ext(1)=1.d0
      Ext(2)=0.d0
      q(1)=0.d0
      q(2)=0.d0
      q(3)=1.d0
c q is the unit wave vector, input the q when you do the calculation
      do 10 i=1,16
      read(5,*)s3(i)
      s3(i)=s3(i)
      read (6,*)(s5ij(i,j),j=1,3)
      s5(i,1,1)=s5ij(i,1)
      s5(i,2,1)=s5ij(i,2)
      s5(i,2,2)=s5ij(i,3)
      s5(i,1,2)=s5(i,2,1)
 10   continue
      do 11 j0=1,4
      read(7,*)(d(j0,i0),i0=1,2)
      d(j0,1)=d(j0,1)/dsqrt(1.d0+rc*rc)
      d(j0,2)=d(j0,2)*rc/dsqrt(1.d0+rc*rc)
 11   continue
      close(5)
      close(6)
      close(7)
      do 15 m=1,13,4
         do 14 i1=1,2
      si(m,i1)=3.d0*(s5(m,i1,1)*d(1,1)+s5(m,i1,2)*d(1,2))
     & -s3(m)*d(1,i1)
      si(m+1,i1)=3.d0*(s5(m+1,i1,1)*d(2,1)+s5(m+1,i1,2)*d(2,2))
     & -s3(m+1)*d(2,i1)
      si(m+2,i1)=3.d0*(s5(m+2,i1,1)*d(3,1)+s5(m+2,i1,2)*d(3,2))
     & -s3(m+2)*d(3,i1)
```

```
      si(m+3,i1)=3.d0*(s5(m+3,i1,1)*d(4,1)+s5(m+3,i1,2)*d(4,2))
     & -s3(m+3)*d(4,i1)
  14      continue
  15    continue
        do 400 mc=0,1000,50
        c1=mc/10.d0
        m1=0
        do 111 i=1,7,2
           do 114 k=1,2
        a1(i,k)=c1*d(1,k)*si(1+m1,1)
        a1(i+1,k)=c1*d(1,k)*si(1+m1,2)
114        continue
           do 115 k=3,4
        i2=k-2
        a1(i,k)=c1*d(2,i2)*si(2+m1,1)
        a1(i+1,k)=c1*d(2,i2)*si(2+m1,2)
  115      continue
           do 116 k=5,6
        i3=k-4
        a1(i,k)=c1*d(3,i3)*si(3+m1,1)
        a1(i+1,k)=c1*d(3,i3)*si(3+m1,2)
  116       continue
            do 117 k=7,8
        i4=k-6
        a1(i,k)=c1*d(4,i4)*si(4+m1,1)
        a1(i+1,k)=c1*d(4,i4)*si(4+m1,2)
  117       continue
        m1=m1+4
  111   continue
        do 100 i=1,8
           do 101 j=1,8
        if(j .eq. i)then
        A(i,i)=1.d0-A1(i,i)
        else
        A(i,j)=-A1(i,j)
        endif
  101     continue
  100   continue
        do 200 j1=1,7,2
        b(j1)=Ext(1)
  200   continue
        do 201 j2=2,8,2
        b(j2)=Ext(2)
  201   continue
      call ludcmp(63)(a,8,8,indx,de)
      call lubksb(63)(a,8,8,indx,b)
      do 300 j=1,7,2
      el(j)=b(j)
      el(j+1)=b(j+1)
  300  continue
       e1d1=el(1)*d(1,1)+el(2)*d(1,2)
```

```
      e1d2=el(3)*d(2,1)+el(4)*d(2,2)
      e1d3=el(5)*d(3,1)+el(6)*d(3,2)
      e1d4=el(7)*d(4,1)+el(8)*d(4,2)
      do 310 i=1,2
      eljdj1(i)=e1d1*d(1,i)+e1d2*d(2,i)+e1d3*d(3,i)+e1d4*d(4,i)
      p(i)=c1*eljdj1(i)/rc
 310  continue
      qp=q(1)*p(1)+q(2)*p(2)
      do 311 i=1,2
      Ave(i) = Ext(i)-2*2*pi*q(i)*qp
c 2 comes from there are two atoms in face center surface structure
 311  continue
      if (p(1) .eq.0.d0 .AND. p(2) .eq. 0.d0)then
      dkai11=0.d0
      dkai22=0.d0
      else
      if (ext(2) .eq. 0.d0)then
      dkai11=p(1)/ave(1)
      dkai21=p(2)/ave(1)
      else
      dkai22=p(2)/ave(2)
      dkai12=p(1)/ave(2)
      endif
      endif
      write(9,62) c1,dkai11,dkai21
 62   format(3f14.4)
 400  continue
      close (9)
      stop
      end
```

Appendix L. File DIJINS.INP

```
 1.d0      1.d0      1.d0
 1.d0     -1.d0     -1.d0
-1.d0      1.d0     -1.d0
-1.d0     -1.d0      1.d0
```

Appendix M. File DIT.INP

```
1.0       0.0       0.0
0.0       1.0       0.0
0.0       0.0       1.0
```

Appendix N. File 2DDINS.INP

```
-1.d0    -1.d0
-1.d0     1.d0
 1.d0    -1.d0
 1.d0     1.d0
```

Appendix O. Dipole Sums For Diamond and Zinc blende crystals

$$S_{ij}(\vec{q},M,m) = 3S_5^{ij}(\vec{q},M,m) - \delta_{ij}S_3(\vec{q},M,m).$$

ADM: 2 fcc sublattice, m=1,2. For $\vec{q}$ along z direction:
$S_{11}(\vec{q},1,1)= S_{22}(\vec{q},1,1)= 16.7550 = 4\,\frac{4\pi}{3}$, $S_{33}(\vec{q},1,1)=-33.5103=-4\frac{8\pi}{3}$,
$S_{11}(\vec{q},1,2)= S_{22}(\vec{q},1,2)= 16.7550 = 4\,\frac{4\pi}{3}$, $S_{33}(\vec{q},1,2)=-33.5103=-4\frac{8\pi}{3}$,
$S_{i\neq j}(\vec{q},1,m)=0.0$. 4 comes from that one fcc sublattice contains 4 atoms.

BDM: 4 fcc sublattice, m=1..4. For $\vec{q}$ along z direction:
$S_{11}(\vec{q},1,1)= S_{22}(\vec{q},1,1)= 16.7550 = 4\,\frac{4\pi}{3}$, $S_{33}(\vec{q},1,1)=-33.5103=-4\frac{8\pi}{3}$,
$S_{11}(\vec{q},1,2)= -17.9158$, $S_{22}(\vec{q},1,2)= 34.0907$, $S_{33}(\vec{q},1,2)=-16.1749$,
$S_{23}(\vec{q},1,2)=57.8424$, $S_{11}(\vec{q},1,3)= 34.0907$, $S_{22}(\vec{q},1,3)= -17.9158$,
$S_{33}(\vec{q},1,3)=-16.1749$, $S_{13}(\vec{q},1,3)=57.8424$, $S_{11}(\vec{q},1,4)= 34.0907$,
$S_{22}(\vec{q},1,4)= 34.0907$, $S_{33}(\vec{q},1,4)=-68.1811$, $S_{12}(\vec{q},1,4)=57.8424$.
All other $S_{i\neq j}(\vec{q},1,m)=0.0$. Notice that $\Sigma_m S_{11}(\vec{q},1,m)=\Sigma_m S_{22}(\vec{q},1,m)=$ $67.0206=16\frac{4\pi}{3}$, there are 16 bond dipoles per unit cell.

Appendix P. Retardation

We give a brief summary of G. D. Mahan[15]'s conclusions here. By using

$$\vec{D} = \vec{E} + 4\pi \vec{P}, \tag{P-1}$$

and

$$\vec{E} = -\frac{1}{c}\frac{\partial}{\partial t}\vec{A} - \nabla \varphi, \tag{P-2}$$

under the Coulomb Gauge $\nabla \cdot \vec{A} = 0$, the Maxwell equations can be rewritten as:

$$\nabla^2 \varphi = 4\pi \nabla \cdot \vec{P}, \tag{P-3}$$

$$\nabla^2 \vec{A} - \frac{1}{c^2}\frac{\partial^2 \vec{A}}{\partial t^2} = -\frac{4\pi}{c}\frac{\partial}{\partial t}(\vec{P} - \frac{1}{4\pi}\nabla \varphi), \tag{P-4}$$

with the assumption that no free charges or currents are present. The right hand side of (P-4) contains the factor

$$\vec{P}_r = \vec{P} - \frac{1}{4\pi}\nabla \varphi, \tag{P-5}$$

which is the rotational part of the polarization vector. One can prove it is rotational by simply proving that

$$0 = \nabla \cdot \vec{P}_r = \nabla \cdot \vec{P} - \frac{1}{4\pi}\nabla^2 \varphi$$

by using (P-3). The irrotational part of polarization vector is

$(1/4\pi)\nabla\varphi$. The electric field also has rotational and irrotational parts. The rotational part is

$$\vec{E}_r = -\frac{1}{c}\frac{\partial}{\partial t}\vec{A}$$

and the irrotational part is $-\nabla\varphi$. In the point dipole model, the polarization $\vec{P}$ is

$$\vec{P} = \frac{1}{V_c}\Sigma_m \vec{p}_m, \tag{P-6}$$

where V_c is the volume of the unit cell and the sum is over all dipoles in the unit cell. The dipole moment $\vec{p}_m$ is proportional to the local electric field at that atomic site

$$\vec{p}_m = \alpha \vec{E}(r_m), \tag{P-7}$$

where α is the atomic polarizability. The local electric field is given

$$\vec{E}(r_m) = \vec{E}_{ext} + \Sigma'_{\ell m'} \frac{3(\vec{x}_{\ell m'}\cdot\vec{p}_{m'})\vec{x}_{\ell m'} - \vec{x}^2_{\ell m'}\vec{p}_{m'}}{x^5_{\ell m'}}, \tag{P-8}$$

where, $\vec{x}_{\ell m} = \vec{r} - \vec{r}_\ell - \vec{r}_m$, $\vec{r}_\ell$ is the lattice vector and $\vec{r}_m$ is the position of the m^{th} base, and $\vec{E}_{ext}$ is the applied electric field.

In an experiment, $\vec{E}_{ext}$ is applied by sending a light beam at the sample. The light beam strikes the surface of the sample and excites the normal modes of the solid which subsequently propagate through

the crystal. Since an oscillating dipole creates both a short range dipole field and a long range radiation field, the latter of which is $\vec{E}_r$. $\vec{E}_r$ is not the applied field, but is instead the normal mode field obtained by the self consistent solution of the interacting dipole problem. So the local field can be equivalently described by Eq.(P-2). Suppose there are N identical atoms per unit cell. The polarization P can then be written as

$$\vec{P} = \frac{Na}{V_c}\left(- \frac{1}{c} \frac{\partial}{\partial t} \vec{A} - \nabla \varphi\right). \qquad \text{(P-9)}$$

Substituting (P-9) into (P-4) we have

$$\nabla^2 \vec{A} - \frac{1}{c^2} \frac{\partial^2 \vec{A}}{\partial t^2} = - \frac{4\pi}{c} \frac{\partial}{\partial t}\left[\frac{Na}{V_c}\left(- \frac{1}{c} \frac{\partial}{\partial t} \vec{A} - \nabla \varphi\right) - \frac{1}{4\pi} \nabla \varphi\right]$$

$$= \frac{4\pi Na}{c^2 V_c} \frac{\partial^2 \vec{A}}{\partial t^2} + \frac{4\pi}{c}\left(\frac{Na}{V_c} + \frac{1}{4\pi}\right) \nabla \frac{\partial}{\partial t} \varphi. \qquad \text{(P-10)}$$

Since the potential φ and $\vec{A}$ have an $e^{i\omega t}$ functional form so (P-9) can be written as

$$\left(\nabla^2 + \frac{\omega^2}{c^2}\right) \vec{A} = - \frac{\omega^2 4\pi Na}{c^2 V_c} \vec{A} + i\omega \frac{4\pi}{c}\left(\frac{Na}{V_c} + \frac{1}{4\pi}\right) \nabla \varphi. \qquad \text{(P-11)}$$

However, the rotational part of the electric field can be written as $\vec{E}_r = - \frac{i\omega}{c} \vec{A}$ allowing (P-11) to be rewritten as

$$(\nabla^2 + \frac{\omega^2}{c^2})\,\vec{E}_r = -\frac{\omega^2 4\pi N\alpha}{c^2 V_c}\,\vec{E}_r + \frac{\omega^2}{c^2}\,4\pi\left(\frac{N\alpha}{V_c} + \frac{1}{4\pi}\right)\nabla\varphi. \qquad \text{(P-12)}$$

If we write the spatial dependence of the $\vec{E}_r$ like $e^{-i\vec{k}\cdot\vec{r}}$, where $k = n\omega/c$ and n is the refractive index, then (P-12) becomes

$$\frac{n^2 - 1}{4\pi}\,\vec{E}_r = \frac{N\alpha}{V_c}\,(\vec{E}_r - \nabla\varphi) - \frac{1}{4\pi}\nabla\varphi$$

$$= P - \frac{1}{4\pi}\nabla\varphi. \qquad \text{(P-13)}$$

Notice the irrotational part of electric field contributes to the rotational part of the polarization since $\vec{P}_r \neq N\alpha E_r/V_c$! This means that when the instantaneous dipole sum is to be taken the retardation has been included. If we put the retardation in the dipole interaction potential we would be putting the retardation in the calculations twice and would be over counting the retardation.

This conclusion is gauge independent, because although the potential depends on the choice of gauge, the physically observable quantities $\vec{E}$ and $\vec{B}$ are independent of the choice of gauge.